MODEL BRICKWORK WALL PANELS UNDER LATERAL LOADING

A Thesis

Submitted for the Degree of

DOCTOR OF PHILOSOPHY

of the

UNIVERSITY OF EDINBURGH

by

KAMAL MOHAMED HAMAD SATTI

B.Sc (Honrs.)

Department of Civil Engineering and

Building Science

(School of the Built Environment)

July 1972

ACKNOWLEDGEMENTS

The author would like to thank Professor A.W. Hendry, Ph.D., D.Sc., F.I.C.E., F.I.Struct.E., F.R.S.E., for granting the opportunity to pursue this study and for his personal guidance and supervision throughout.

Thanks are also due to Dr. S.R. Davies, B.Sc., Ph.D., M.I.C.E., for his assistance with the theoretical analysis, and to the British Ceramic Research Association for supply of model bricks, and my wife and parents for their enormous sacrifices.

Finally the author wishes to thank the staff of the Edinburgh Regional Computing Centre for their services, all workshop and technical personnel, in particular Mr. R.S. Elder for their valuable assistance, Mr. R. MacKenzie and Mr. R. Beverage who produced the photographic work and Miss E. McNamara for skillfully typing the thesis and Mrs. E. Ezzi for her general help.

NOTATION

M_i : component of the ultimate moments in the direction of the axis of rotation

θ : rotation of the resultant of ultimate moments

M_x : component of M_i in the X-axis

M_y : component of M_i in the Y-axis

θ_x : component of θ in the X-axis

θ_y : component of θ in the Y-axis

W : external work done by loading

Z : virtual displacement of a point in plate

p : applied loading

L : length of plate

w : displacement of a mesh point

U_n : nodal displacement vector

$w_{,xx}$: second derivative of w with respect to x

D_1 : $\frac{Et^3}{12(1-v^2)}$

D_2 : vD_1

D_3 : $D_1(1 - v)/2$

α : height to length ratio

t : thickness of panel

v : Poisson's ratio

E : modulus of elasticity

k : factor expressing the proportion of load on the vertical side

μ : coefficient of friction between the brickwork and steel suppo

m_1 : moment due to flexural strength of brickwork

m_2 : moment due to restraining action of friction between panel and supports

f_t : modulus of rupture of brickwork

F : Axial precompression on walls

A B S T R A C T

The purpose of the work reported in this thesis was to investigate whether the yield line and finite element methods could be used to estimate the lateral load capacity of model brick walls, in conjunction with experimentally established values of modulus of rupture. Model brick walls of varying dimensions, thicknesses, support conditions and axial precompressions were tested under uniform lateral load. Analyses were carried out using the yield line and finite element methods for comparison with the experimental results. Good agreement between measured and calculated loads and deflections was found.

Reported also are the results of tests carried out on full scale wallettes and prisms to investigate the modulus of rupture of brickwork, using five types of bricks and two of mortars. Simple transverse tests for studying the modulus of rupture at axes of bending parallel to or at 45° or 90° to the mortar bed joints are described. Possible effects on modulus of rupture of variables such as suction rate, modulus of rupture, crushing strength of the bricks and the brickwork are reported.

The effect of axial precompression on lateral load capacity and rigidity of walls is also included.

CHAPTER 1

1.1 GENERAL INTRODUCTION

Brick masonry is primarily a loadbearing material with relatively large compressive strength. It was used exclusively as such, and walls possessed gravity stability because of the mass of the wall and the superimposed floor loads. Under such design conditions, flexural and tensile strengths were not a consideration.

The trend of the last years, however, has been in the direction of walls with less and less lateral support and with little or no superimposed loads to make them gravity-stable. Warehouses and shops with high walls, which cannot be justified on the basis of gravity stability, are quite common. Moreover, many modern wall designs for schools or offices have strip windows and large door openings which interrupt the beam action.

Transverse strength of brick masonry walls is small and highly variable in character. It is usually not directly recognised by most building codes. Indirectly, the transverse or flexural resistance of masonry walls is controlled by providing either the horizontal or vertical support intervals not to exceed eighteen times the nominal wall thickness. Now increased, however, allowable extreme fibre stresses that would permit rational analysis is indeed lacking. In some types of walls, CP III, 1970[1], defines certain allowable stresses.

The source of the transverse strength in a masonry assemblage is the bond at/

at the interface between the brick and mortar. Although the precise nature of this bond is not completely understood, research indicates that the following variables influence this mechanism:

1. Brick characteristics
   (a) absorption or suction rate at time of laying.
   (b) type (solid, perforated, frogged) and surface roughness, including texture.
2. Mortar characteristics
   (a) flow and water retentivity
   (b) type and cement content
   (c) thickness of mortar bed
   (d) curing conditions and duration
   (e) workability.
3. Workmanship

Basically, bond is largely influenced by the battle between the brick's capacity to absorb water and the mortar's ability to retain it for proper hydration at the interface. Bricks having a suction of 20 $gm/dm^2/mm$ or less are generally considered satisfactory. It is this initial rate of water absorption that is of most importance in obtaining good bond between brick and mortar. It is also important that mortar shall have a flow after suction greater than 70% of the initial flow. This is a measure of its water retentivity and workability.

Since it is the internal curing condition of the bond interface that is important here, it is questionable whether the external curing of the wall greatly/

greatly aids the bond. As air curing conditions are the only ones usually practicable, attention is better directed to aiding the internal hydration by controlling water retention, which can be accomplished by admixtures in the mortar mix and by changing the suction of the bricks by wetting before they are laid.

Traditionally, masonry has been built by rule-of-thumb methods. Most building Codes reflect these arbitrary limitations as to height and thickness of masonry. In most cases designed walls have had satisfactory bearing capacity, however, the factor of safety might have been unduly high thus resulting in uneconomical design. Where failure has occurred, in adequately supported wall panels, it has been by bond failure at the brick mortar interface although in panels with good bond strength, tension failure in the bricks and mortar has taken place. The introduction of rational design provisions into a code allows the engineer to utilise masonry not in accordance with these arbitrary restrictions, but with regards to its structural properties.

Due to insufficient knowledge of the structural mechanics of laterally loaded masonry walls, the lateral load capacity could not be determined analytically. Existing design methods are based on empirical data and highly approximate calculation methods and are not considered to be a rational approach to the design problem. A rational design must be based on a method that is representative for the performance of the structure in use.

As a rule, however, national building codes with a few exceptions are restricting the use of masonry walls by not allowing tensile stresses to occur in such walls. If this rule was strictly enforced it would mean that unreinforced/

unreinforced masonry walls could not be used as infill panels or in the top storeys of buildings where the vertical loads are small.

There are several reasons why tensile stresses are not allowed, one being the lack of better design methods. To develop stress analysis design methods, test data for masonry walls must be available to verify the methods.

A combination of vertical and horizontal loading is common. Combined loading tests are important because exterior walls in loadbearing masonry carry both lateral and compressive loads. Below ground the walls may be subjected to soil pressure. The compressive load increases the flexural strength, and when cracking occurs it does not necessarily result in immediate collapse of the wall, which may be sufficiently stabilised by the effect of the vertical loading.

1.2 REVIEW OF PREVIOUS WORK

All walls, whether designed to support vertical load or not, are liable to be subjected to lateral loading, as for example from wind or from materials stacked against them. As the tensile strength of brickwork is low and variable, cracking may occur for even small lateral loads if the wall is thin or if insufficient support is given to the perimeter of the wall.

Cracking in itself may not lead to collapse, however, for the cracked wall may be stabilised by the action of any vertical loading it supports. Alternatively, if restraint to edge movement is afforded by the rest of the structure the wall may resist further lateral load by acting as a flat dome. This/

This later action can occur when a brick panel is built into or against a steel framework and tests have been made at the Building Research Station to examine the lateral strength of such panels as reported by Thomas[2]. Some single and cavity full size walls were tested with and without reinforcement, the lateral loading being applied by means of hydraulic jacks at 16 points through a distributing system of steel joists.

Davey[3] reported a few tests carried out by the Building Research Station. Two sets of 4½ in. panels, 4 ft 6 in long and 9 ft high were tested using two different strength bricks. Both sets included walls built in 1:3 cement, sand mortar, 1:1:4 cement, lime, sand mortar, and 1:2:9 cement, lime, sand mortar. The walls were all loaded with a direct end load of 1 ton per sq ft and the lateral load was applied horizontally half-way up the wall. In all cases failure occurred by the breaking of the bond between the mortar and the bricks in a horizontal course. There was an increase in the strength of the brick mortar bond as the cement content of the mortar increased but the increase was not proportional. Although in the second series of tests very much stronger bricks were used, this did not result in proportionally greater failure strength, indicating that the mortar bond is to a greater extent the factor determining the lateral stability of a wall.

The next problems to be considered were those arising when the wall is used in a structural framework. In this case the wall could be either restrained or simply supported around its entire periphery.

In the first tests undertaken the walls were loaded laterally by means of hydraulic jacks on 16 points of its surface. Later, air pressure was used to/

to give uniform pressure loading on the walls. Air was pumped into a rubber bag enclosed between one side of the wall and a concrete slab. The reaction due to the air pressure was taken by connecting the slab with tie bars to a concrete frame on the other side of the test wall.

In one series two walls were tested with all edges free, that is the walls were not subjected to edge forces in the plane of the wall. Two other walls had their edges built into a steel channel surround to simulate the conditions of a panel in a steel framed building. One wall had free edges and a direct load applied to the top.

Where the edges were free the load to cause cracking was not exceeded as the wall was further deformed. When edge restraint was provided, the walls developed appreciable dome action and the capacity of the wall to resist lateral load was increased.

Another series of tests using a weaker brick strength produced very similar results.

Tasker[4] initiated simulated wind load tests on full size test walls using contiguous canvas bags. He tested two 9 in no-fines concrete walls, one 9 in brick wall and an 11 in brick cavity wall, with a view to studying the stresses involved and the action of these walls under pressure, and to presenting an analysis for all types of external masonry walls likely to be used in construction for domestic buildings. Only incomplete conclusions have been drawn from these tests due to their limited scope and number.

Bradshaw/

Bradshaw and Entwisle[5] discussed the problems associated with lateral wind loading on external brickwork infill panels of the uppermost storeys of buildings where vertical precompression is very small. Only an approximate method of design for safe panel sizes and thicknesses to resist given wind loading was introduced, based on bending moments similar to those for two-way span reinforced concrete slabs with torsional resistance[6].

The Structural Clay Products Research Foundation[7,8,9,10] reported transverse tests on vertically spanning brick walls of various thicknesses using either the inflated bag method or two line loads at the outer quarter points of the wall.

Thompson, Johnson and Wheeless[11] presented a report based on a series of flexural tests on masonry bonded hollow walls of varying widths, percentages of headers and sizes of brick. A systematic analysis of the results of the tests and the effects of the basic parameters involved in the structural capacity of masonry bonded hollow walls is presented. The influence of the section modulus, percentage of headers, mortar compressive strength, and bond effectiveness on the resisting moment and modulus of rupture of the walls is discussed.

Monk[12] carried out some lateral tests on walls and found that major wall rupture did not occur at loads lower than the yield strength load; hence this value is unaffected by redistribution of stresses due to failure. He also noted two observations from the crack patterns. Cracks at the corners show evidence of the restraining moments generated by corner continuity. The shorter walls, not restrained at their tops, failed primarily as horizontal beams./

beams. He also found that wall strength determined by the third-point loading method was less than that obtained with uniform loading.

National Concrete Masonry Association[13] performed flexural tests on masonry walls in the vertical and horizontal spans for providing information which can be used as a basis for the engineered design of concrete masonry.

Brick cavity walls of different support conditions have been tested by uniform lateral loading at The Norwegian Building Research Institute[14] to study their stiffness and strength to provide a better understanding of their structural mechanics.

Dial gauge readings indicated that both wythes got approximately the same deflections and the strain gauge readings on steel ties connecting the wythes indicated that about half the load was carried by each wythe. Hence it was concluded that the bending moment caused by lateral loads is divided between the wythes according to their stiffness in bending.

The test data for the walls have been used to verify theoretical calculation methods, and design tables worked out based on the test results and a computer program for elastic plates.

Haseltine, Thomas, West and Hodgkinson[15] reported some tests on vertically spanning brick walls carried out at the Laboratories of the British Ceramic Research Association. The walls, which were storey high, were placed under a known precompression while the lateral load was applied by means of an air bag.

The/

The tests established that at low pre-loads (5000 lb/ft run) failure is entirely geometrical and that the strengths of the mortar and the bricks play little or no part in the total resistance to lateral loading. As the pre-loads increases, the mode of failure changes, introducing an element of crushing at mid-height of the wall on the laterally loaded face (Fig 1.1)

It was suggested that these patterns of failure seem to account for the shape of the lateral load-precompression curves (Fig. 1.2)

Although the precise relationship between lateral load and precompression at very high levels of precompression has not been investigated, the range covered is adequate for practical purposes.

The effects of end restraints on the load capacity were tested on one 9 in-wall with returns. At a precompression of 5000 lb/ft run this wall failed in a yield line pattern of cracks at a load more than twice that of the equivalent wall without returns. It seems likely that the effect of returns at one or both ends of a wall must be to stiffen it and thus increase in some degree the lateral load resistance and also, of course, change the hinge failure to that of a yield line pattern.

Grenley, Cattaneo and Pfrang[16] reported flexural tests of precompressed, vertically spanning brick walls. Two mortars were selected; a conventional and a high-bond strength one to illustrate what can be accomplished in engineered masonry as better mortars become available, permitting a masonry structure to more fully utilize the inherent high strength of the individual brick. The increase in the flexural strength of masonry walls due to applied edge-load was also reported and interaction diagrams for such systems presented.

An/

An investigation which centres on the effect of precompression, wall length and returns on the transverse strength of full scale brick cavity walls was reported by Hendry, Sinha & Maurenbrecher[17]. The test walls formed part of a full scale building thus having similar end conditions and similar precompressions to those in practice. The cavity walls were uniformly loaded on their inner leaf, both in precompression and transverse load. A simple theory was proposed for walls supported in various ways, taking into account the arching effect resulting from vertical restraint. Results of the investigation are reproduced in Tables (1.1) and (1.2).

1.3 METHOD OF ANALYSIS

Two calculation methods have been used based on The Yield-Line and Finite Elements Methods. The former predicts the ultimate load and the latter is essentially an elastic analysis method. Both are assumed to be valid until the instant of cracking, at which in most cases full pattern development was achieved, and where equilibrium of bending moments and compatibility of deformations is still applicable. Both of these methods have been extensively applied for the analysis of reinforced concrete slabs of any shape with varying conditions of support and under any combinations of loading.

Structures continuously or occasionally under load obviously have to be made safe against failure, and so it is vitally important to determine their strength through tests and calculations. Such a study must often by supplemente by calculations of the deformations, since it is often necessary to keep the deformations within appropriate limits; in other words, besides having a certain/

certain strength, the structure must have a certain degree of rigidity. These subjects are covered by the two branches of study: strength of material of materials and theory of elasticity, the latter was generally being by far the more widely applied.

This bias has led in the past to a certain reluctance to accept, if not to actual distrust of, methods of calculation which are not based on the theory of elasticity, although in most cases the result calculated according to the theory of elasticity will be an idealised figure, since the materials do not follow Hooke's law to the point of failure, and the deformations can not be reckoned as infinitesimal. The result based on the strength of materials criteria will be realised in practice, however, since these make use of the particular features of failure.

It is therefore quite natural that the first attempts to analyse loadbearing structures should have been made on the strength of materials theory; but they have been calculated on the basis of elastic theory, and they have not therefore been developed to the best advantage.

Except in the simplest case of spanning between two parallel supports it is uneconomical to design a wall panel as if it consisted of a series of beams laid side by side. Elastic methods of analysis of two-way spanning slabs have been developed and have been in use for many years, but they are so complicated mathematically that in practice the data obtained from standard cases are generally provided in the form of tables of bending moments, etc[6], for various slab proportions and support conditions, and have been applied to non-loadbearing brickwork panels by Bradshaw and Entwisle[5]. For slabs of irregular/

irregular shape, elastic analysis is hoplessly complicated and a solution may be beyond the ability of even the best mathematician unless a computer is available. This, however, is not true when employing an ultimate load method of analysis and solutions can be obtained for slabs of any shape, with any support conditions, and under any combinations of loading.

From the above review it will be seen that the work done previously on the lateral strength of brick walls was not comprehensive and most of it was concerned with the strength when walls were spanning vertically. Only a limited number of tests were carried out on walls supported from more than two sides to allow the verification of any suggested method of analysis.

TABLE 1.1

MORTAR AND BRICKWORK STRENGTHS.

Test No	Mortar Strength lbf/in^2	Average Age days	Brickwork Strength lbf/in^2	Average Age days	Notes
1	2430	16	2630[1]	17	1. 9" brickwork cubes
2	1290	36	3940[1]	36	
3	1825	10	850	10	All brickwork specimens tested with plywood top and bottom
4	1700	13	1060	12	
5	2090	12	800	9	
6	1245	9	1050	16	
7	1235	12	1020	10	
8	1140	9	1075	11	
9	1310	19	1180	20	
10	1910	9	945	8	
11	1415	11	1080	14	
12	2090	17	1240	21	
13	2595	23	950	23	
14	2000	14	1175	15	
15	2135	21	800	21	
16	2050	12	1020	13	
17	2475	26	995	20	
18	3265	39	810	39	

TABLE 1.2

TEST RESULTS

Test No	Returns	Overall Length ft in	‡ Length/Height Ratio	Thickness in	Cross-sectional Area of wall in^2	Load on Wall tons	Stress lbf/in^2	Max. Uplift in	Max. Lateral Load		Ratio Exp./Simple Theory
									Exp. lbf/in^2	Theory* lbf/in^2	
1	NONE	4'0"	0·5	8·4	403	-	-	-	10·5	-	-
2	NONE	4'0"	0·5	8·4	403	-	-	0·72	12·2	-	-
3	NONE	4'1"	0·5	4" 3" 4" CAVITY	196	14·4	165	0·11	2·3	2·3	1
4	NONE	4'1"	0·5	"	196	12	137	0·11	2·0	1·9	1·05
5	ONE	4'6"	0·52	"	216	16	166	0·09	3·8	2·3	1·7
6	ONE	4'6"	0·52	"	216	13·4	139	0·12	3·7	1·93	1·9
7	NONE	8'2"	1.0	4"	392	12·2	70	0·18	1·1	0·97	1·15
8	NONE	8'2"	1·0	4"	392	13·1	75	0·17	0·95	1·04	0·95
9	ONE	8'6"	1·0	4" 3" 4" CAVITY	408	16-18·5	88-102	0·15	2·2	1·22-1·41	1·8-1·6
10	ONE	8'6"	1·0	"	408	13·6	75	0·17	2·3	1·04	2·2
11	TWO	8'11"	1·0	"	428	13·3	70	0·15	3·0	0·97	3·1
12	TWO	8'11"	1·0	"	428	15	79	0·11	3·4	1·1	3·1
13	ONE	15'4"	1·9	"	736	23	70	0·14	0·8	0·97	0·85
14	ONE	15'6"	1·9	"	744	26·5	80	0·15	0·9	1·1	0·8
15	ONE	4'4"	0·5	"	209	13·5	145	0·11	3·5	2·02	1·75
16	ONE	6'2"	0·75	"	296	14	106	0·11	2·5	1·47	1·7
17	TWO	12'9"	1·5	"	612	15	55	0·12	1·7	0·76	2·2
18	TWO	15'0"	1·8	"	720	17	53	0·08	1·4	0·74	1·9

Notes: Height of all walls 8'0"; Theoretical Max. Uplift for 8·4" thick walls = 1·46"
4" " " = 0·33"

‡ Length without return

* Theory without return

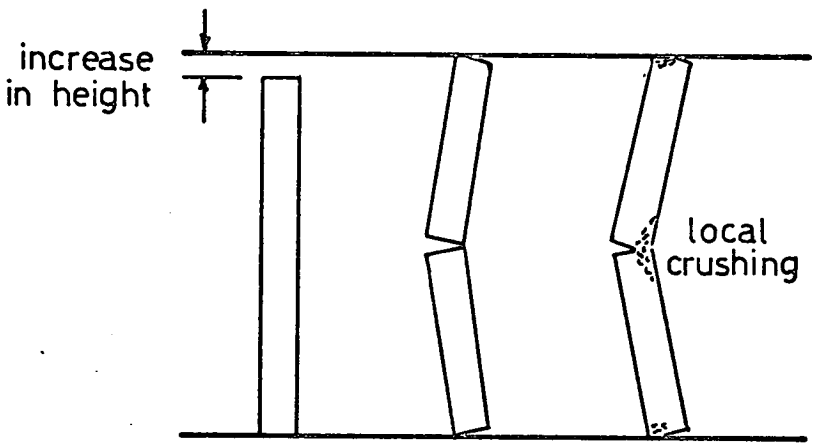
increase
in height
local
crushing

FIG. 1.1

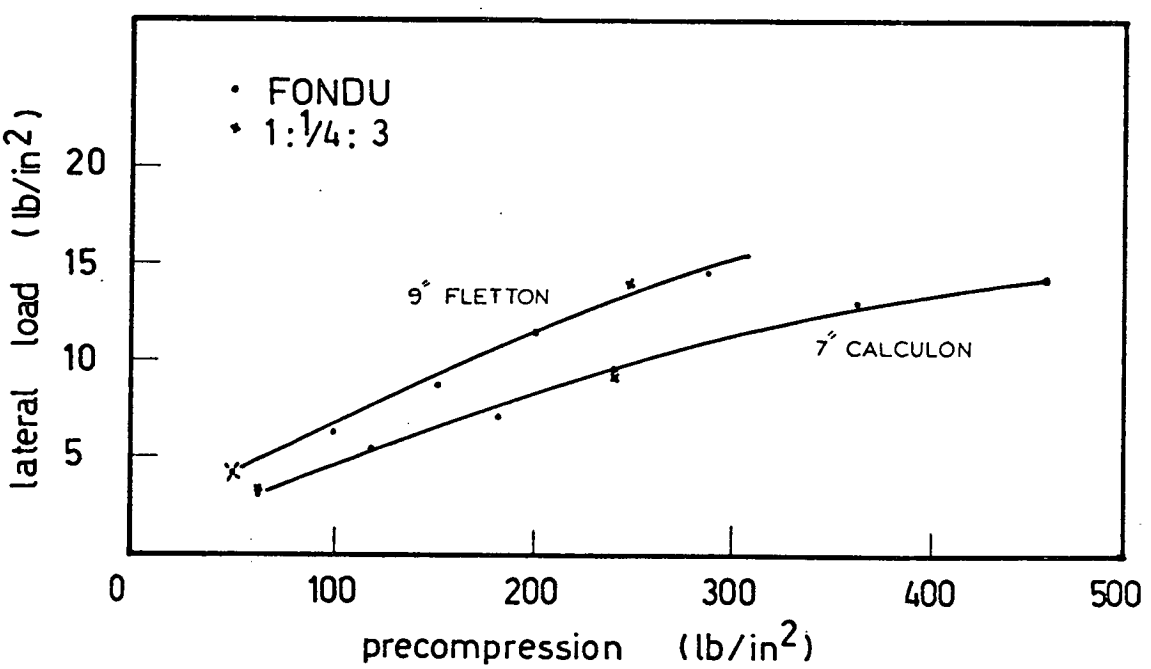
• FONDU
• 1:¼: 3
9" FLETTON
7" CALCULON
lateral load (lb/in²)
precompression (lb/in²)
0
100
200
300
400
500
5
10
15
20

FIG. 1.2

CHAPTER 2

YIELD-LINE METHOD

2.1 GENERAL

If it is assumed that failure occurs when a certain function of the stresses reaches a specific limiting value, then failure will generally start at a single point in the body under stress.

A brittle material will lose completely its capacity to take up the stresses at failure, and the stresses must therefore be borne by the adjoining sections; these are already stressed almost to the failure point, however, and therefore reach this point when the extra stress is imposed. The next adjoining sections then also lose their capacity to take up not only the extra stresses, but the original stresses as well, and sections adjoining these are stressed to the point of failure, and so on. In this way, the failure immediately spreads over an extensive area, which completely loses its capacity to bear stresses and in many cases the whole of the body's carrying capacity will then be exhausted.

It was observed in the majority of tests that failure took place along all yield lines simultaneously with no cracks being detected previously and in some cases accompanied with a sound. Therefore no sections or points in the walls had lost their ability to take up stresses before the others, and so all yield lines were assumed to have attained the maximum bending moment and yield stress at the same time. So it could be stated that this assumption would/

would be a direct result of two facts: the fact that the brickwork being a brittle material would lose its capacity to take up stresses once its yield stress is exceeded. The other fact is the experimental observation that failure of the walls was along all yield lines at the same time with no cracks appearing at earlier stages.

2.2 INTRODUCTION

Any theory of failure must be based on a hypothesis of failure which, in association with certain geometrical assumptions, lead to the determination of the state of stress. If the failure hypothesis says anything about the failure sections, certain patterns of fracture lines, such as yield lines in plastic bodies, are defined by it, and it will therefore be right to call these theories mathematical yield-line theories. Two cases of failure are possible: yield in three dimensions, and yield over certain failure surfaces or along yield lines for plane problems.

Development of the mathematical yield-line theory for plastic plates is new compared to elastic analysis. The condition of failure is that the maximum bending moment corresponds to the ultimate load. Studies show that the mathematical yield-line theory is just as complicated a tool as the mathematical theory of elasticity, and so the obvious course seems to be to formulate a simplified yield-line theory, in just the same way as the simplified theory of elasticity has been evolved side by side with the mathematical theory of elasticity. It is suitable, particularly for thin plates, to formulate a complete theory, and this was done by K.W. Johansen in a special section of his book "Yield-Line Theory"[18]. Some of the steps

treated/

treated are considered here:

Treatment of the purely geometrical features of plates; a study being made of the way in which the yield pattern depends upon the type of support used. This shows that the yield pattern depends upon the axes of rotation of the individual parts of the plate and the relation between the rotations.

Then the work equation - which serves to determine the ultimate moment, when the yield pattern is assumed to be known - is derived by the principle of virtual work. The yield pattern can also be determined through the work equation, however, it being shown that the correct yield pattern is that one of all the geometrically possible yield patterns which gives the biggest ultimate moment.

The work equation is of inestimable value for practical calculations, since the ultimate moment can be determined directly from an estimated yield pattern. With it an excellent approximate value can be obtained for the ultimate moment. For these calculations it is not even necessary to remember the formulae for the nodal forces; once one has learned how the work equation is formulated, one can solve most practical problems with this equation alone.

Also the nodal forces are defined and determined, i.e. a system of forces which are statically equivalent to the shear forces and torsional moments in the failure sections or yield lines. They are determined only with equilibrium equations and failure hypothesis. When the nodal forces have been determined in this way, the yield pattern and ultimate moment can be determined by means of the equilibrium equations for the various sections

of/

of the plate.

The theory is based on energy and kinematic principles and leads to an upper bound on the collapse load. That is the true collapse load is either equal to or less than that calculated by yield line analysis and therefore essentially unsafe predictions are made. The collapse load is determined by equating the external work done by applied loads to that dissipated internally along the yield lines of an assumed collapse mechanism. This leaves much choice to the analyst in selecting the collapse configuration, and although there are certain well defined procedures to aid in the proper selection, one is never sure that the lowest possible collapse load has been determined even after analysing many possible mechanism patterns.

The greatest drawback of the method is the impossibility of predicting what internal generalised stress states exist within the portions of the plate bounded by supports and yield lines.

A further limitation is the absence from the analysis of the effects of membrane action on the collapse load. This has lead to very conservative estimates of the collapse load for slabs in which in-plane forces are significant.

Even with its limitations, the yield line method has and continues to stimulate interest in the limit behaviour of slabs. Its greatest advantage is its simplicity of application and even though theoretically it leads to an upper bound on the collapse load, it seldom overestimates the experimental collapse load. This is primarily why it has been so well accepted.

For/

For the practical application of the yield line method excellent texts have been produced by Jones[19] and Wood and Jones[20].

2.3 FORMATION OF THE YIELD-LINE THEORY

The first stage of the ultimate load analysis of any plate is to predict the yield-line pattern of failure. The ultimate resistance moment along the yield lines can be calculated and by analysing the panel at the failure condition, the value of the load which is in equilibrium with these moments can be found.

As with most methods of analysis certain assumptions are made, which from tests are known to be reasonably true. Since the curvature along the yield lines is larger than the curvature of the parts between the yield lines, which are still behaving elastically, then it is quite reasonable to assume that the elements between the yield lines remain plane, and that all deformations take place in the yield lines. Since the intersections between inclined planes are straight lines, it follows that the yield lines, which are the intersections between the plane elements are also straight.

In order that the plate may deflect, the plane elements must rotate about certain axis; and it is a necessary condition of deformation that the yield line, or intersection line between two adjacent elements, passes through the intersection of the axes of rotation of these plane elements. Generally the axes of rotation will lie along the lines of support.

2.3.1 VIRTUAL WORK METHOD /

2.3.1 VIRTUAL WORK METHOD

Once a failure pattern has been postulated two methods of analysis are available in order to find the relation between the ultimate resistance moment in the plate and the ultimate load. One method has been called the equilibrium method. When using this method it is usually necessary to study the equilibrium of each of the elements into which the plate is divided by the yield lines. Equilibrium equations are obtained from each element, by equating internal and external moments and by resolving vertical forces, and to find the desired solution the resulting equations are solved simultaneously.

The second method of solution is the well-known principle of virtual work. Since the moments and the load are in equilibrium when the yield line pattern has formed, the slightest increment in load will cause the structure to deflect. When this increase in load is infinitesimal, the work done on the plate while the yield lines are rotating must be equal to the loss of work due to the load deflecting. Thus, if a point on the plate is given a virtual deflection, Z, displacements in the form of rotations compatible with this deflection take place along the yield lines. The internal work done on the plate will be the sum of the rotations in the yield lines multiplied by the resisting ultimate moments, while the external loss of work will be the sum of the loads multiplied by their respective deflections. When the internal and external work is equated, we have the relation between the ultimate resistance moments and the ultimate load.

If we assume that the yield pattern is known, the axes of rotation and the rotios/

ratios of the rotations will also be known. A set of simultaneous rotations is then used as virtual displacements. Since all that happens between the parts of a plate is a rotation, not a translation, the shear forces do not do any work in the plate as a whole. For a part of a plate which undergoes rotation, θ, the work done by the ultimate moments will be the produce of, θ, and the component in the direction of the axis of rotation of the resultant M_i, of the ultimate moments for the part of the plate in question. Expressed in vector language, it will be $(mi \cdot \theta)$ i.e. the scalar product of the vectors, M_i, and θ. If, M_i, has components, M_x, and M_y, corresponding to two axes at right-angles to each other, and θ, components θ_x, and θ_y, we get

$$(M_i \cdot \theta) = M_x \cdot \theta_x + M_y \theta_y \qquad \ldots\ldots(2.1)$$

The right-hand side of the equation is the sum of the work done by the component moments, since, M_x, does no work for the rotation θ_y, nor does M_y do any for θ_x.

In order to obtain an expression for the external work, we choose a convenient point in the plate and give it a virtual displacement, Z. The deflections of all parts of the plate can now be expressed in terms of Z and hence the loss of work due to this displacement of the load may be calculated from the equation:

$$\Sigma(W \cdot Z) = \Sigma \iint p \cdot Z \, dxdy \qquad \ldots\ldots(2.2)$$

The/

The principle of virtual work then gives

$$\Sigma(M_i.\theta) \quad + \Sigma\iint p.Z \, dxdy \quad = \quad 0 \qquad \ldots\ldots(2.3)$$

in which the summation extends over all the parts of the plate, since only then is the work done by the shear forces zero.

For the square plate shown in Fig. (2.1), the total internal work done in yield line, ac, is given by

$$\Sigma(M_i.\theta)_{ac} \quad = \quad \sqrt{2} \quad L.m \quad \frac{2\sqrt{2}}{L} \quad = \quad 4.m \qquad \ldots\ldots(2.4)$$

The work done in yield line, bd, is the same as in ac, hence

$$\Sigma(M_i.\theta) \quad = \quad 8.m \qquad \ldots\ldots(2.5)$$

The centre of gravity of each of the triangular elements deflects one-third hence

$$\Sigma(w.Z) \quad = \quad \tfrac{1}{3} pL^2 \qquad \ldots\ldots(2.6)$$

writing $\Sigma(M_i.\theta) \quad = \quad \Sigma(W.Z.)$ we find that

$$m \quad = \quad \frac{pL^2}{24} \qquad \ldots\ldots(2.7)$$

Expressions for other plates with varying dimensions and boundary conditions are given in detail in Appendix (A.1)

2.4 MOMENT/

2.4 MOMENT OF RESISTANCE OF BRICKWORK

While data on the transverse strength of brick masonry walls are not as extensive as those available on the compressive strength of walls and piers, transverse tests of specimens, constructed of materials representative of those used in construction, provide data from which it is possible to estimate the expected transverse strength of brick masonry walls if the type of workmanship and curing conditions are maintained the same.

The resistance of brick walls to lateral forces applied normal to the face of the wall depends primarily upon the bond strength of the mortar joints through which failures normally occur. Bond between mortar and brick is materially affected by mortar composition and flow, suction of the bricks when laid and the technique of forming the mortar joint. Obviously, incompletely filled joints, due to furrowing or partial filling, develop much less strength than completely filled joints.

The location of lateral supports has an important effect on the resistance of masonry walls to lateral forces. When the supports are spaced vertically and the bed joints are normal to the span, failure of walls subjected to transverse loading is usually at a bed joint and results from failure of the bond between mortar and masonry units. However, when lateral supports are spaced horizontally with bed joints parallel to the span, failure resulting from transverse/

transverse loading often occurs in the unit, as well as in the mortar joints.

Moment of resistance of the brick walls was determined by flexural tests of brick panels made from the same materials as the walls and kept in the same conditions. They were loaded using the third-point method as simply supported beams. The resulting moments of resistance from these tests were used in the yield-line formulae to estimate the lateral load capacity of the brick walls. These moments of resistance were obtained through the modulus of rupture and section modulus of the test panels.

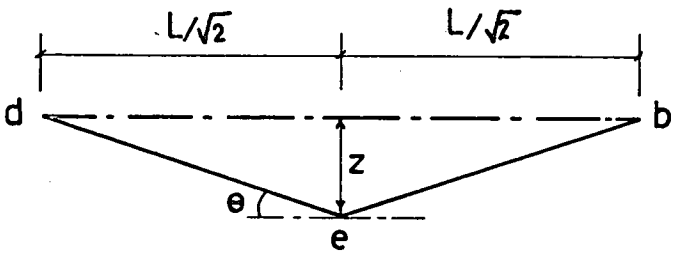

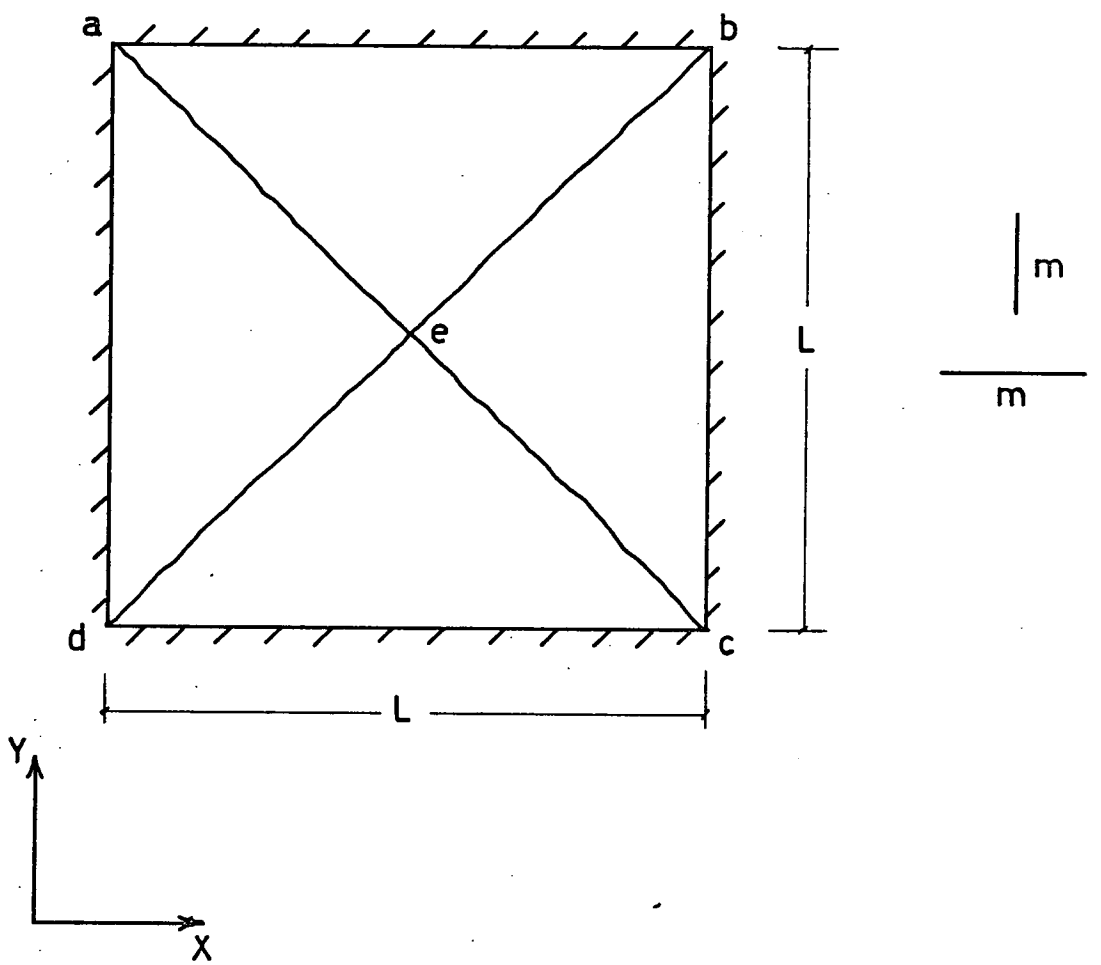

FIG. 2.1

CHAPTER 3

THE FINITE ELEMENT METHOD

3.1 INTRODUCTION

The behaviour of plates under transverse loading has received considerable attention since the first attempts of plate analysis. For well over a century many analysts developed and improved upon the theories of plate bending by elastic analysis. Westergaard[21] has summarised the historical development of plate theory and described the early tests to investigate the collapse behaviour of reinforced concrete slabs. A comprehensive work on the theory of plates and shells by Timoshenko and Woinowsky-Krieger[22] now forms the standard reference for most investigators.

In view of the complexity of plate bending problems it is hardly surprising that numerical methods are being applied to their solution[23]. One such method that has gained appreciable popularity in recent years is the finite element method. This method is a more physically obvious one than previous methods such as the finite difference. The structure is divided into a number of small elements connected at their nodal points, where displacement continuity, in the purely elastic case, and discontinuity, by introducing plastic rotations, together with equilibrium of nodal forces is established. The solution of the problem follows using standard structural procedures.

The/

The majority of finite element development effort has been devoted to systems involving one or two dimensional elements: frames, plane stress systems, plates, shells, and combinations of such components. However, the method is equally applicable for the solution of problems in the difficult, but important, field of three dimensional elasticity.

The dominant reason why the finite element method has been accepted so quickly and applied so extensively in engineering practice is its complete generality. The same basic theory, indeed, a single basic computer program, may be employed in the analysis of structural systems ranging from simple plane trusses to elastic solids of arbitrary geometry. To implement a general computer program of this type, it is necessary only to include in the element sub-routine library, programs for evaluating the stiffness of each type of element required in any given structural idealisation.

3.2 ORIGIN

The finite element method was developed in the U.S.A. in 1956[24]. Since its beginning in the aircraft industry, the method has become very popular in many other fields. Principal researchers into the development and application of finite elements have been Clough[25] in U.S.A. and Zienkiewicz[26, 27] in the U.K. Many other authors have contributed to the popularity of the method. Almost all available literature on the procedures and use of finite elements is reported in two texts[27, 28].

3.3 PHILOSOPHY/

3.3 PHILOSOPHY

The finite element method is essentially a generalisation to three dimensions of the classical structural analyses of skeletal structures. The basic concept of the method is not new. The structure when analysed is approximated by a finite number of elements interconnected at a finite number of nodes. The structure is a mathematical assembly of physical elements. There is no approximation required in the mathematical procedures, only in the choice and physical assembly of the elements. This is the basic difference between the finite element and finite difference methods. The finite difference method gives an approximate mathematical solution to the exact continuum whereas the finite element method gives an exact mathematical solution to an approximate continuum.

By dividing the continuum into elements of various sizes and shapes, all material properties of the original system can be retained within the individual elements. This capacity of the method to cope with arbitrary material properties is a principal attribute of the method. Of equal importance, is the facility to deal with cut-outs, irregularly shaped boundaries and any type of applied loading.

The basic steps in any finite elements analysis are the structural idealisation or subdivision into elements, the derivation of individual element properties and the assembly of elements into a physical structure. The number of different shaped elements should be kept to a minimum, so as to reduce the amount of initial comput - ation/

ation of element stiffness characteristics.

The element stiffness properties describe the nodal force displacement response of the element. The elements are assembled into a substitute structure using the well known matrix structural methods, satisfying equilibrium of nodal forces and compatibility of corresponding displacements.

Either of two approaches to matrix analysis, force or displacement approach, can be used in the finite element formulation. The development of the force method has been traced by Argyris[29]. A summary of both and a comparison have been made by Gallagher[30].

3.4 BENDING OF PLATES.

A full account of the finite element method as applied to plate bending problems has been given by Zienkiewicz[27]. In solutions presented the starting point has been based on the classical plate theory assumptions and subject to precisely the same limitations.

The state of deformation of a plate has been entirely described by the lateral displacement, w, of the middle plane of the plate, and continuity conditions between elements imposed not only on this quantity but on its derivatives. At each node, therefore, three conditions of equilibrium and continuity have been imposed.

Determination/

Determination of suitable shape functions giving complete slope continuity on the interfaces between various elements is much more complex. It is, however, relatively simple to obtain shape functions which, while preserving continuity of, w, may violate the slope continuity between elements, though naturally not at the nodes where continuity is imposed. These have been labelled by Zienkiewicz as non-conforming shape functions.

3.5 THE ELASTIC ELEMENT STIFFNESS MATRIX FOR RECTANGULAR ELEMENT

3.5.1 Shape Functions

At each node of a rectangular element of a plate coinciding with the x, y plane, displacements, U_n, are introduced. These have three components: a displacement in the Z direction, and two rotations about the x and y axes respectively. The nodal displacement vector can be defined as follows at a node i

$$U_i = \begin{vmatrix} w_i \\ \theta_{xi} \\ \theta_{yi} \end{vmatrix} = \begin{vmatrix} w_i \\ -\left(\frac{\partial w}{\partial y}\right)_i \\ \left(\frac{\partial w}{\partial x}\right) \end{vmatrix} \quad \ldots\ldots(3.1)$$

The element displacement will, as usual be given by the listing of the nodal displacements, now totalling four

U_i /

$$U = \begin{vmatrix} U_i \\ U_j \\ U_k \\ U_l \end{vmatrix} \qquad .....(3.2)$$

The shape functions must be defined in terms of U, i.e. in terms of twelve parameters

$$w = a_1+a_2x+a_3y+a_4x^2+a_5xy+a_6y^2+a_7x^3+a_8x^2y+a_9xy^2+a_{10}y^3+a_{11}x^3y+a_{12}xy^3 \qquad .....(3.3)$$

The constants a_1 to a_{12} can be evaluated by writing down the twelve simultaneous equations linking the values of w, and its slopes at the nodes when the coordinates take up their appropriate values. These have been defined in matrix form by

$$U = Ca \qquad .....(3.4)$$

where C is a twelve by twelve matrix depending on nodal coordinates and, a, is a vector of the twelve unknown constants.

3.5.2 Stress and Strain Matrices

These relationships depend upon the nodal displacements such that all internal generalised stresses can be determined at each node in the plate, once the displacements are known. These generalised stresses for isotropic plate bending are given by

M_x /...

$$\begin{vmatrix} M_x \\ M_y \\ M_{xy} \end{vmatrix} = \begin{vmatrix} D_1 & D_2 & 0 \\ D_2 & D_1 & 0 \\ 0 & 0 & D_3 \end{vmatrix} \begin{vmatrix} -w, xx \\ -w, yy \\ w, xy \end{vmatrix} \quad \ldots\ldots(3.5)$$

$$D_1 = \frac{Et^3}{12(1-\nu^2)}, \quad D_2 = \nu D_1, \quad D_3 = D_1(1-\nu)/2$$

In general matrix terms, if we state

$$K = \begin{vmatrix} -w, xx \\ -w, yy \\ w, xy \end{vmatrix} = Ba \qquad \ldots\ldots(3.6)$$

Then

$$M = DK = DBa$$
$$= DBC^{-1}U \qquad \ldots\ldots(3.7)$$

which is an expression of the generalised stresses in terms of the element nodal displacements.

3.5.3 Nodal Forces

The components of each nodal force must correspond to the nodal displacement components. These nodal forces are equivalent statically to the boundary stresses and distributed loads on the element. This is true if we impose an arbitrary virtual nodal displacement and equate the external and internal work done by the various forces and stresses during that displacement.

For/

For the element there are twelve force components given as

$$F = \begin{vmatrix} F_i \\ F_j \\ F_k \\ F_l \end{vmatrix} \qquad .....(3.8)$$

3.5.4 Stiffness Matrix

This is expressed by the relation between the nodal force and displacement and can be obtained by making use of the principle of virtual work. If virtual displacements of unit magnitudes are introduced at the element nodes in the directions of the nodal forces, the external work will be

$$W_e = \delta U \; F = I \; F = F \qquad .....(3.9)$$

where $\delta U = I$, the identity matrix.

The internal work will be the product of the generalised stresses and their corresponding strains,

$$W_i = \iint (\delta k)^T \; M \, dx \, dy \qquad .....(3.10)$$

But $\delta k = BC^{-1} \delta U = BC^{-1} I = BC^{-1}$ and $M = DBC^{-1}U$, hence

$$W_i = \iint (BC^{-1})^T DBC^{-1} U \, dx \; dy$$

Now/

Now, for $W_e = W_i$ we get an expression for the nodal force in terms of the nodal displacement

$$F = \left[(C^{-1})^T \iint B^T D B \, dx dy \, C^{-1} \right] U$$

and the element elastic stiffness matrix becomes

$$K = (C^{-1})^T \left[\iint B^T D B \, dx \, dy \right] C^{-1} \qquad \text{.....(3.11)}$$

3.6 ASSEMBLY OF THE ELEMENTS

After each element in the structure is considered and its stiffness matrix derived relative to the element coordinate axes, these elements are assembled into the final structure. Then equilibrium of nodal forces and compatibility of nodal displacements can be achieved. Since the elements are considered to be joined only at their corners, the bending and twisting internal generalised stresses are only approximations to the actual values.

With this displacement method of finite elements, the basic unknowns are the nodal displacements. Through proper force-displacement relationships the stiffness matrices for each element are derived. In addition, the elastic bending theory provides the necessary internal generalised stress relationships, and when combined with the assumed displacement function the internal generalised stress matrices are established. By applying the usual procedures of structural stiffness matrix methods, the plate continuum can be assembled/

assembled once the element stiffness matrices are known.

When the plate structure is assembled the resulting nodal force-displacement relationships form a set of simultaneous linear equations. Since the nodal forces must be in equilibrium with any applied loading, the matrix of nodal forces can be replaced by a matrix of applied loads. Solution of these equations produces the nodal displacements for the entire structure. From the displacements, the principal stresses can be obtained, and whenever these exceed the yield strength failure occurs. In order to trace the spread of failure from node to node the behaviour is assumed to be a linear function of the displacements, which is true in the elastic response.

Now it seems unnecessary to use elements where boundaries are on the lines of plastic action since the aim is to allow the plate to develop the failure pattern without imposing any initial conditions on the kinematics of the collapse mechanism or having to change the element shapes before a complete solution is obtained.

3.7 COMPUTER PROGRAM

The program GC21, which has been available in the Department was used. It is based on the finite elements method and proved to be very helpful in determining the load capacities and patterns of failure of the model brick walls.

3.7.1 Aim of the Program/

3.7.1 Aim of the Program

This program allows calculation of the displacements, internal moments and reactions of a plate of any shape in bending. The plate can be supported in any possible way and loaded by any external force.

The plate can be of constant or variable thickness. It can be simply supported or clamped on separate points or along segments of straight line. The values of the displacement at some points can also be imposed. The external forces are formed by distributed vertical loads, concentrated loads, or bending moments applied to the boundary. Several load cases can be processed in the same run.

The numerical calculation is performed by the finite element method. The curved boundary is treated as polygonal lines; the plate divided into triangular and rectangular elements; both types can be used together in a same computation.

3.7.2 Establishment of The Mesh

Let us consider a plate in the rectangular system (x,y); the boundary and lines of support of the plate are formed by segments of straight line. We set on this plate a mesh of trinagles and rectangles: the sides of the rectangles are parallel to the x and y axes. The mesh points or nodes are the vertices of the triangles or rectangles; the lines of mesh points are not necessarily rectilinear, but do not intersect./

intersect. A segment of straight line of support is also composed of sides of triangles and rectangles and its end points are mesh points. From a practical point of view, we use rectangles where possible. An element of the mesh is one of the triangles or rectangles. So, between two lines of mesh points, there is a line of elements formed by triangles and rectangles.

We number the lines of elements and the lines of mesh points consecutively; the line of elements number, n, lying between the lines of mesh points numbers, n and n + 1. In a line of mesh points we number the mesh points consecutively; similarly, in a line of elements we number the elements consecutively; the lines of mesh points and the lines of elements are run over in the same direction.

In the finite element method, the vertical displacement w(x,y) of the middle plane of the plate is expressed with the help of variables associated to each mesh point. In this program six variables are associated to each mesh point: w, w_x, w_y, w_{xx}, w_{yy}, w_{xy} which are the values of the displacement and its derivatives of first and second order i.e. $w_x = \frac{\partial w}{\partial x}$ ....etc. The displacement on a triangular or rectangular element is then represented by polynomials in x and y. At first, the program calculates the values of the displacement and of its derivatives at the mesh points; then the internal moments and the reactions are deducted from the displacements. Principal stresses are also obtained from displacements. The finite element is an approximate method; the precision of the results depends upon the number of elements. The approximate solution/

solution converges to the exact one when the dimensions of the elements tend to zero.

3.7.3 Input Data

The general line of the preparation of the data is indicated; a complete flow chart, 1, is given in Appendix A.2. The general data includes:

(a) A title

(b) Elasticity modulus and Poisson's coefficient

(c) Number of lines of mesh points.

(d) The numbers of the extreme mesh points of each line.

(e) A parameter which specifies the desired results.

(f) A parameter which allows to print the intermediate results if there is a mistake.

(g) Thickness of the plate

(h) Coordinates of the mesh points

(i) External loading, and

(j) Boundary conditions of the plate.

3.7.4 Output of the Results

The desired results are specified by the value of a parameter. The complete set of results include for each load case:

(a) The displacements and moments at mesh points:

w,/

w, w_x, w_y, M_x, M_y, M_{xy}

(b) The vertical reactions and the clamped moments are calculated for all the mesh points where boundary conditions are imposed. These reactions are always concentrated values at the mesh points. The sum of the vertical reactions allows to verify the equilibrium of the entire plate.

3.8 PRINCIPAL STRESSES

Another program has been written and used for the calculation of the principal stresses at all nodes from the displacements obtained from the original program. A general outline of this program is given in flow chart 2 in Appendix (A.2).

CHAPTER 4

ANALYSIS OF MODEL BRICK WALLS

4.1 USING THE YIELD-LINE THEORY

In Table (4.1) expressions, based on the Yield-Line Theory, of bending moments per unit length for panels of variable dimensions and support conditions are given.

When the panel is supported on all four sides it will tend to span in two directions and failure may be by tensile bond, shear bond or tension in the brick and perpend joints, depending on the panel dimensions, as shown in Figs. (4.1), (4.2), (4.3). In the case of a panel supported from three sides and free at the top, the upper part will tend to span in a horizontal direction between the supports. The lower part will tend to span in two directions and failure of the panel would be as indicated for the above case.

The bending moment (m) occurring in a panel can approximately be evaluated using beams made from the same materials, tested in flexure in addition to the moment of resistance developed by the restraining action of shear at the supports. The sum of these two moments of resistance gives only an approximate estimate of the actual bending moment in the panel, because it is clear that the test beams simulate the action at the vertical yield line which is believed to develop a lower moment of resistance than the inclined ones/

ones. Also the flexural strength is influenced by so many factors which could be variable from one point or part of the wall to another. The one-third point method used for testing beams gives a lower estimate of the flexural strength than does U.D.L.

4.1.1 Model Walls Under Lateral Loading

The analysis of panels by the yield-line theory is true at the instant of cracking at which the bending moment is a constant value at the lines of failure and the panel is about to fail.

For a panel supported from three sides the yeild-line theory gives the following expression for the ultimate moment per unit length

$$m = \frac{pL^2}{24}\left(\sqrt{3 + {}^1/_{4\alpha^2}} - {}^1/_{2\alpha}\right)^2 \qquad \ldots\ldots(4.1)$$

where p = lateral load, lb/in^2

L = Length of panel, in

α = height to length ratio

The above equation, (4.1), can be written in the form

$$m = pL^2/K \qquad \ldots\ldots(4.2)$$

where $K = 24 \Big/ \left(\sqrt{3 + {}^1/_{4\alpha^2}} - {}^1/_{2\alpha}\right)^2$

The variation of K with panel dimensions is shown in Fig. (6.4)

From test beams the portion of the resisting moment in the panel developed/

developed due to the flexural strength of the brickwork is given as

m_1 lb-in (Table 4.2),

and that due to the restraining action of friction between the panel and the supports is

$$m_2 = \mu \frac{p_o \alpha L . L . k_o}{\alpha L} \frac{t}{2}$$

$$= \frac{\mu p L^2 k}{L} \frac{t}{2} \quad \ldots\ldots(4.3)$$

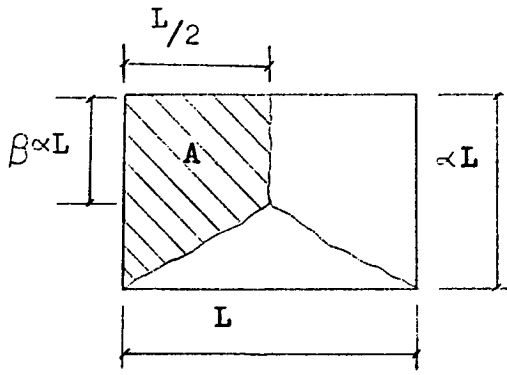

where t = thickness of panel

k = factor expressing the proportion of load on the vertical sides

μ = coefficient of friction between the brickwork and the steel supports

$$\beta = \frac{1}{2\alpha^2}\left(\sqrt{1/4 + 3\alpha^2} - 1/2\right)$$

$\alpha = 0.85$, $\alpha^2 = 0.72$

$\therefore \beta = 0.73$

$$A = \frac{\alpha L^2}{2}\left(\frac{0.73 + 1}{2}\right)$$

$$= 0.433\, \alpha L^2$$

$\therefore$ $\underline{k = 0.433}$

Variation of k with L/H is shown in Fig (4.4)

Now $m = m_1 + m_2$

$= p L^2/K$

where K is a factor depending on panel dimensions and support conditions.

Now we can write

$$\frac{pL^2}{K} = m_1 + \frac{\mu p L^2 k_o}{L} t/2$$

hence

$m_1/$

$$m_1 = pL^2 \left({}^1/K - \frac{\mu kt}{2L} \right) \qquad \text{.....(4.4)}$$

and therefore

$$p = \frac{m_1}{L^2 \left({}^1/K - \mu kt/2L \right)} \qquad \text{.....(4.5)}$$

which gives the estimated lateral pressure causing failure of the panel.

Now if we consider model wall A2 with L = 20 in:
αL = 17 in; t = 0·75 in; k = 0·433; $\alpha = {}^{17}/_{20} = 0{\cdot}85$; Using equation (4.1) we get K= 16, then

$$p = \frac{m_1}{20^2 \left({}^1/16 - 0{\cdot}7 \times 0{\cdot}433 \times 0{\cdot}75/40 \right)} = \frac{m_1}{22{\cdot}76}$$

From flexural tests on brickwork beams m_1 = 22·7 lb-in., hence

$$p = {}^{22{\cdot}7}/_{22{\cdot}76}$$

$$= \underline{\underline{0{\cdot}99}} \text{ lb/in}^2$$

Similar treatment has been given to all half-brick model walls and a summary of the results is listed in Table (4.3) together with the experimental results and dimensions.

One brick model walls were of variable dimensions as well, and were tested with either three or four supports, with or without vertical precompression. For those model walls which were supported on three sides/

sides the same above procedure of analysis was used. Again, in case of model walls supported from four sides the same method was used except that the expression for the bending moment (m) will be different from that given by equation (4.1). For the square model panels designated by (E), m will be equal to

$$m = pL^2/24 \qquad \text{.....(4.6)}$$

and so K = 24. Results of these square panels are given in Table (4.4). The rectangular ones designated by (G) and supported from all four sides have

$$m = \frac{p(\alpha L)^2}{24}\left(\sqrt{3+\alpha^2} - \alpha\right)^2 \qquad \text{.....(4.7)}$$

and hence $K = 24/\alpha 2 \left(\sqrt{3+\alpha^2} - \alpha\right)^2$

Rectangular model walls G when supported from three sides assume the second mode of failure shown in Appendix (A.1) where the value of the bending moment is given by

$$m = \frac{p(\alpha L)^2}{24}\left(\sqrt{4 + 9/\alpha^2} - 2\right) \qquad \text{.....(4.8)}$$

and $K = 24/\alpha^2 \left(\sqrt{4 + 9/\alpha^2} - 2\right)$

Results of the rectangular panels can be found in Table (4.5)

4.1.2 Model Walls Under Combined Axial And Lateral Loadings

The treatment of model walls under combined loading is more or less the same as for walls under lateral load, only the necessary adjustment is/

is made to take into account the effect of the precompression in increasing the estimated value of the flexural moment of resistance (m) of the walls.

These model walls are expected to resist higher lateral pressures as the precompression is assumed to act like prestressing under certain conditions, and in this way the modulus of rupture of the precompressed walls exceeds the actual modulus of rupture of the brickwork.

The stress diagram at failure of the precompressed walls will be as shown in the figure below which can be explained as follows:

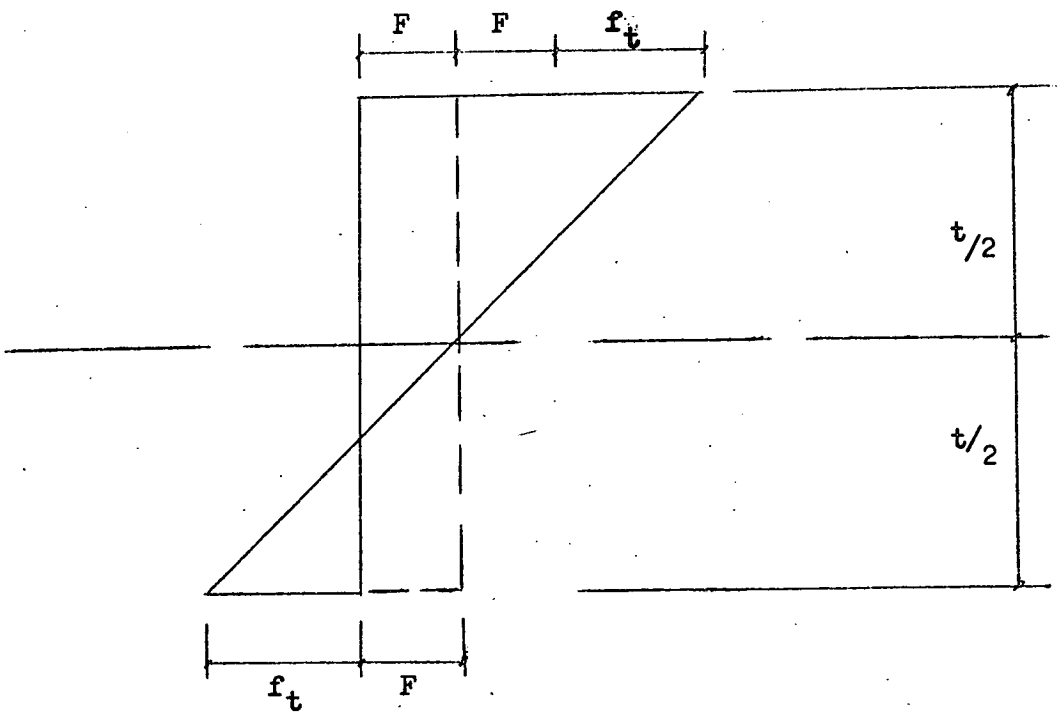

On loading laterally a precompressed wall, the action of the lateral load tends to relief the tension zone from the effect of the precompression (F lb/in^2) and starts to build up additional precompression on the compression zone which initially had the same F lb/in^2 precompression as the tension zone. So when all precompression is released from the tension zone and it starts to mobilize its original tensile strength (f_t lb/in^2), made up of the modulus of rupture of brickwork, to resist increasing lateral load there already exists at the compression zone twice as much compressive stress as the applied axial precompression.

Now the moment of resistance of the precompressed walls can be estimated with the help of the stress diagram above

$$m = (f_t + F)\frac{bt^2}{6}$$

where f_t = modulus of rupture of brickwork,
F = axial precompression on wall,
t = wall thickness

For walls under axial precompression F = 50 lb/in^2 and a modulus of rupture of f_t = 137 lb/in^2 and thickness t = 1·5 in., the moment of resistance developed is

$$m = \frac{(137 + 50) \times 1{\cdot}5^2}{6}$$

$$= \underline{\underline{70}} \text{ in-lb}$$

On/

On the other hand the bending capacity of walls under axial precompression F = 100 lb/in^2 and having the same modulus of rupture and thickness as above, can be estimated as follows

$$m = \frac{(137 + 100) \times 1.5^2}{6}$$

$$= \underline{89} \text{ in-lb}$$

Now these resistance moments are used together with the formulae derived from The Yield-Line Theory, presented in Table (4.1), to estimate the lateral load capacities of axially precompressed walls. Results of these treatments are given in Tables (4.4), (4.5) and (4.6).

4.2 ANALYSIS OF THE MODEL BRICK WALLS BY THE FINITE ELEMENT METHOD

4.2.1 Outline and Analytical Procedure

The situation being investigated is that of a panel loaded laterally by a uniformly distributed load. From the tests carried out it was observed that model walls free from precompression failed with no previous signs of cracking. Now, knowing that brickwork is a brittle material and so loses its bending strength completely once it is exceeded, it could be assumed that bending moments were maintained equal at all critical sections until failure. So the same stress value should prevail throughout sections of failure, and indeed this is the case for square panels supported from their all four edges/

edges and hence analysis was carried out assuming as a failure criterion the existence at the nodes near the corners of the panel of tensile principal stresses which are in excess of the modulus of rupture of brickwork. This stress field at failure can be determined directly and the pattern predicted from a plot of contours representing the tensile principal stresses.

Analysis of the model walls has been carried out using the computer program, based on the finite element method, mentioned earlier (3.7). The walls were divided into a reasonable number of elements and values of the elastic modulus, Poisson's ratio, thickness and dimensions inserted, and boundary conditions imposed. The load which will satisfy the failure criterion, i.e. cause nodes near the corners of panels to have tensile principal stresses which are greater than the modulus of rupture of brickwork, was also inserted. The value of this load was estimated by first applying a small load to the panel in question, then studying the resultant stress field at the nodes and finally scaling the applied small load by multiplying it by the ratio of modulus of rupture of the brickwork and the tensile principal stress due to the small load at the node nearest to the corner of the plate. This is the failure load of the plate and produces tensile principal stresses the contours of which when drawn verify the yield line pattern of failure of the walls.

4.2.2 Results

(i) Half brick model walls

A/

A few walls of this series were anslysed, and failure pressures, deflections and patterns of failure obtained. These are given in Figs. (4.5), (4.6), (4.7) and (4.8). Table (4.7) presents pressures and deflections at failure.

(ii) One-brick model walls

Selected walls from the three series of one-brick model walls were analysed. Failure loads, deflection and patterns of failure are presented in Figs. (4.9), (4.10), (4.11), (4.12) and (4.13), and Table (4.8).

TABLE 4.1

Bending Moments Expressions for Simply Supported Panels Developed Using the Yield-Line Method.

Support conditions	Ratio of Panel Dimensions 'L/H'					
	0·5	0·75	1·0	1·25	1·5	2·0
Three sides supported	$\frac{WL}{11}$	$\frac{WL}{12}$	$\frac{WL}{14}$	$\frac{WL}{16}$	$\frac{WL}{19}$	$\frac{WL}{22}$
Four sides supported	$\frac{WL}{14}$	$\frac{WL}{19}$	$\frac{WL}{24}$	$\frac{WL}{30}$	$\frac{WL}{38}$	$\frac{WL}{57}$

TABLE 4.2

Model Wall No	Modulus of Rupture		Section Modulus $in^3 \times 10^{-2}$	Moment of Resistance in-lb
	Average lb/in^2	Coefficient of variation, %		
A1	180	11	9·37	16·9
A2	242	11	9·37	22·7
A3	177	35	9·37	16·6
B1	192	29	9·37	18·0
B2	208	18	9·37	19·5
C1	238	8	9·37	22·3
C2	214	13	9·37	20·0
C3	209	12	9·37	19·6
E	137	11	37·5	51·4
G, H	133	25	37·5	50·0

TABLE 4.3

Half-Brick Model Walls-Three Sides supported

Model Wall No	A1	A2	A3	B1	B2	C1	C2	C3
Dimensions (in)	20x17x$\frac{3}{4}$	"	"	12x16x$\frac{3}{4}$	"	24x16x$\frac{3}{4}$	"	"
Experimental failure load 'lb/in^2'	1·45	1·0	0·65	1·8	2·1	0·9	0·8	0·67
Load using Yield-Line Theory 'lb/in^2'	0·74	0·99	0·73	1·67	1·81	0·72	0·65	0·63

TABLE 4.4

One-Brick Model Walls 16" x 16" x 1½"

Precompression lb/in²	0				50		100		50		100	
support conditions	Three sides supported		Four sides supported		Three sides supported		Three sides supported		Four sides supported		Four sides supported	
Wall No	E1	E2	E3	E4	E5	E6	E7	E8	E9	E10	E11	E12
Experimental failure load lb/in²	2·6	2·9	5·25	5·15	4·7	4·2	5·9	5·7	7·2	8·4	9·2	10·7
Load using Yield-Line Theory lb/in²	3·1		5·4		4·35		5·9		7·45		10·0	

TABLE 4.5

One-Brick Model Walls 32" x 16" x 1½"

Precompression lb/in^2	0			50		100		
Support conditions	3 sides supported	4 sides supported		3 sides supported	4 sides supported	3 sides supported		4 sides supported
Wall No	G1	G3	G4	G5	G10	G7	G8	G12
Experimental failure load, lb/in^2	1·10	2·6	2·9	1·65	4·0	2·10	3·35	4·85
Load using Yield-Line theory lb/in^2	1·10	2·8	2·8	1·71	4·4	2·3	2·3	6·0

TABLE 4.6

One-Brick Model Walls 8" x 16" x 1½"

Precompression lb/in^2	0				50		100	
Boundary conditions	3 sides supported		4 sides supported		3 sides supported	4 sides supported	3 sides supported	4 sides supported
Model Wall No	H1	H2	H3	H4	H6	H9	H7	H12
Experimental failure load, lb/in^2	6·8	8·1	9·7	12·5	11·8	15·8	14·9	21
Load using Yield-Line Theory lb/in^2	8·6		11·0		13·7	17·7	18·6	24·0

TABLE 4·7

Half-Brick Model Walls Results of Finite Element Method

Model Wall No.	A2	A3	B1	C3
Failure Load (lb/in^2)	1·10	0·79	2·1	0·66
Mid-Top Deflection (in x 10^{-3})	48·9	35·2	31·2	50·9
Central Deflection (in x 10^{-3})	30·9	22·3	23·8	31·2

TABLE 4·8

One-Brick Model Walls Results of Finite Element Method

Model Wall No	E1	E3	G1	H1	H3
Failure Load (Lb/in^2)	3·25	5·10	1·20	10	15
Mid-Top Deflection (in x 10^{-3})	85·6	-	26·8	19·5	-
Central Deflection (in x 10^{-3})	58·8	47·2	15·1	16·4	21·6

FIG. 4.1 BOND FAILURE WITH LOAD NORMAL TO FACE

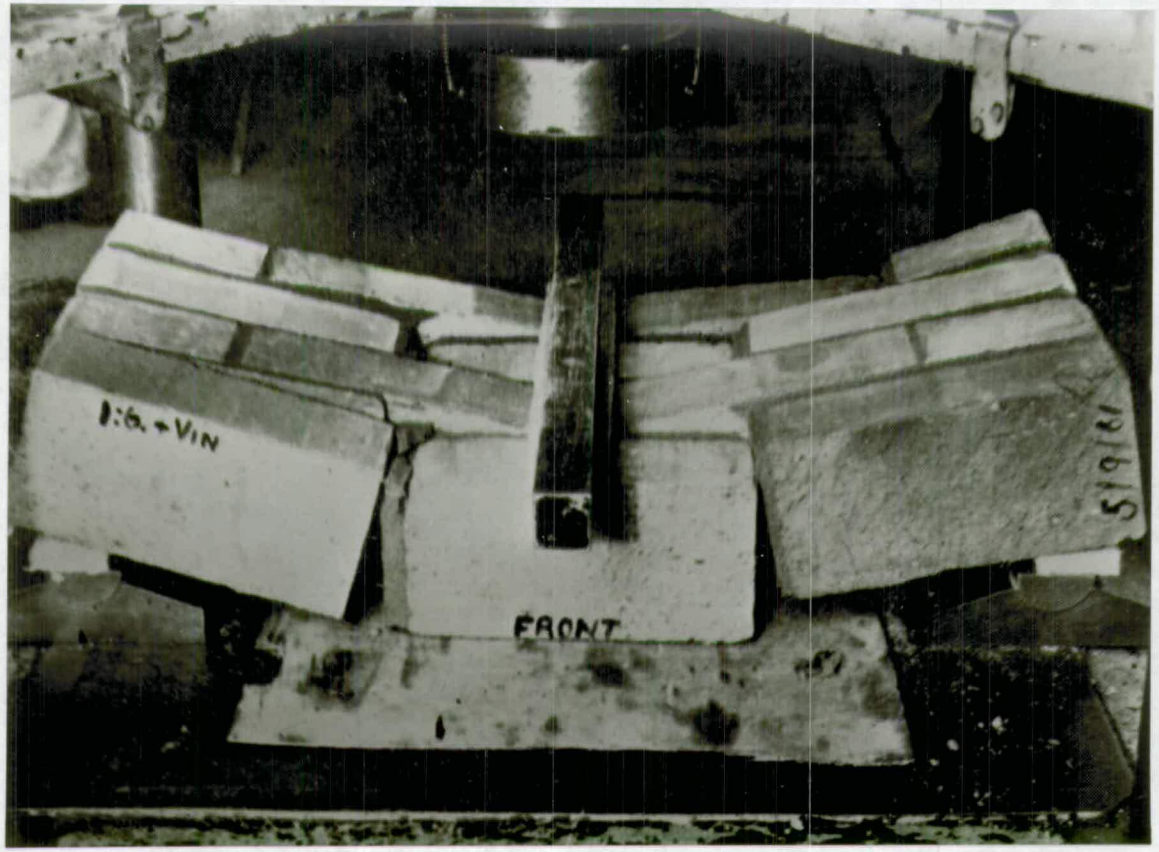

FIG. 4.2 FAILURE OF BOND

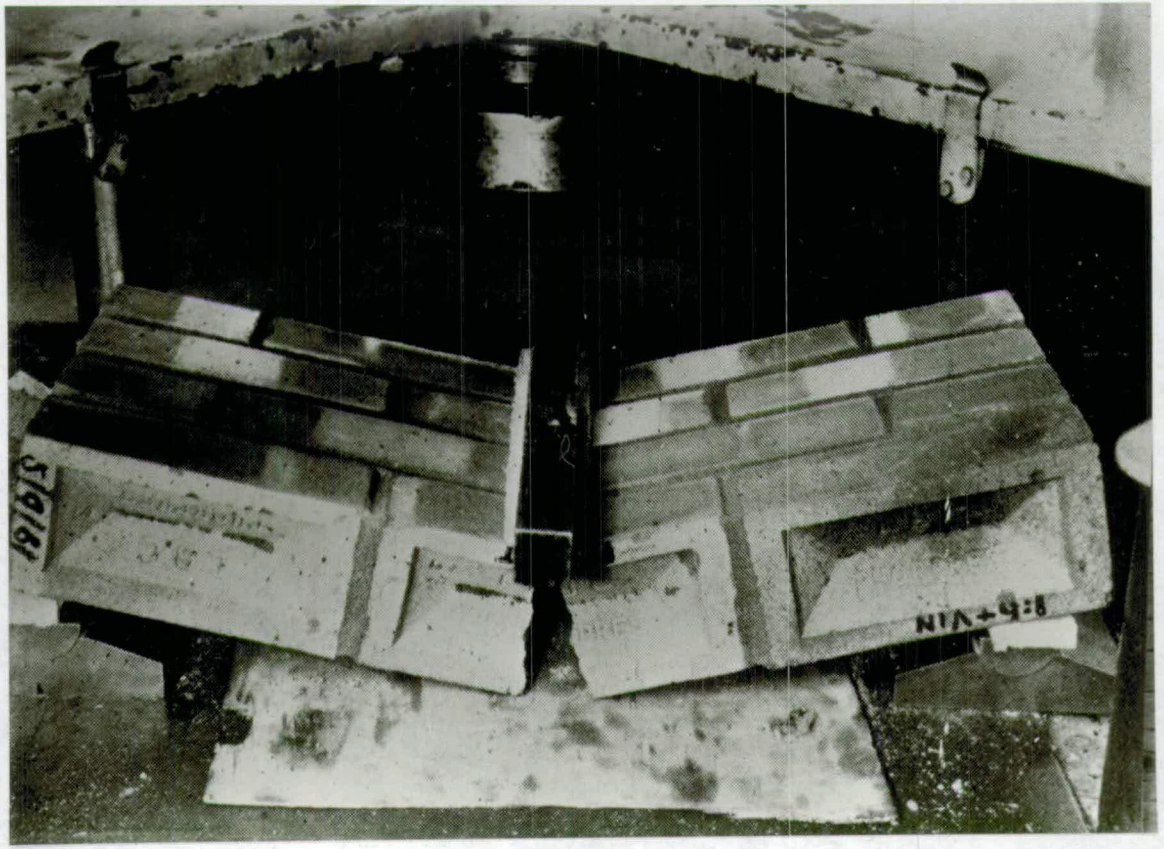

FIG. 4.3 FAILURE OF BRICK IN TENSION

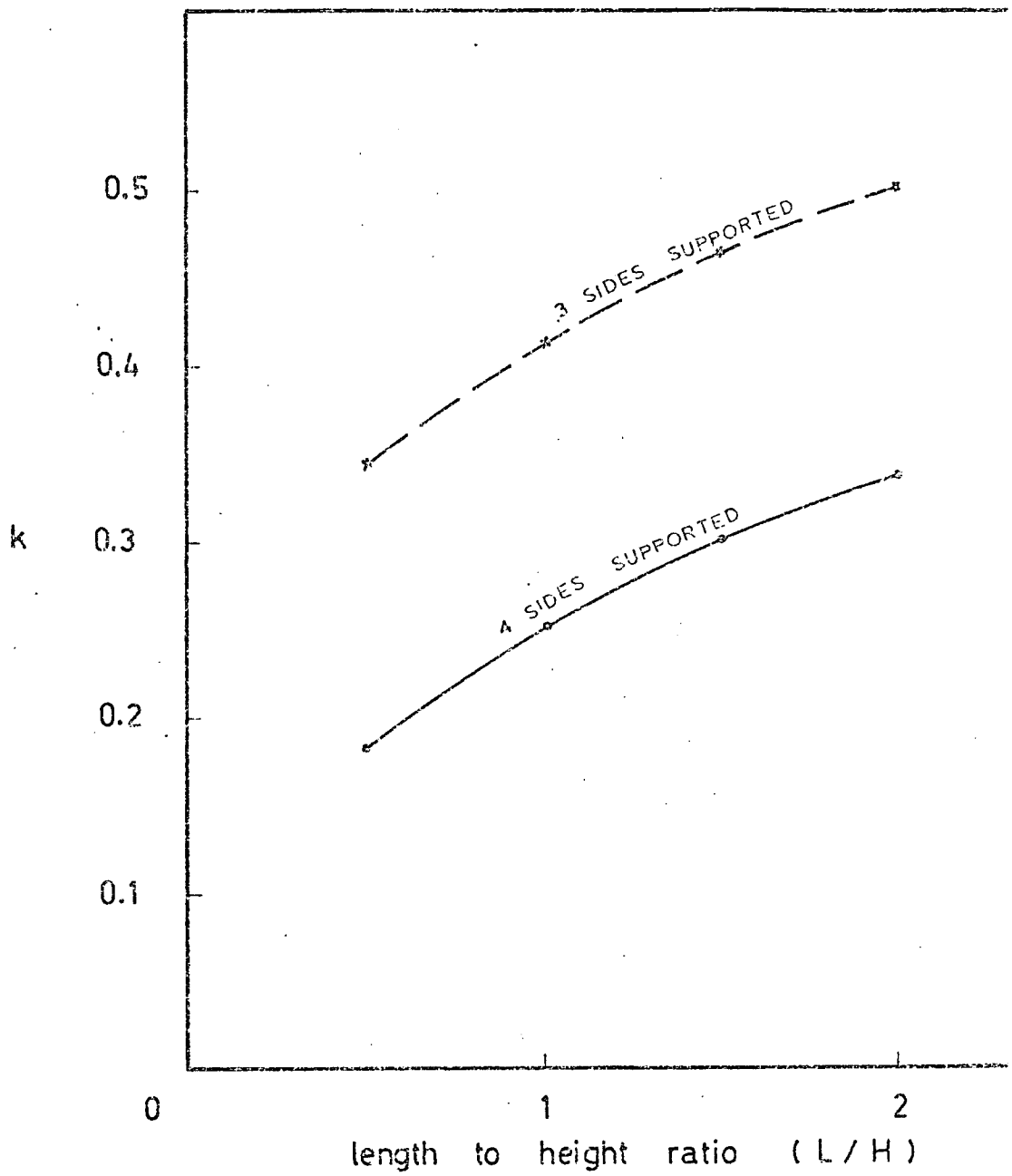
0.5
0.4
0.3
0.2
0.1
k
0
1
2
3 SIDES SUPPORTED
4 SIDES SUPPORTED
length to height ratio (L / H)

FIG. 4.4

model wall A2

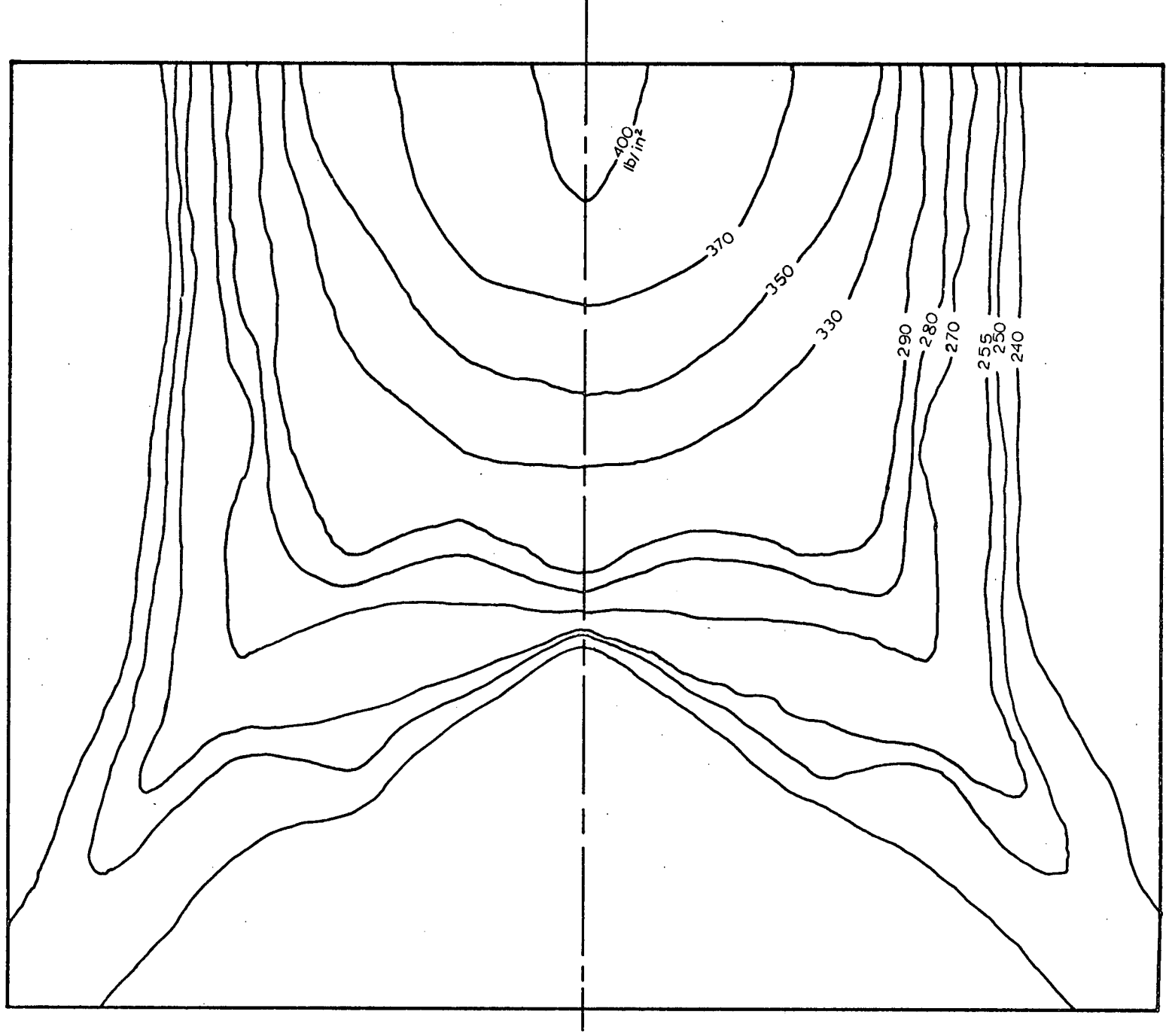

FIG. 4.5: CONTOURS OF TENSILE PRINCIPAL STRESSES

model wall A3

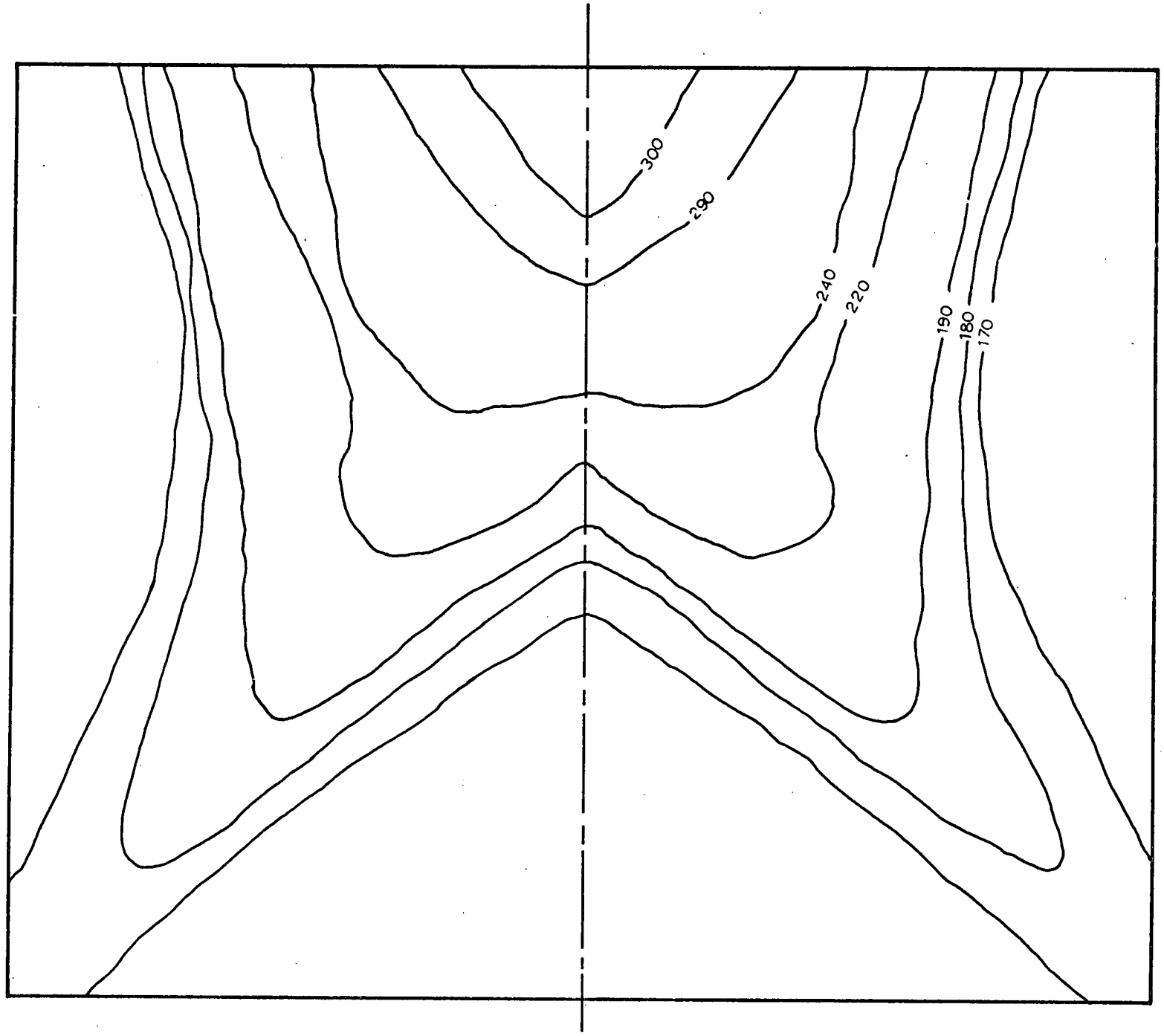

FIG 4.6: CONTOURS OF TENSILE PRINCIPAL STRESSES

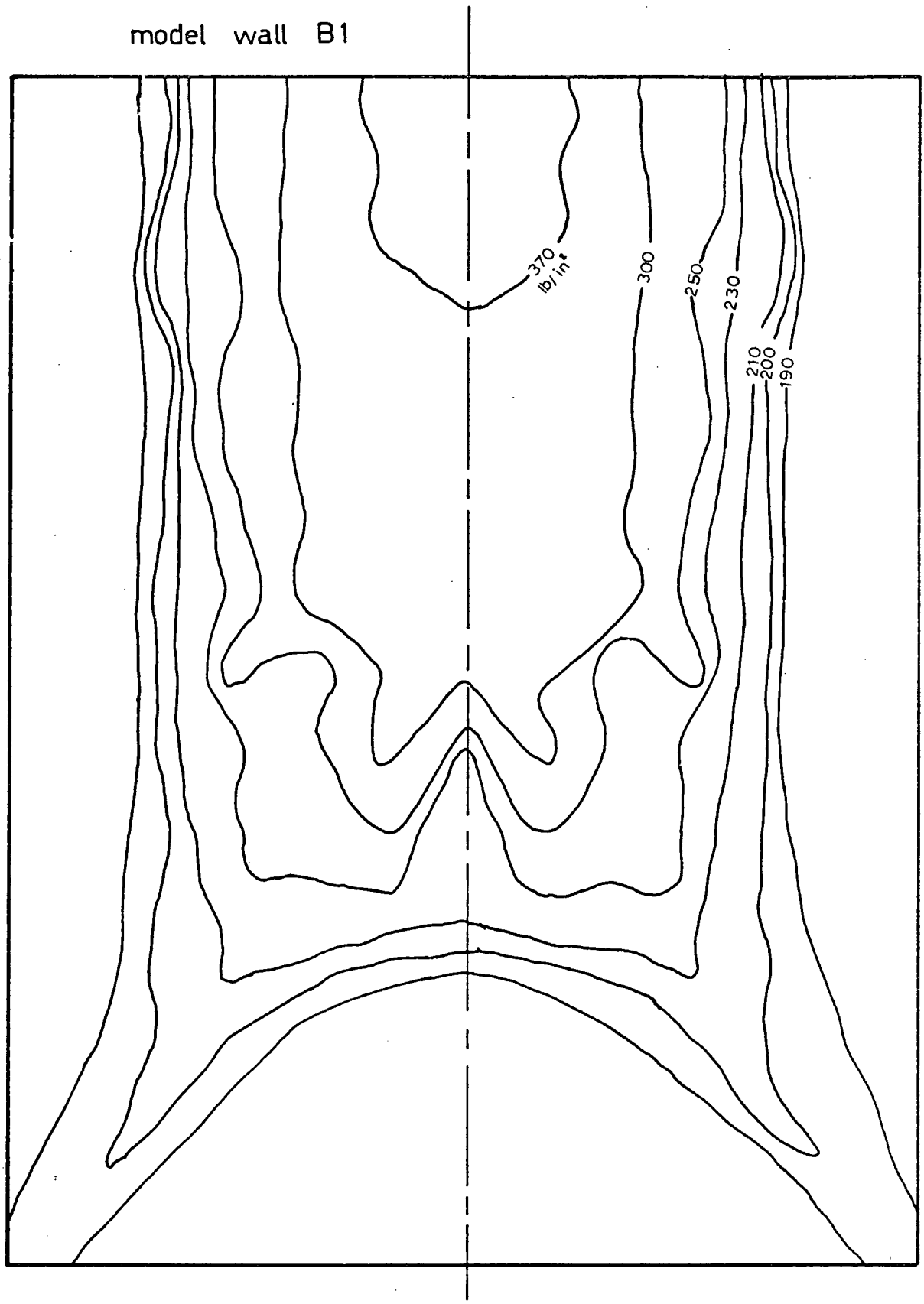

FIG. 4.7 : CONTOURS OF TENSILE PRINCIPAL STRESSES

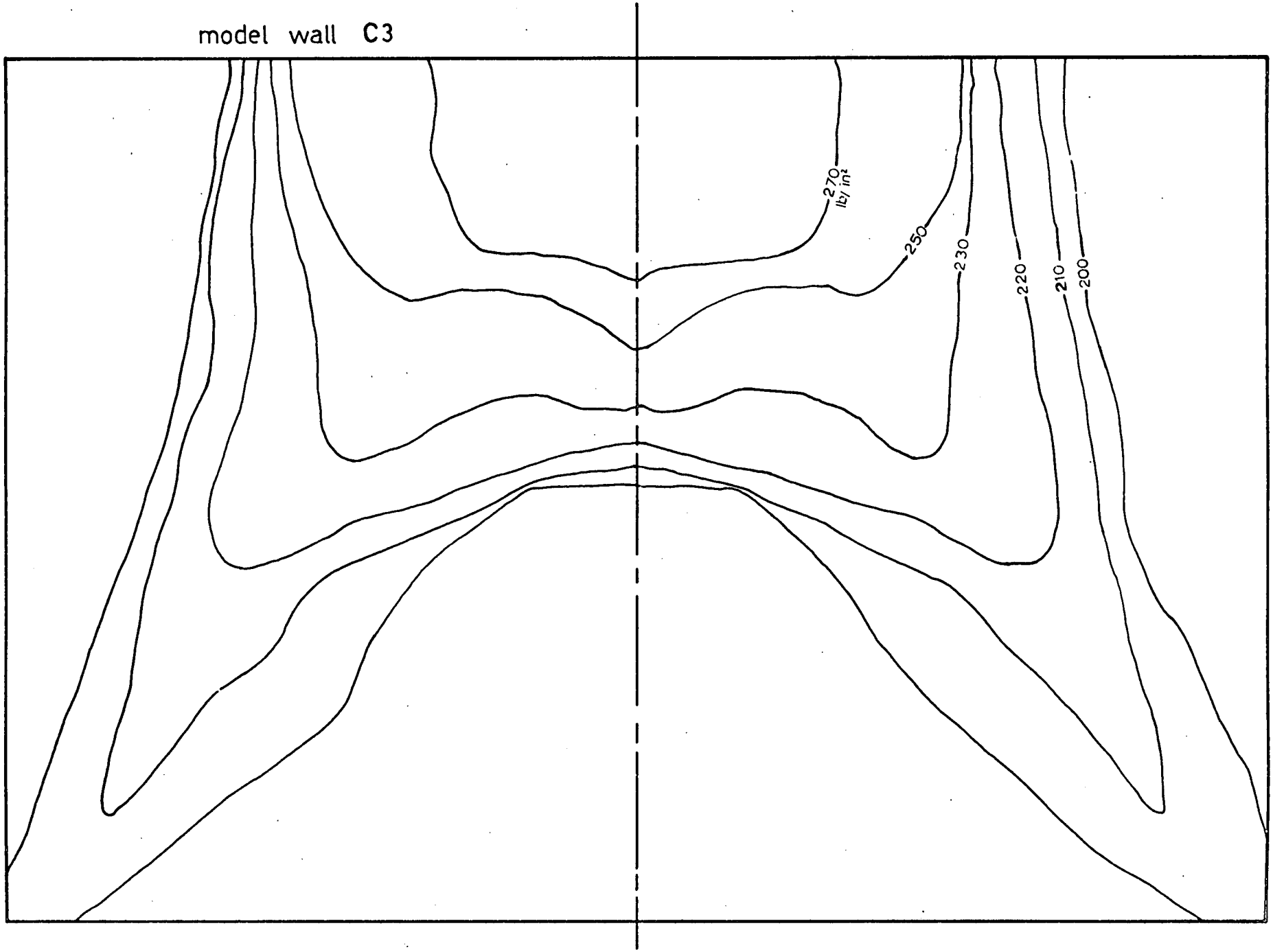

FIG 4.8· CONTOURS OF PRINCIPAL TENSILE STRESSES

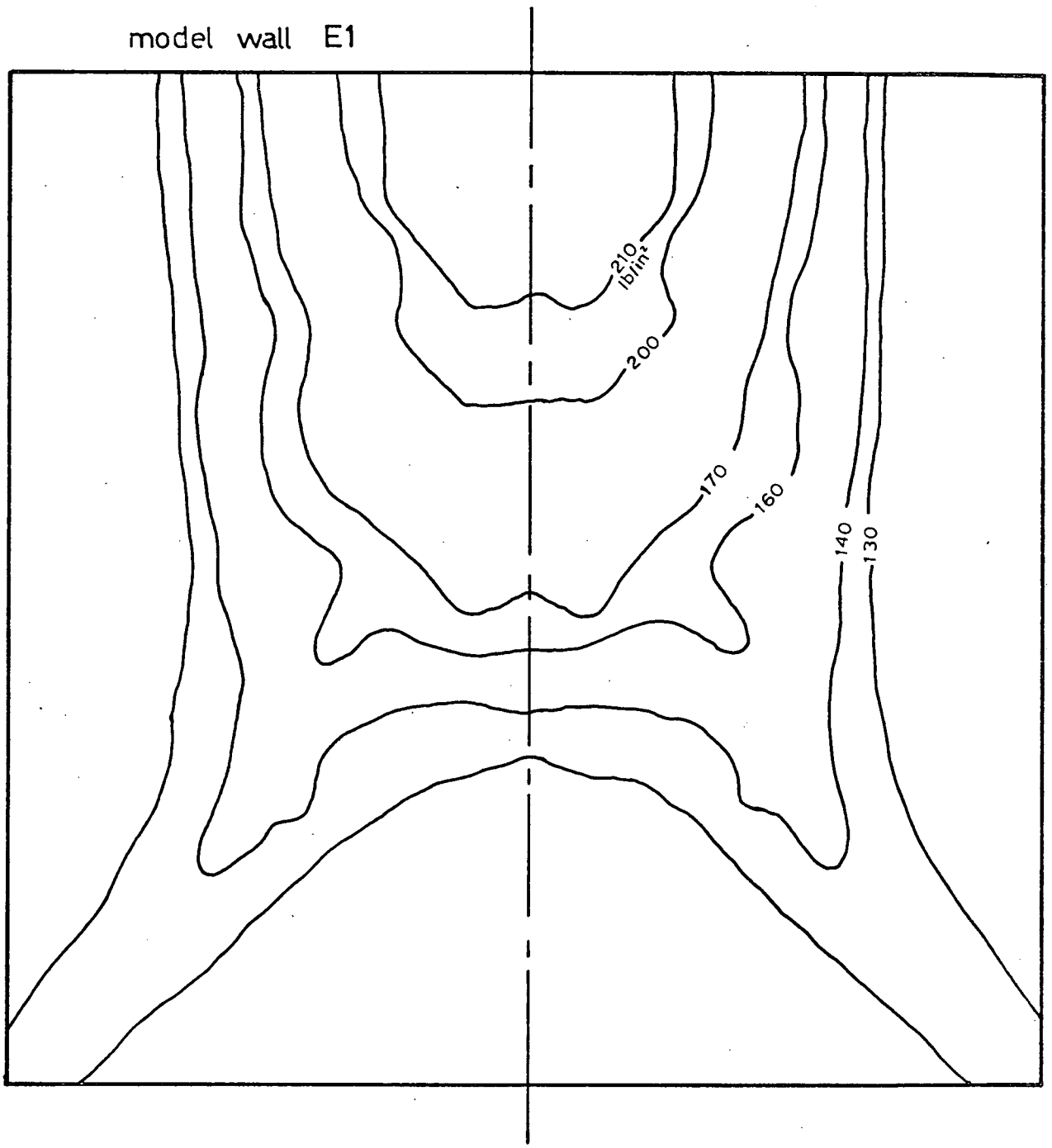

FIG 4.9: CONTOURS OF TENSILE PRINCIPAL STESSES

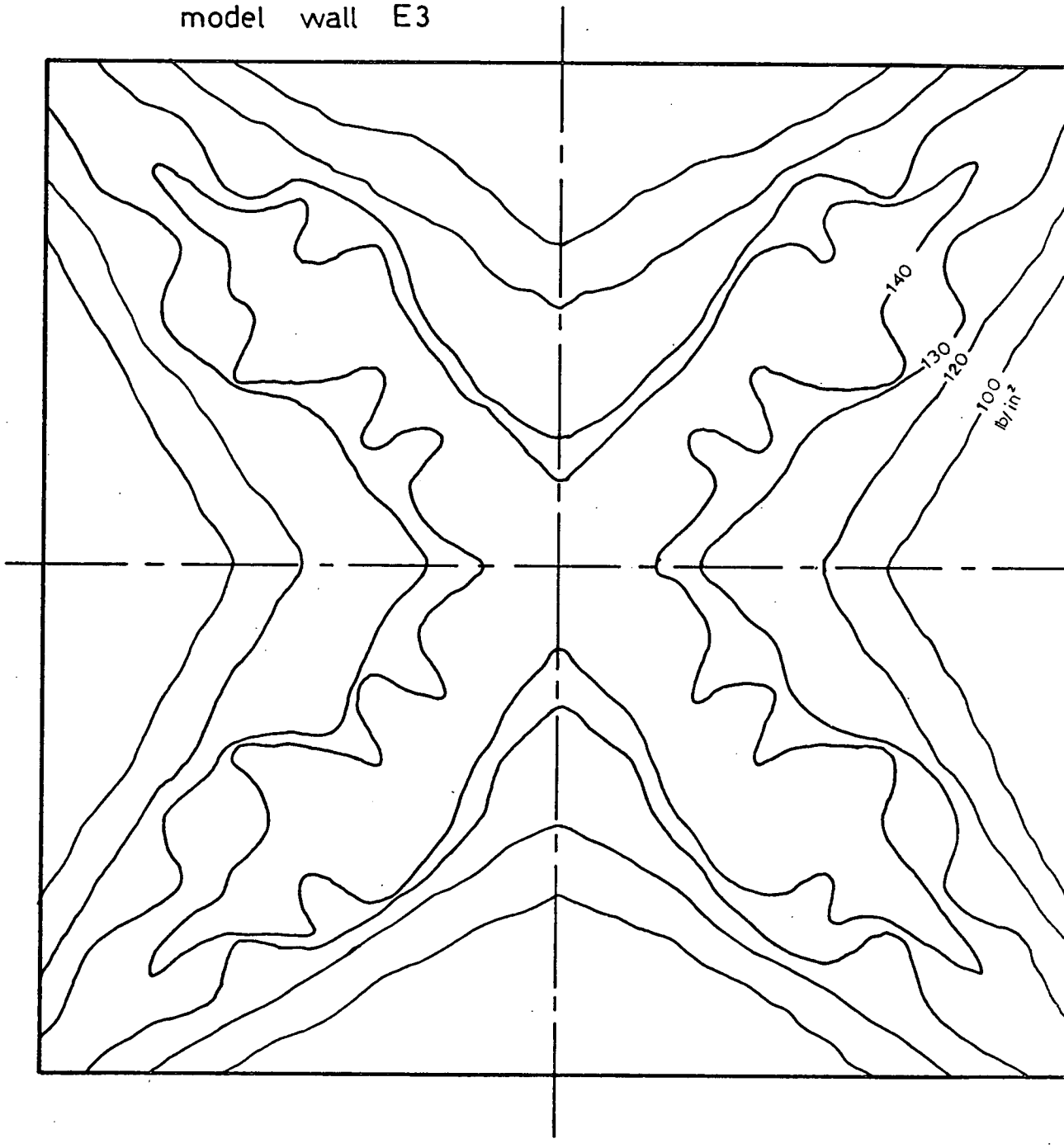

FIG. 4.10: CONTOURS OF TENSILE PRINCIPAL STRESSES

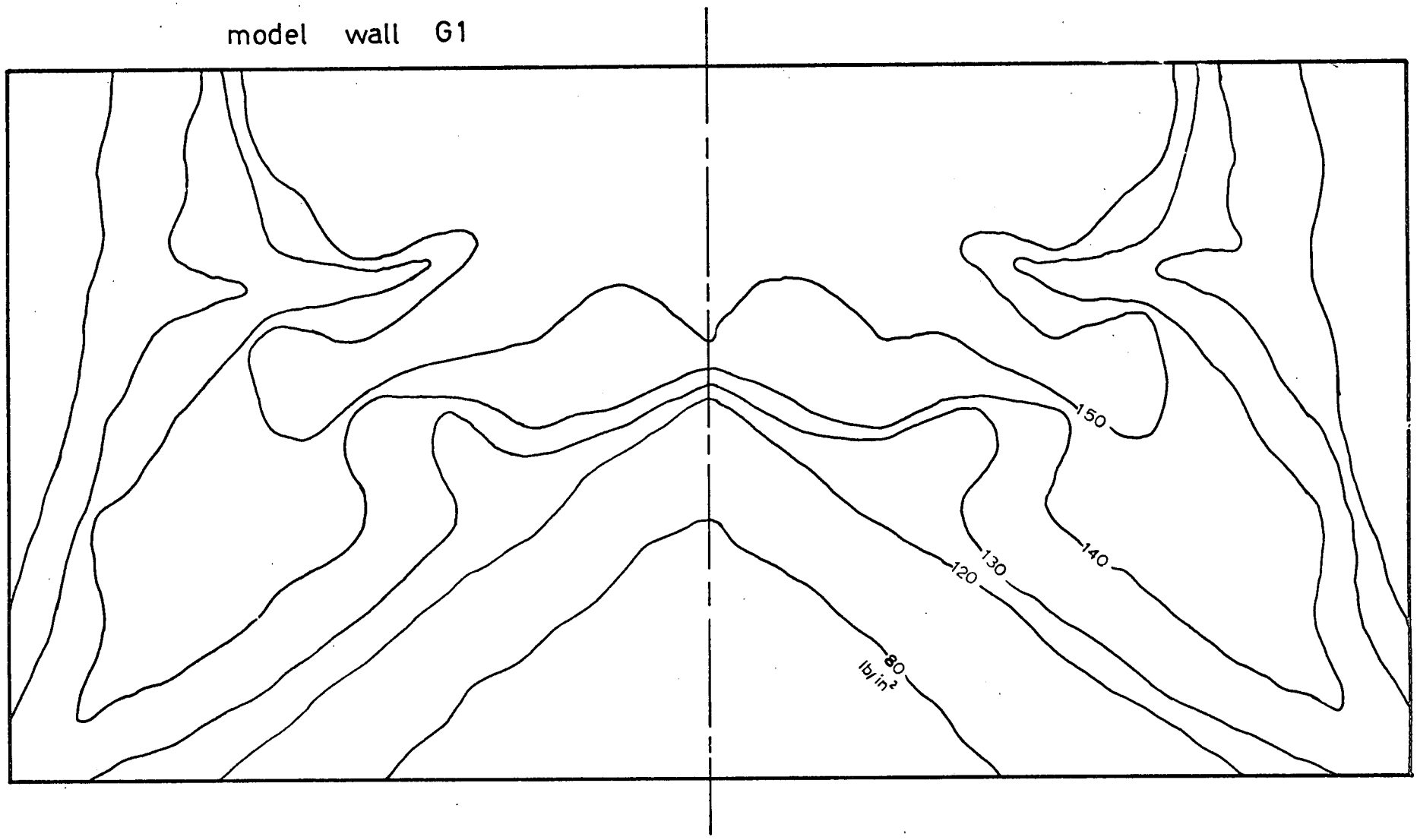

FIG. 4.11: CONTOURS OF TENSILE PRINCIPAL STRESSES

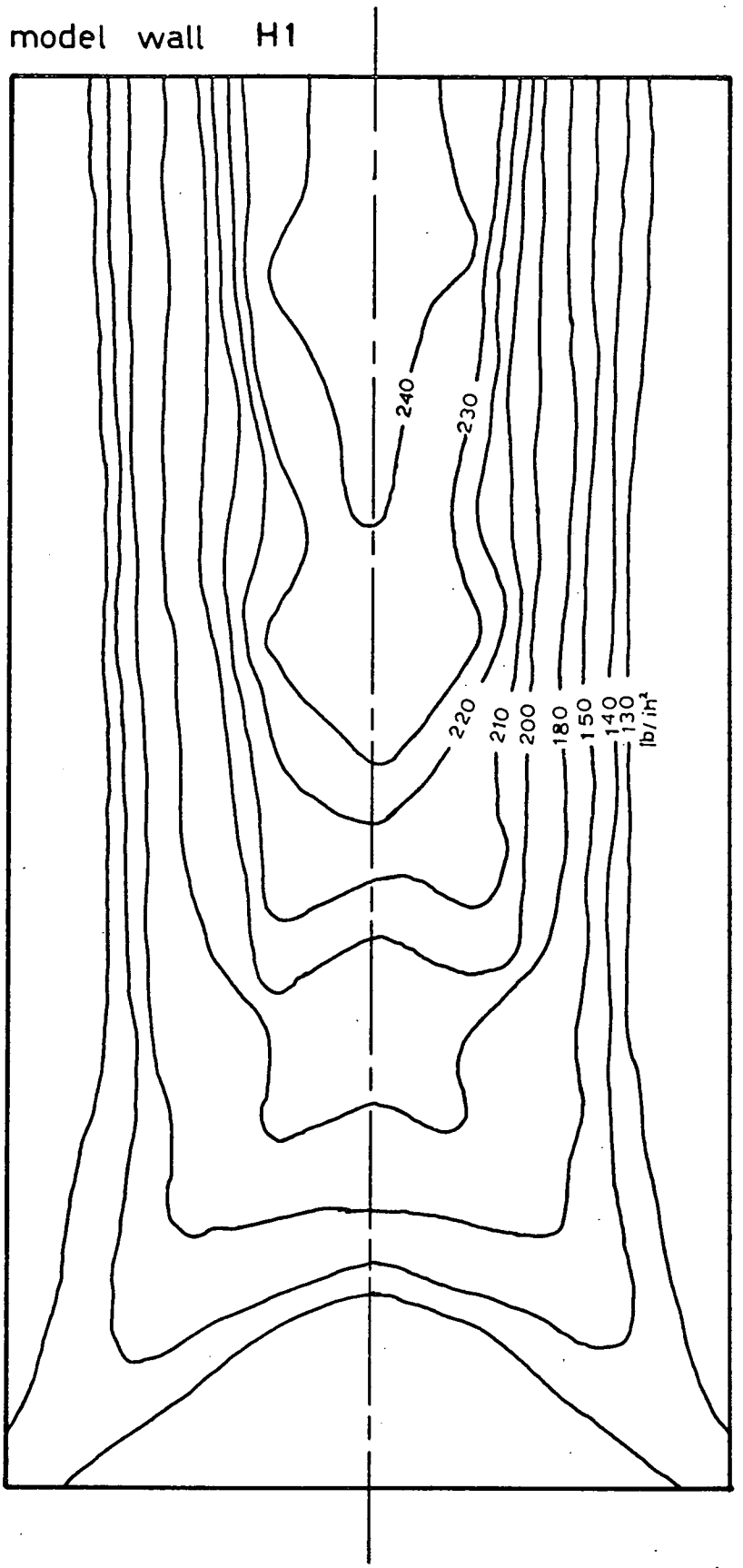

FIG 4.12: CONTOURS OF TENSILE PRINCIPAL STRESSES

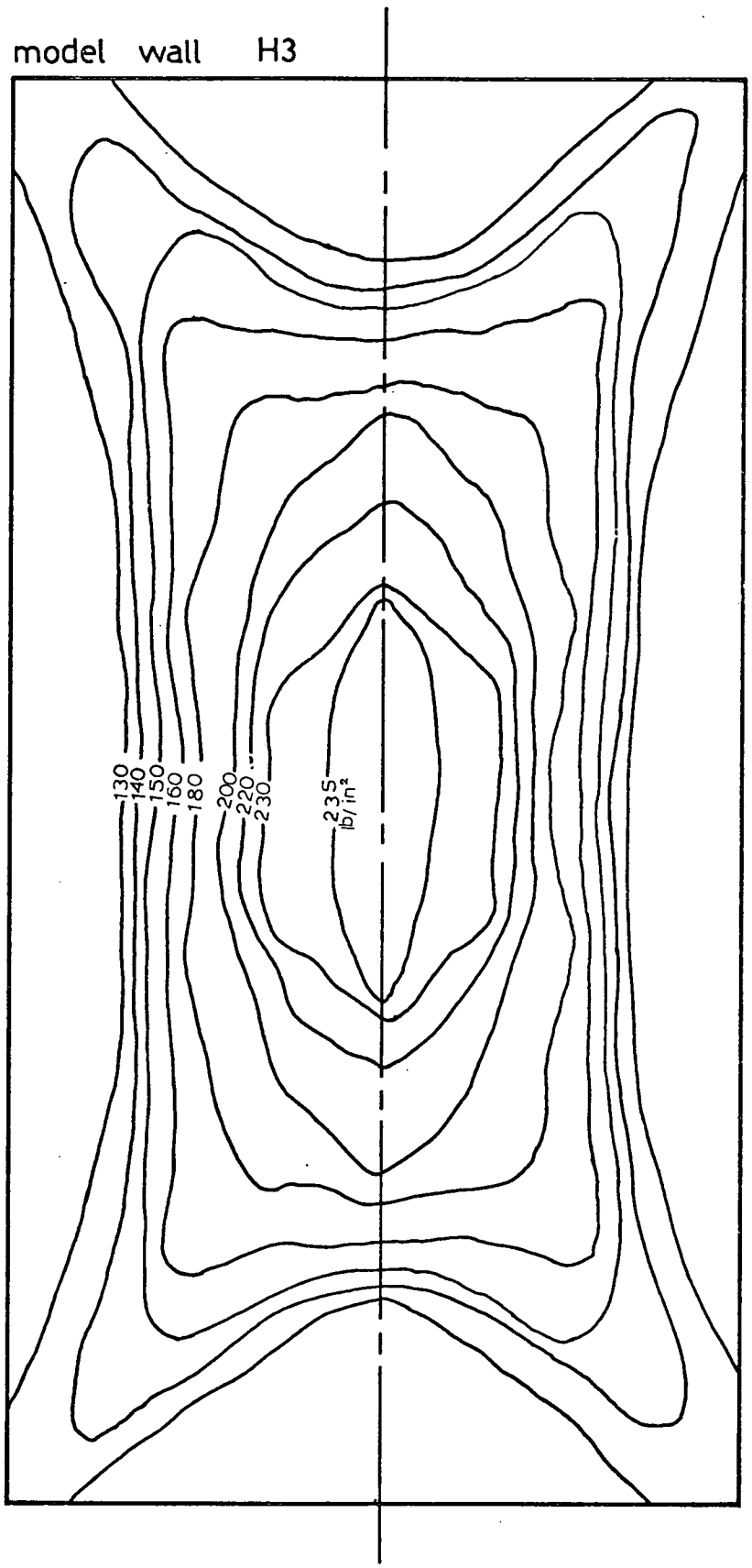

FIG. 4.13: CONTOURS OF TENSILE PRINCIPAL STRESSES

CHAPTER 5

EXPERIMENTAL TESTS AND INVESTIGATIONS

5.1 MATERIALS

5.1.1 Bricks

One-sixth scale model bricks were used in carrying out this work. Those used in the construction of half-brick model walls, representing a thickness at full scale of $4\frac{1}{2}$ in., had an average crushing strength of 3775 lb/in^2. For one-brick model walls bricks with average crushing strengths of 3331 and 3980 lb/in^2 were used.

5.1.2 Cement, Sand and Mortar

Rapid hardening "ferrocrete" cement was used for the cement/sand mortar used throughout this work. The sand was Leighton Buzzard No. 19 of $^{25}/_{52}$ grading. Mortar strength is given in Table (5.1).

5.2 TEST SPECIMENS.

These included both half and one-brick model walls, which were built in wooden moulds using wetted bricks and filled vertical joints. The walls were kept in their moulds under wet sacks for seven days and then left to cure under normal laboratory conditions until tested.

5.2.1 Half/

5.2.1 Half-brick Thick Model Walls

These were tested on three supports. A total of eight walls of varying dimensions were tested together with beams of three or four courses made from the same materials and under the same conditions. 1:3 cement/sand mortar by weight was used for these walls. The average crushing strength of 1 x 1 x 1 in. cubes was 2700 lb/in^2. The average crushing strength of the brickwork itself was 2325 lb/in^2, Table (5.1).

5.2.2 One-Brick Thick Model Walls

These were tested simply supported on either three or four sides, with or without precompression. The length/height ratios of the three types tested were: i) $^L/_H$ = 1.0, series E, 12 walls tested; ii) $^L/_H$ = 2.0, series G, 8 walls tested; iii) $^L/_H$ = 0.5, series H, 8 walls tested. Nominal thickness was 1.5 in for all these walls. 1:4 cement/sand mortar by weight of average crushing strength between 1400 and 1690 lb/in^2 was used. The average values of the crushing strength of the brickwork cubes were 1700 and 2060 lb/in^2.

5.2.3 Test Beams

The moduli of elasticity and rupture of the brickwork were determined using test beams between 8 and 12 in. long, with three or four courses wide. They were tested on simple supports and loaded at one-third points with two concentrated loads. Results are given in Tables (5.2)/

(5.2),(5.3), (5.4).

5.2.4 Test Apparatus

A steel rig of two main parts was designed and used for testing. The first part consists of two I-sections vertically erected on the horizontally placed web of a channel. One of the I-sections can slide freely on a steel rod, along the channel to give the required span for the wall to be tested. A steel rod fixed to either I-section constitutes the vertical supports for the panel. The second part consists of a stiff steel plate bolted to two channel sections to act as a reaction frame for the rig. The two parts are held together using bolts, with a rubberised canvas air bag sandwiched between the test wall, placed in the first part, and the steel plate of the second part. The air bag is equipped with an inlet valve delivering air from a compressor, and an outlet connected to a mercury manometer for recording the uniform pressure on the test wall.

Vertical precompression on walls was applied using a lever system and loading beams. Fig (5.1) presents a general view of the steel rig

5.2.5 Test Procedure

All the walls were tested on simple supports. Half-brick and a number of one-brick walls were tested free of precompression, whereas/

whereas the rest of the one-brick walls were tested taking an axial precompression of either 50 or 100 lb/in^2 before lateral loading was applied.

After the test walls were taken to the testing rig they were fitted with dial gauges at various points for the measurement of wall deflections. Uniform loading of the walls was achieved by inflating the air bag, between the test wall and the reaction steel frame, by small increments of pressure from the air compressor. The rate of loading was maintained approximately constant. Readings of the dial gauges and the difference in height of mercury in the two manometer columns were taken at each load increment. This was repeated each time the applied load was increased until failure of the wall. Tables (5.5), (5.6), (5.7) and (5.8) give measured deflections for the applied loads for all model walls.

5.3 EXPERIMENTAL INVESTIGATIONS

5.3.1 Behaviour of Walls Under Test

The general behaviour under load of half and one-brick model walls is outlined. Wall designation, dimensions, support conditions and amount of precompression can be found in Tables (4.2), (4.3), (4.4) and (4.5).

It was clear that the test walls failed in a yield line pattern of/

of cracks which could be compared with that obtained for reinforced concrete slabs under similar conditions. But, of course, there are differences in the manner of formation of the pattern of failure in each case. In slabs it is gradual and cracks are apparent well before failure, but in the brickwork walls no cracks were there before final failure. This could be due to the brittle nature of the brickwork and its low tensile strength.

(i) Half-Brick Thick Model Walls.

Walls of this series were designated by the letters A, B and C. These walls produced sudden failure with no cracks detected previously. Exception is wall A1 which had a slight difference in its boundary conditions: the three supported edges of the wall had a layer of mortar applied to them and then left to set in position in the testing rig for 24 hrs. before loading to failure. So in this case the wall would have developed semi-fixity which allowed the wall to develop cracking before failure. Cracking started vertically at the middle of the free edge and spreading diagonally towards the extreme corners with increasing load. When the full yield pattern of cracks has developed no fresh cracks were formed with increasing load until failure of the wall took place along the existing set of cracks. Figures (5.2) to (5.9) show the patterns developed at failure.

(ii) One-Brick Thick Model Walls Without Precompression

These/

These walls failed suddenly in some cases producing a sound, with no cracks being visible before complete failure. Mostly failure lines followed mortar joints, and in many test walls splitting of the bricks was quite common in vertically running failure lines and to a lesser degree in inclined ones. Figures (5.10), (5.11), (5.12), (5.13) and (5.14) indicate the failure patterns.

(iii) Axially precompressed One-Brick Thick Model Walls

One-brick model walls supported from three sides and axially precompressed with 50 or 100 lb/in^2 and with their length to height ratio ($^L/_H$) = 1 or 2 failed, like those model walls without precompression, suddenly with a sound and no cracks observed before failure Model walls from the same two series when taking the same level of precompression but have all four sides supported experienced cracking and full yield pattern formation before failure. Failure occurred at later stages accompanied by a loud sound; in one case the test wall burst out with some bricks flying to about 8 ft. and crushing of the bricks was noticed. Hence, in the first instance, the vertical precompression added to the overall strength of the model walls without changing the manner of failure, whereas in the second, in addition, it contributed to the general stability thus producing a change of the way of failure. The model walls were stable enough under the combined effect of the precompression and the supports to resist further increments of pressure after they had developed the full crack-pattern. Figs. (5.15) to (5.18) give the failure pattern.

A/

A model wall with three sides supported, length to height ratio of 0.5 and axial precompression of 50 lb/in^2 failed suddenly, under lateral load, before any cracks could appear. The vertical line of failure was two lines from the free edge which ran into one line through the middle of the wall where it joined the other two inclined ones to complete the usual pattern. When the same type of wall under similar support conditions was axially precompressed with 100 lb/in^2 and then loaded laterally, cracking preceeded complete failure of the wall. Now, here the vertical failure line did not come along the middle of the wall but was shifted to the left side of it. Factors which could account for this include variable workmanship and variable reactions at the different points of application of the precompression.

It should be noted that, in general, the same yield line pattern of failure was observed for both half and one-brick walls when precompressed or free from precompression when bound by the same support conditions.

5.3.2 Formation of Crack Pattern

Experiments on model brick walls have shown that at failure a characteristic pattern of cracks is formed. Consider, for example, one square wall under uniform lateral pressure, simply supported on all four sides. With increasing load the wall behaved elastically up to a certain stage, then greater deflections were obtained for the same load increments so that the load-deflection curve was always shifting/

shifting away from a straight line. Then suddenly, with increasing load, the wall failed with lines of failure extending from the centre right to the corners of the wall and there was no chance for observing any cracks before complete failure took place. It was noticed that lines of failure followed mortar joints most of the time and went through the bricks occasionally.

At this stage, since the yield lines can propagate no further, and the resistance moments along the yield lines are almost at their ultimate values, the wall is carrying the maximum possible load. Now excessive deflections and a state of unstable equilibrium occurs leading to the complete failure.

In the case of a wall supported from three sides it could be that cracking starts first at the middle of the free edge then extending vertically downwards and progresses towards the extreme corners. But this happens so fast that it is almost impossible to see where cracking has started and only the final pattern is there to be observed. This is due to the brittle nature of the brickwork which causes it to lose its capacity to take up stresses at failure, and the stresses must therefore be borne by the adjoining sections; these are already stressed almost to the point of failure, however, and therefore reach this point when the extra stress is imposed. The next adjoining sections then also lose their capacity to take up not only the extra stresses, but the original stresses as well, and sections adjoining these are stressed to the point of failure, and so on. In this way, the/

the failure immediately spreads over the whole wall whose carrying capacity will then be exhausted.

5.3.3 Variation of Deflections With Applied Loads

Measured deflections from tests showed reasonable consistancy for various model wall spans. For half-brick walls of different lengths Figs. (5.19) and (5.20) give the variation of the measured deflections with applied lateral loads. As expected, the wall with the smallest length had the least deflection for the same lateral load, the height being virtually the same for all walls. This is also the feature of the variation of deflections with applied lateral loads for one-brick model walls with or without precompression as shown in Figs. (5.21), (5.22), (5.23) and (5.24). The measured deflections of walls of the same dimensions, boundary conditions, materials and thickness are compared when these walls are precompressed or free from the precompression. The precompression, predictably, tends to reduce deflections for identical walls under equal lateral loads as indicated in Figs. (5.25), (5.26), (5.27) and (5.28).

5.3.4 Variation of Lateral loads with $^{L}/_{H}$ Ratio

The failure lateral loads for walls of different thicknesses, support conditions and precompressions vary in a decreasing manner with increasing $^{L}/_{H}$ ratio, but the relation is by no means linear, as shown by Figs. (5.29) and (5.30).

5.3.5 Variation/

5.3.5 Variation of Lateral Loads with Precompression

Lateral loads causing failure of walls increased with increasing precompression, the rate of increase being greater as the wall length became shorter. This is shown approximately in Fig. (5.31) for one-brick walls supported from three and four sides respectively, although higher precompressions would be needed for such tests to know the exact variation.

TABLE 5.1

Brick Strength lb/in^2	Mortar Ratio cement/sand by wt.	Mortar Strength lb/in^2	Brickwork Strength lb/in^2
3775	1:3	2700	2325
3331	1:4	1400	1700
3980	1:4	1690	2060

TABLE 5.2

Modulus of Elasticity, x 10^6 lb/in^2

1·46	0·95	0·91	1·10	average = 1·13
1·33	1·02	0·80	1·50	

TABLE 5·3

Modulus of Rupture, lb/in^2

Model Wall No	A1	A2	A3	B1	B2	C1	C2	C3
1	160	252	110	250	166	224	201	197
2	200	250	244	140	251	251	193	178
3	180	260	140	230	190	210	211	158
4		195	214	150	226	266	246	214
5		252					217	247
6								224
Average	180	242	177	192	208	238	214	209
Coefficient of variation %	11	11	35	29	18	8	13	12

TABLE 5·4

Modulus of Rupture, lb/in^2

Model Walls	1	2	3	4	5	6	Average	Coefficient of Variation %
E	152	114	146	139	148	124	137	11
G, H	142	98	123	108	134	194	133	25

TABLE 5.5

Support conditions	Dimensions (in)	Test wall No	Lateral load (lb/in^2)	Deflections (in x 10^{-3})	
				centre	mid-top
Three sides simply supported	20x17 x $\frac{3}{4}$	A1	0	0	0
			0·1	2	6
			0·2	7	16
			0·3	13	27
			0·4	19	37
			0·5	24	47
			0·6	28	55
			0·7	33	63
			0·8	39	71
			0·9	44	79
			1·0	50	88
			1·2	61	104
			1·3	73	120
			1·4	90	140
			1·45	97	151
		A2	0	0	0
			0·13	2	3
			0·25	5	6
			0·38	8	14
			0·50	10	17
			0·63	16	24
			0·75	20	29
			0·88	25	34
			1·00	29	41
	20x17x$\frac{3}{4}$	A3	0	0	0
			0·125	8	6
			0·25	15	14
			0·375	22	17
			0·55	34	25
			0·65		
Three sides simply supported	12x16x$\frac{3}{4}$	B1	0	0	0
			0·45	1	-
			0·55	2	1
			0·60	3	2
			0·70	4	-
			0·80	5	3

TABLE 5.5 (CONTD...)

Support conditions	Dimensions (in)	Test wall No	Lateral load (lb/in^2)	Deflections ($in \times 10^{-3}$)	
				centre	mid-top
Three sides simply supported	$12 \times 16 \times \frac{3}{4}$	B1	1·00	10	7
			1·20	12	9
			1·45	17	12
			1·80	31	27
		B2	0	0	0
			0·40	0·4	-
			0·50	0·7	0·4
			0·65	2	2
			0·80	3	4
			1·00	5	6
			1·28	8	9
			1·43	11	14
			1·60	15	20
			1·75	19	28
			1·88	24	42
			2·10	30	52
	$24 \times 16 \times \frac{3}{4}$	C1	0	0	
			0·10	2	
			0·23	7	
			0·33	12	
			0·45	28	
			0·58	33	
			0·60	36	
			0·75	60	
			0·78	79	
			0·80	90	
			0·85	125	
			0·88	146	
			0·90	169	
Three sides simply supported	$24 \times 16 \times \frac{3}{4}$	C2	0	0	0
			0·10	6	7
			0·20	12	16
			0·33	21	27
			0·45	30	37
			0·50	34	42
			0·55	39	47
			0·63	46	55
			0·70	54	65
			0·75	64	78
			0·80	84	104
			0	0	0

TABLE 5.5 (CONTD...)

Support conditions	Dimensions in	Test Wall No	Lateral Load (lb/in^2)	Deflections (in $x10^{-3}$)	
				centre	mid-top
		C3	0	0	0
			0•2	5	7
			0•38	16	18
			0•48	19	23
			0•58	25	30
			0•63	29	36
			0•68	35	-
			0•70	-	-

TABLE 5.6

Test walls dimensions, 16 x 16 x $1\frac{1}{2}$ in

Support conditions	Precompression (lb/in^2)	Test Wall No	Lateral Load (lb/in^2)	Deflections ($in \times 10^{-3}$)	
				centre	mid-top
Three sides simply supported	Nil	E1	0 0·45 0·60 0·80 1·10 1·55 1·70 1·95 2·20 2·50 2·60	0 7 10 12 16 22 24 29 32 40	0 3 7 11 15 30 32 40 49 60
Four sides simply supported	Nil	E3	0 0·10 0·55 0·90 1·60 2·00 2·50 3·00 3·50 4·00 4·50 5·00 5·25	0 3 10 19 31 38 45 53 62 72 83 93 101	
Four sides simply supported	Nil	E4	0 0·25 0·55 0·93 1·43 2·00 2·53 3·00 3·75 4·50 5·15	0 4 9 18 27 41 46 59 70 89 106	
			0 0·1 0·7	0 0·1 0·2	0 1 3

TABLE 5·6 (CONTD....)

Support conditions	Precompression (lb/in^2)	Test Wall No	Lateral Load (lb/in^2)	Deflections (in x 10^{-3})	
				centre	mid-top
Three sides simply supported	50	E5	1·2	2	4
			1·7	4	6
			2·1	6	10
			2·7	8	15
			3·1	10	17
			3·7	14	21
			4·1	-	24
			4·7	18	29
Three sides simply Supported	50	E6	0	0	0
			0·7	17	30
			1·2	35	54
			1·7	48	70
			2·2	57	95
			2·7	73	117
			3·2	90	142
			3·7	106	172
			4·2		
	100	E8	0	0	0
			0·7	2	8
			1·8	7	19
			2·7	11	36
			3·2	15	54
			3·7	25	73
			4·2	44	102
			5·7		
		E9	0	0	
			0·4	6	
			0·7	12	
			1·2	24	
			1·7	38	
			2·2	50	
			2·7	58	
			3·2	72	
			3·7	82	
			4·2	92	
			4·7	104	
			5·2	120	
			5·7	136	
			7·2	cracking	
			10·2		

TABLE 5·6 (CONTD....)

Support conditions	Precompression (lb/in^2)	Test Wall No	Lateral load (lb/in^2)	Deflections (in $x10^{-3}$)	
				centre	mid-top
Four sides simply supported	50	E10	0	0	0
			0·8	6	
			1·2	13	
			1·7	17	
			2·2	22	
			2·7	26	
			3·2	35	
			3·7	44	
			4·2	57	
			4·7	69	
			5·2	83	
			5·7	94	
			6·2	110	
			6·7	122	
			7·2	135	
			8·4	cracking	
			12·3		
Four sides simply supported	100	E11	0	0	
			0·7	10	
			1·2	33	
			2·2	47	
			2·7	62	
			3·2	70	
			4·2	80	
			4·7	101	
			5·2	109	
			5·7	119	
			6·2	129	
			6·7	139	
			7·2	152	
			7·7	163	
			8·2	174	
			8·7	186	
			9·2	cracking	
			14·5		
			0	0	
			0·2	2	
			0·7	10	
			1·7	17	
			2·2	21	
			3·2	32	
			3·7	36	
			4·2	42	

TABLE 5·6 (CONTD....)

Support conditions	Precompression (lb/in^2)	Test Wall No	Lateral load (lb/in^2)	Deflections (in $x10^{-3}$)	
				centre	mid-top
Four sides simply supported	100	E12	4·7	50	
			5·7	71	
			6·7	93	
			7·2	103	
			8·2	127	
			8·7	139	
			9·2	149	
			9·7	161	
			10·2	169	
			10·7	cracking	
			11·2	196	
			11·7	209	
			12·2	233	
			12·7	250	
			13·2		

TABLE 5·7

Test walls dimensions, 32 x 16 x 1½ in

Support conditions	Precompression (lb/in^2)	Test wall No	Lateral load (lb/in^2)	Dimensions ($in \times 10^{-3}$)	
				centre	mid-top
Four sides simply supported	Nil	G3	0	0	
			0·7	42	
			1·2	96	
			1·7	182	
			2·0	260	
			2·3		
		G4	0	0	
			0·2	12	
			0·7	61	
			1·0	74	
			1·2	123	
			1·4	179	
			1·7	233	
			2·1	314	
			2·3	408	
			2·45	573	
			2·6		
Three sides simply supported	50	G5	0	0	0
			0·2	12	18
			0·45	22	23
			0·70	30	45
			1·00	40	59
			1·20	52	78
			1·45	65	98
			1·65		
	100	G8	0	0	0
			0·50	15	20
			1·00	27	40
			1·25	33	53
			1·55	47	67
			1·90	71	85
			2·25	94	95
			2·55	111	117
			2·85	130	144
			3·15	157	181
			3·35		

TABLE 5·7 (CONTD.....)

Support conditions	Precompression (lb/in^2)	Test Wall No	Lateral load (lb/in^2)	Deflections (in $\times 10^{-3}$)	
				centre	mid-top
Four sides simply supported	50	G10	0	0	L/4
			0·3	8	7
			0·8	16	16
			1·2	44	41
			1·7	72	66
			2·2	109	96
			2·7	168	137
			3·2	197	
			4·0		
	100	G12	0	0	L/4
			0·30	10	9
			0·65	19	18
			0·95	27	25
			1·25	41	36
			1·55	52	48
			1·85	90	70
			2·15	122	95
			2·45	139	119
			2·75	178	146
			4·85		

TABLE 5·8

Test walls dimensions, 8 x 16 x 1½ in.

Support conditions	Precompression (lb/in^2)	Test Wall No	Lateral Load (lb/in^2)	Deflections (in x 10^{-3})	
				centre	mid-top
Three sides simply supported	Nil	H1	0	0	0
			1	20	35
			2	52	66
			3	82	97
			4	106	124
			5	130	160
			6	152	195
			6·8		
Four sides simply supported	Nil	H3	0	0	
			1	17	
			2	37	
			3	52	
			4	72	
			5	95	
			6	137	
			7	182	
			9·7		
Three sides simply supported	50	H6	0	0	0
			1	16	9
			2	22	21
			3	58	38
			4	92	53
			5	113	66
			6	146	83
			7	163	96
			8	188	113
			11·8		
	100	H7	0	0	0
			1	11	9
			2	23	22
			3	37	35
			4	54	44
			5	100	56
			6	114	68
			7	174	84
			8	229	98
			14·9		

TABLE 5·8 (CONTD...)

Support conditions	Precompression (lb/in^2)	Test Wall No	Lateral load (lb/in^2)	Deflections (in $x10^{-3}$)	
				centre	mid-top
Four sides simply supported	50	H9	0	0	$\frac{3}{4}h, L/2$
			1	6	4
			2	11	8
			3	18	15
			4	28	25
			5	39	40
			6	57	53
			7	74	69
			8	89	88
			9	109	103
			10	137	128
			15·8		
	100	H12	0	0	$\frac{3}{4}h, L/2$
			1	7	6
			2	19	16
			3	39	33
			4	59	50
			5	75	64
			6	87	76
			7	100	92
			8	112	106
			9	125	118
			10	145	131
			21		

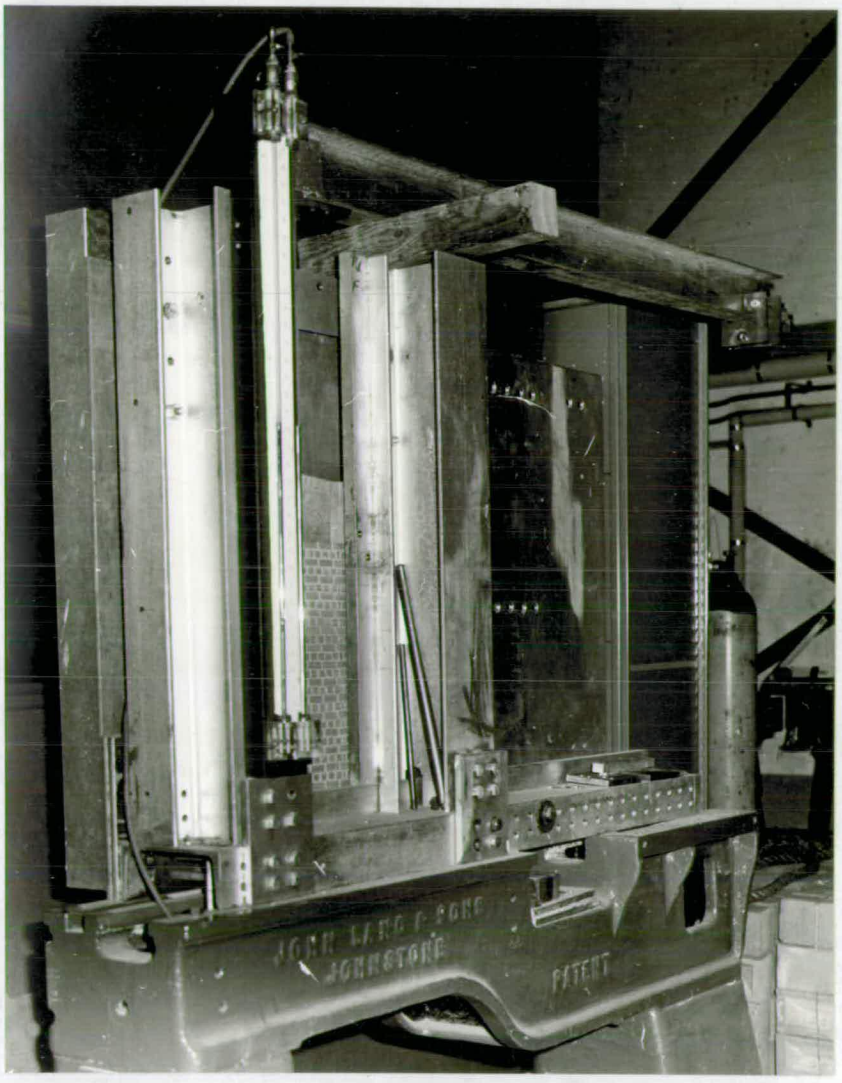

FIG. 5.1 GENERAL VIEW OF TESTING RIG FOR MODEL WALLS

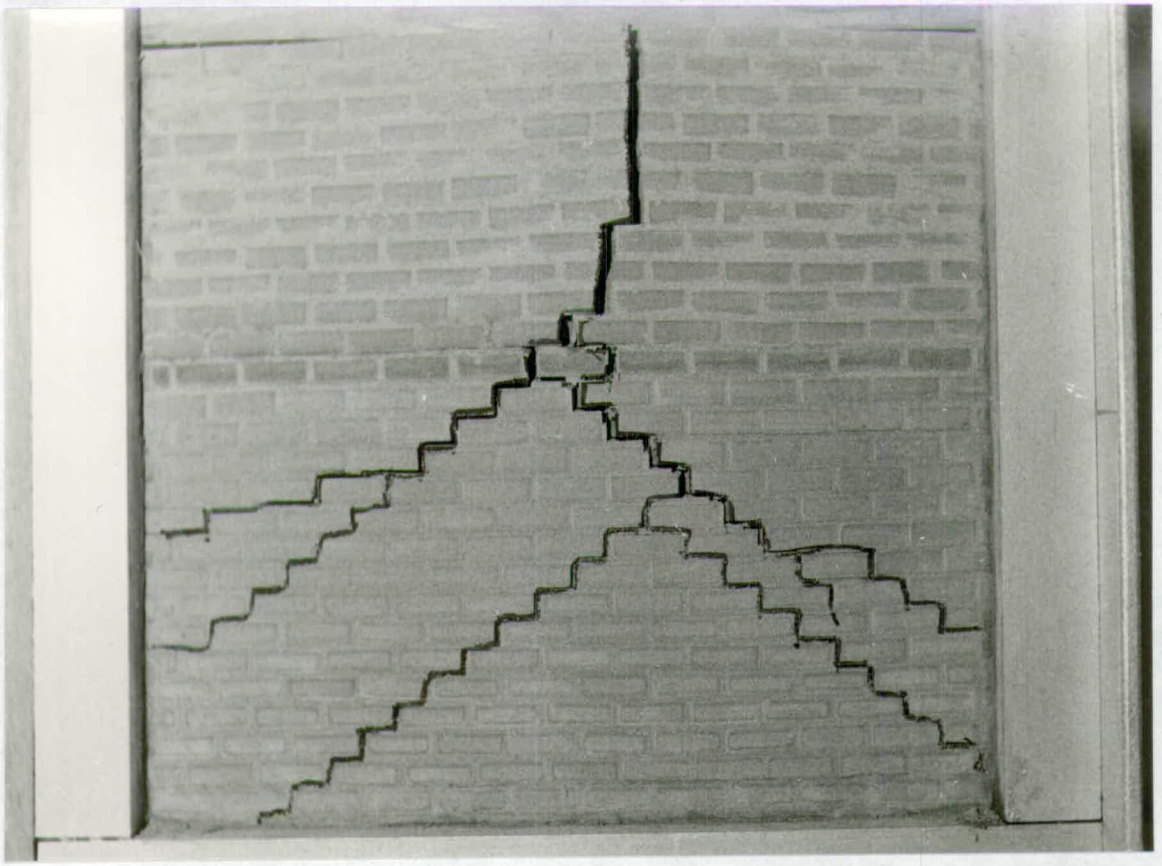

FIG. 5.2 FAILURE OF WALL A2 - 3 SIDES SUPPORTED

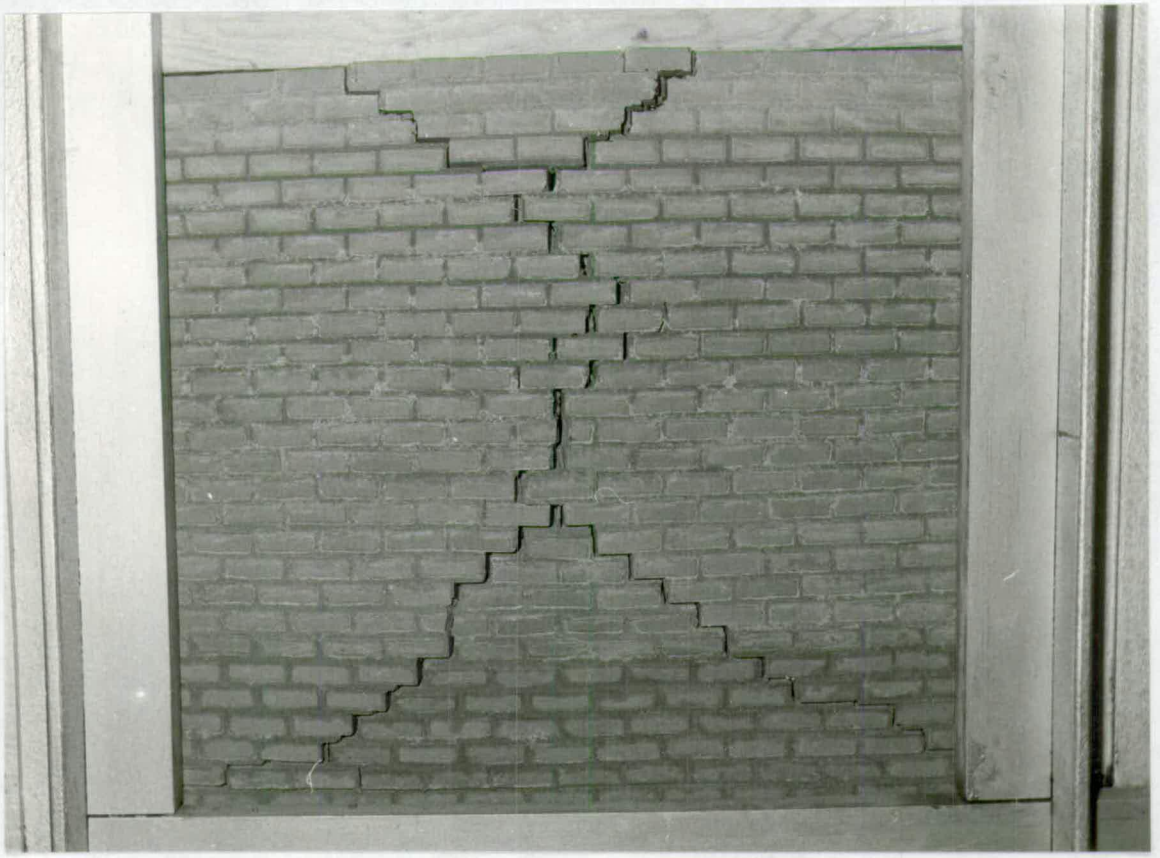

FIG. 5.3 FAILURE OF WALL A3 - 3 SIDES SUPPORTED

Fig. 5.4 FAILURE OF WALL B1 - 3 SIDES SUPPORTED

FIG. 5.5 FAILURE OF WALL B2 - 3 SIDES SUPPORTED

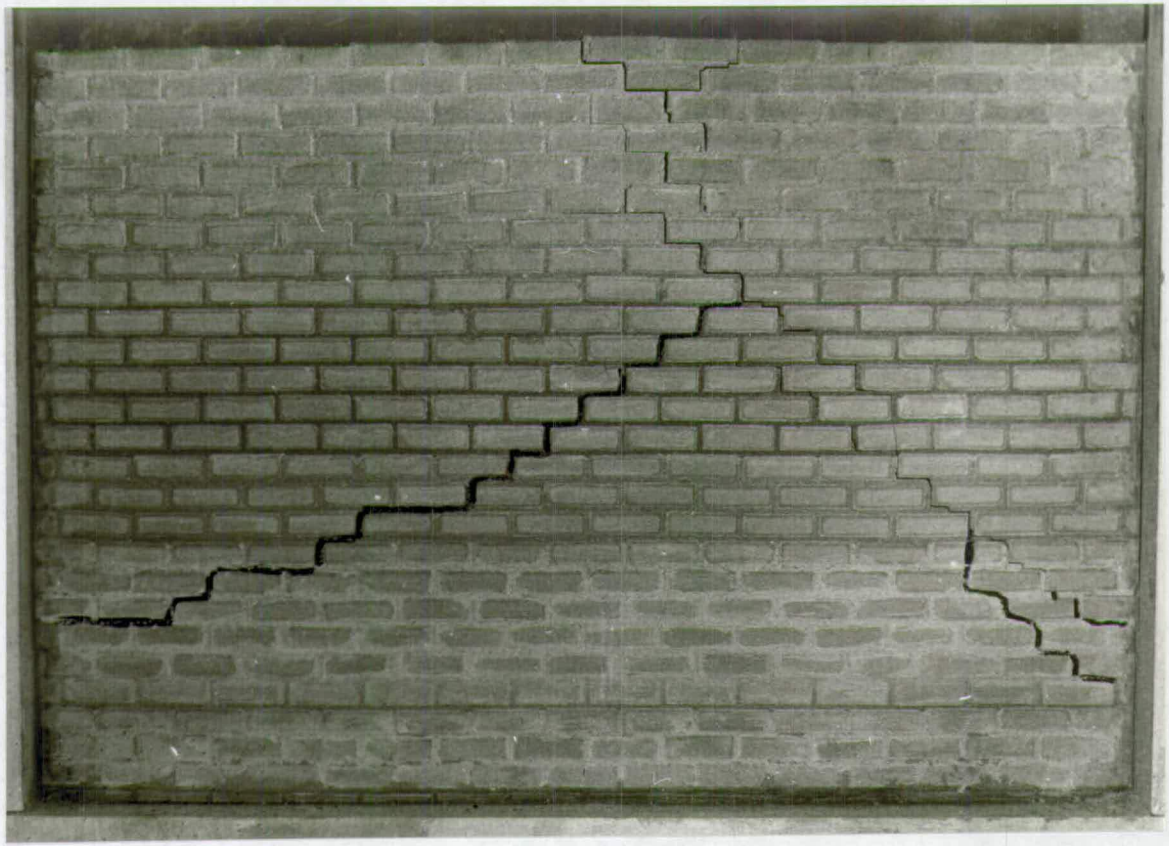

FIG. 5.6 FAILURE OF WALL C2 - 3 SIDES SUPPORTED

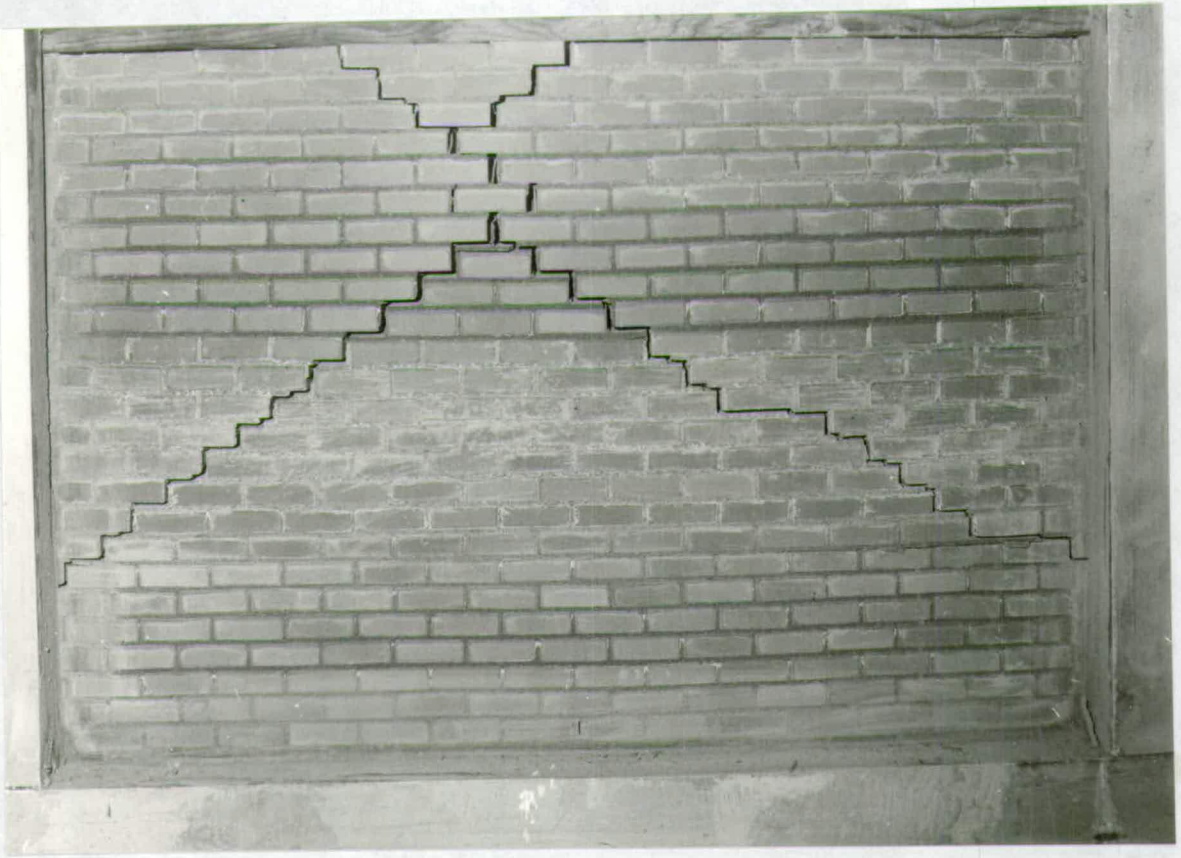

FIG. 5.7 FAILURE OF WALL C3 - 3 SIDES SUPPORTED

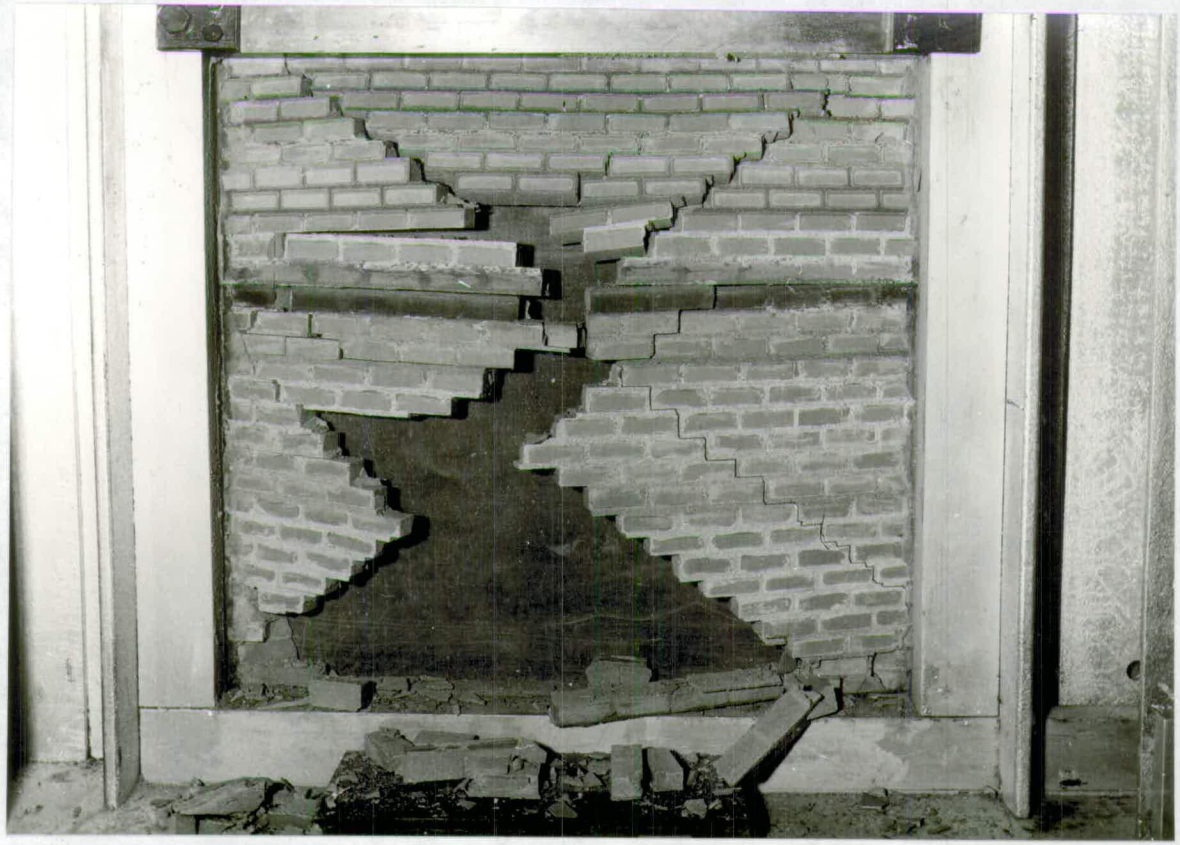

FIG. 5.8 FAILURE OF WALL D1 - 4 SIDES SUPPORTED

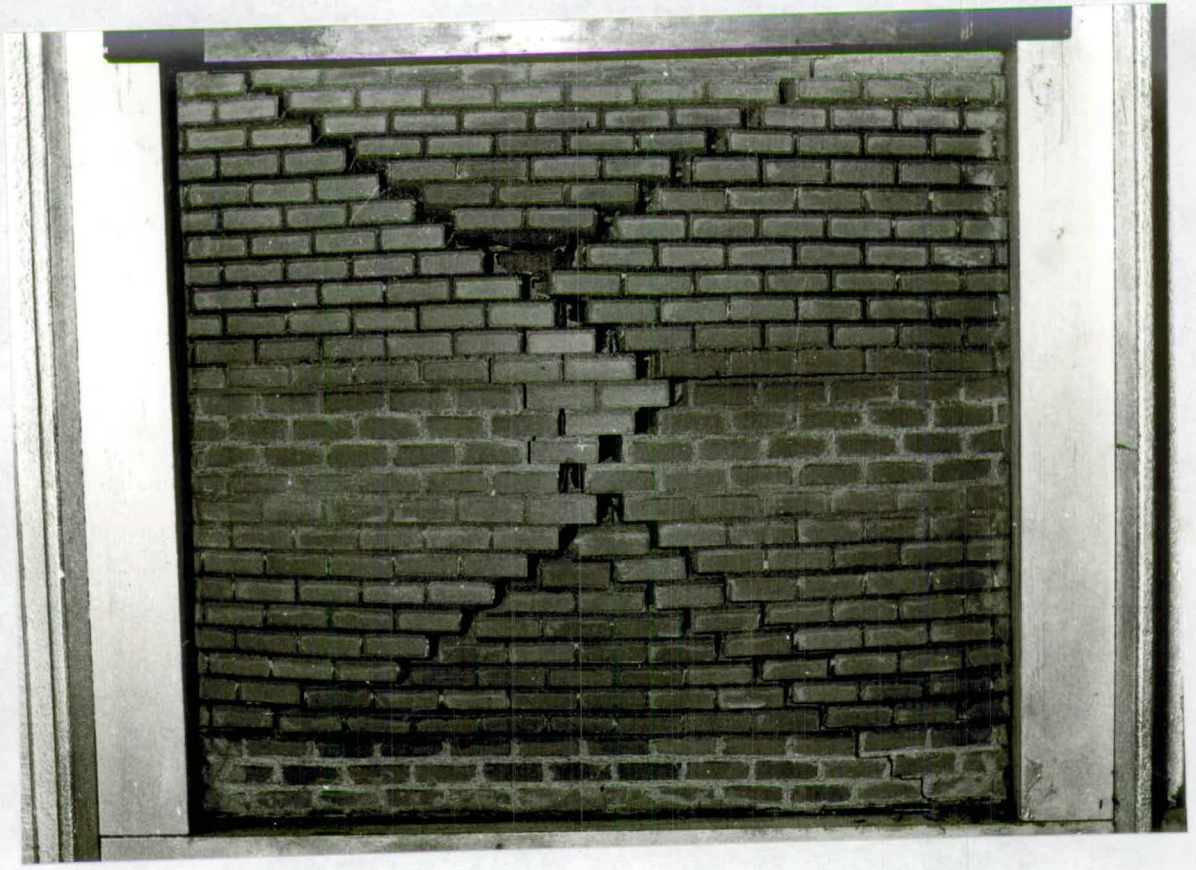

FIG. 5.9 FAILURE OF WALL D2 - 4 SIDES SUPPORTED

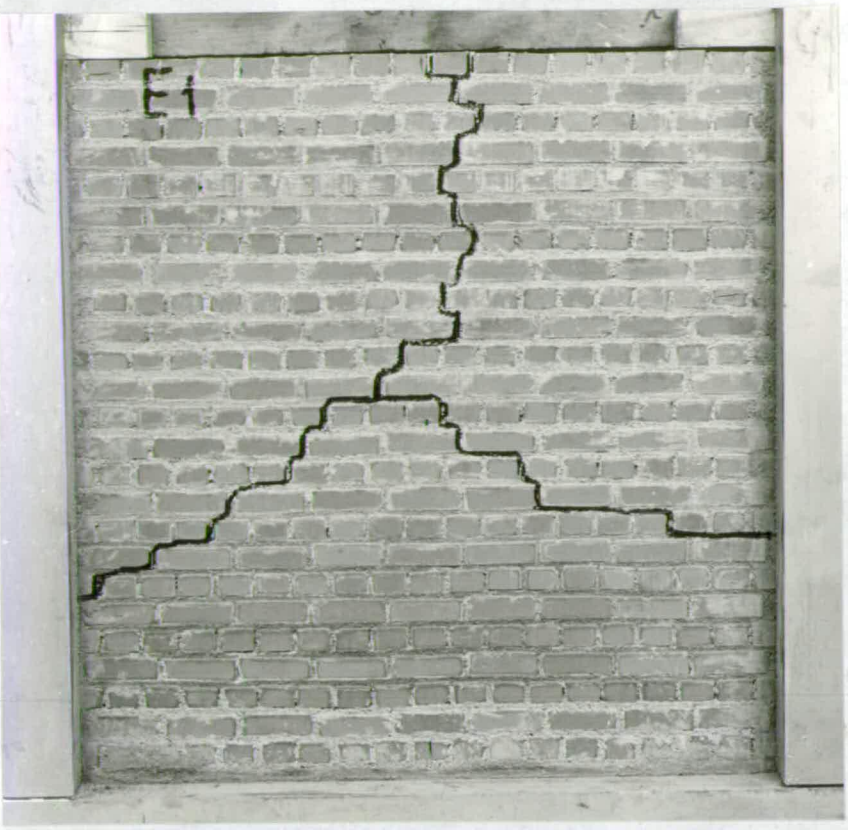

FIG. 5.10 FAILURE OF WALL E1 - 3 SIDES SUPPORTED

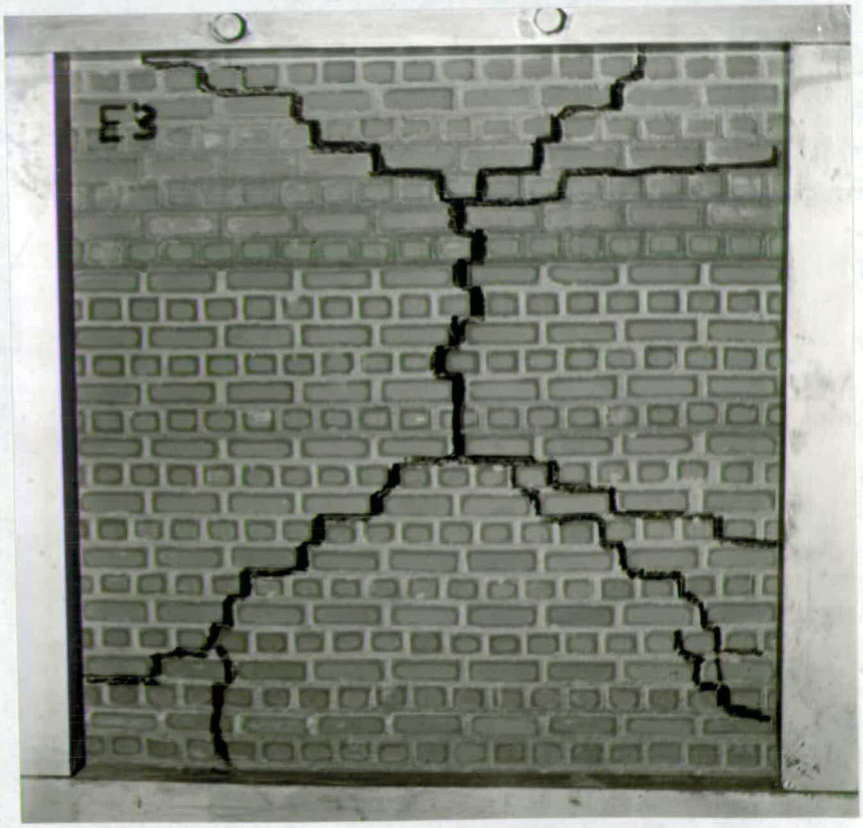

FIG. 5.11 FAILURE OF WALL E3 - 4 SIDES SUPPORTED

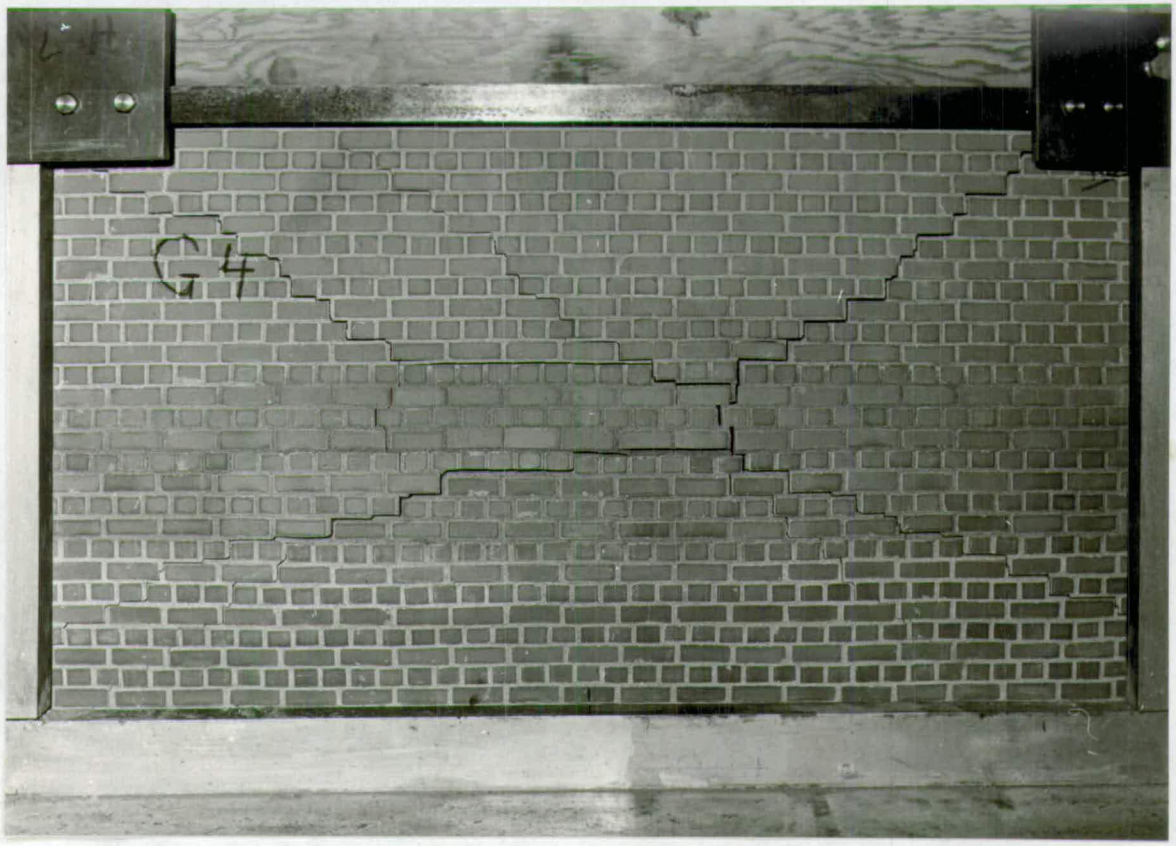

FIG. 5.12 FAILURE OF WALL G4 - 4 SIDES SUPPORTED

FIG. 5.13 FAILURE OF WALL H1 - 3 SIDES SUPPORTED

FIG. 5.14 FAILURE OF WALL H3 - 4 SIDES SUPPORTED

FIG. 5.15 FAILURE OF WALL E7 - 3 SIDES SUPPORTED

PRECOMPRESSION = 100 LB/IN^2

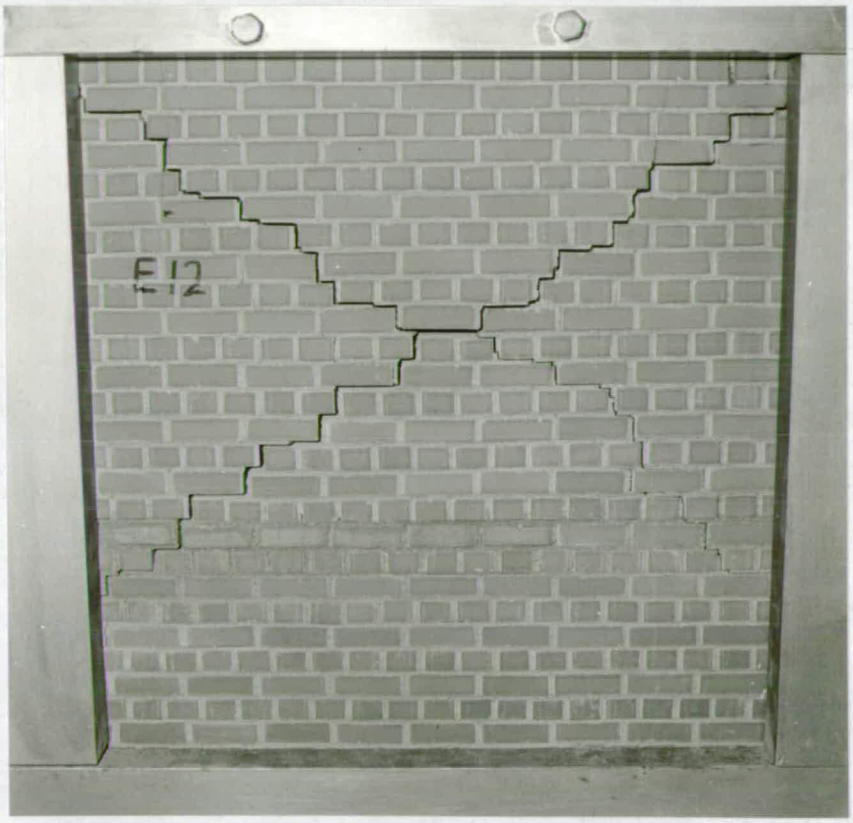

FIG. 5.16 FAILURE OF WALL E12 - 4 SIDES SUPPORTED

Compression = 100 lb/in^2

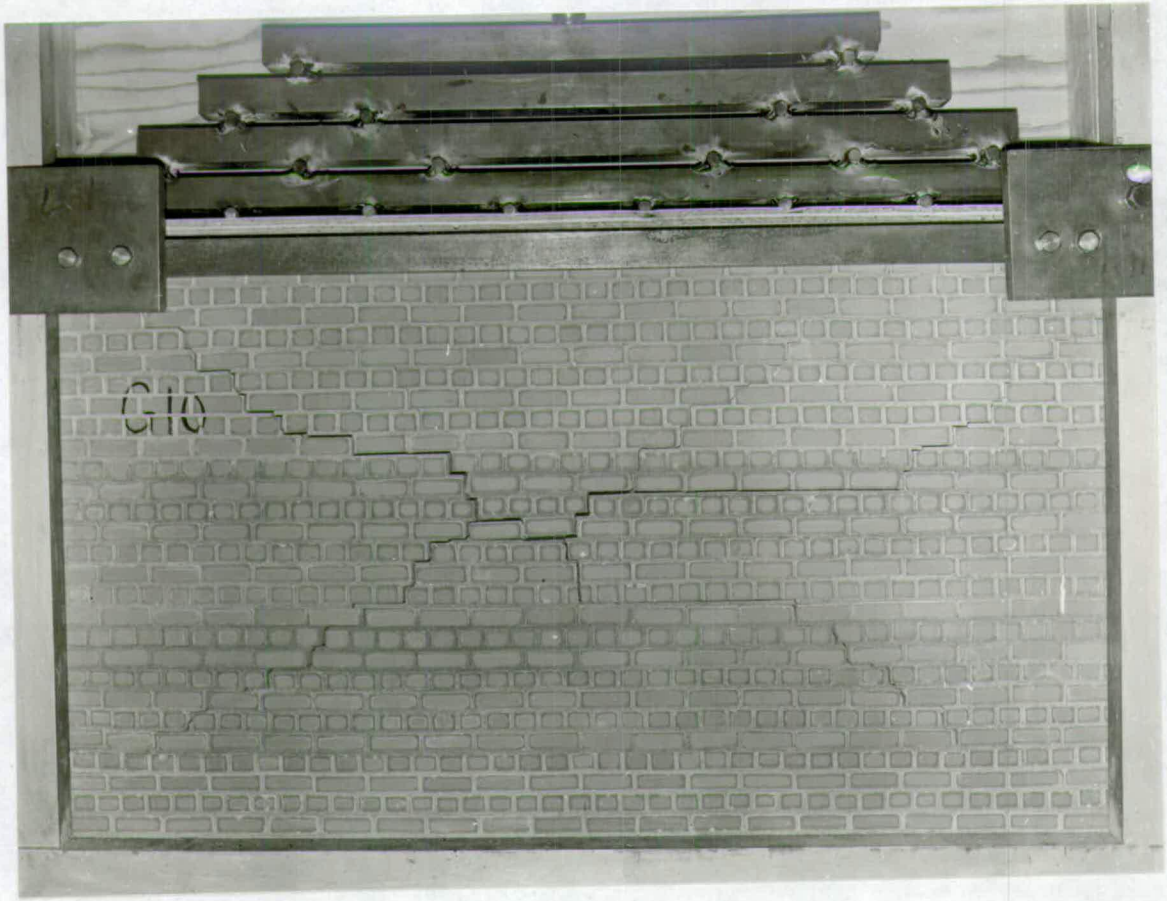

FIG. 5.17 FAILURE OF WALL G10 - 4 SIDES SUPPORTED

Precompression = 50 lb/in^2

FIG. 5.18 FAILURE OF WALL H6 - 3 SIDES SUPPORTED

PRECOMPRESSION = 50 LB/IN^2

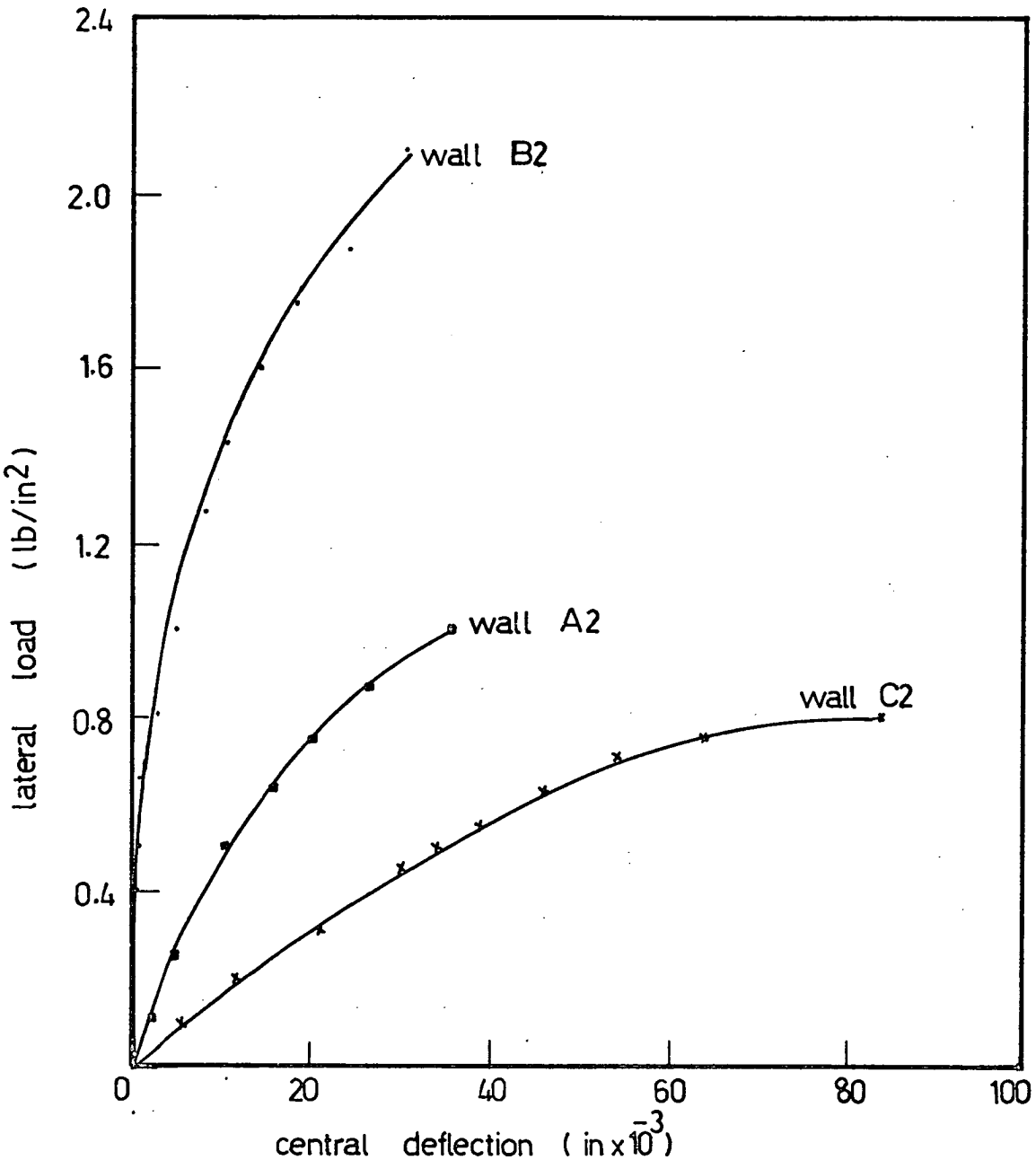

FIG. 5.19 VARIATION OF DEFLECTION WITH LATERAL LOAD

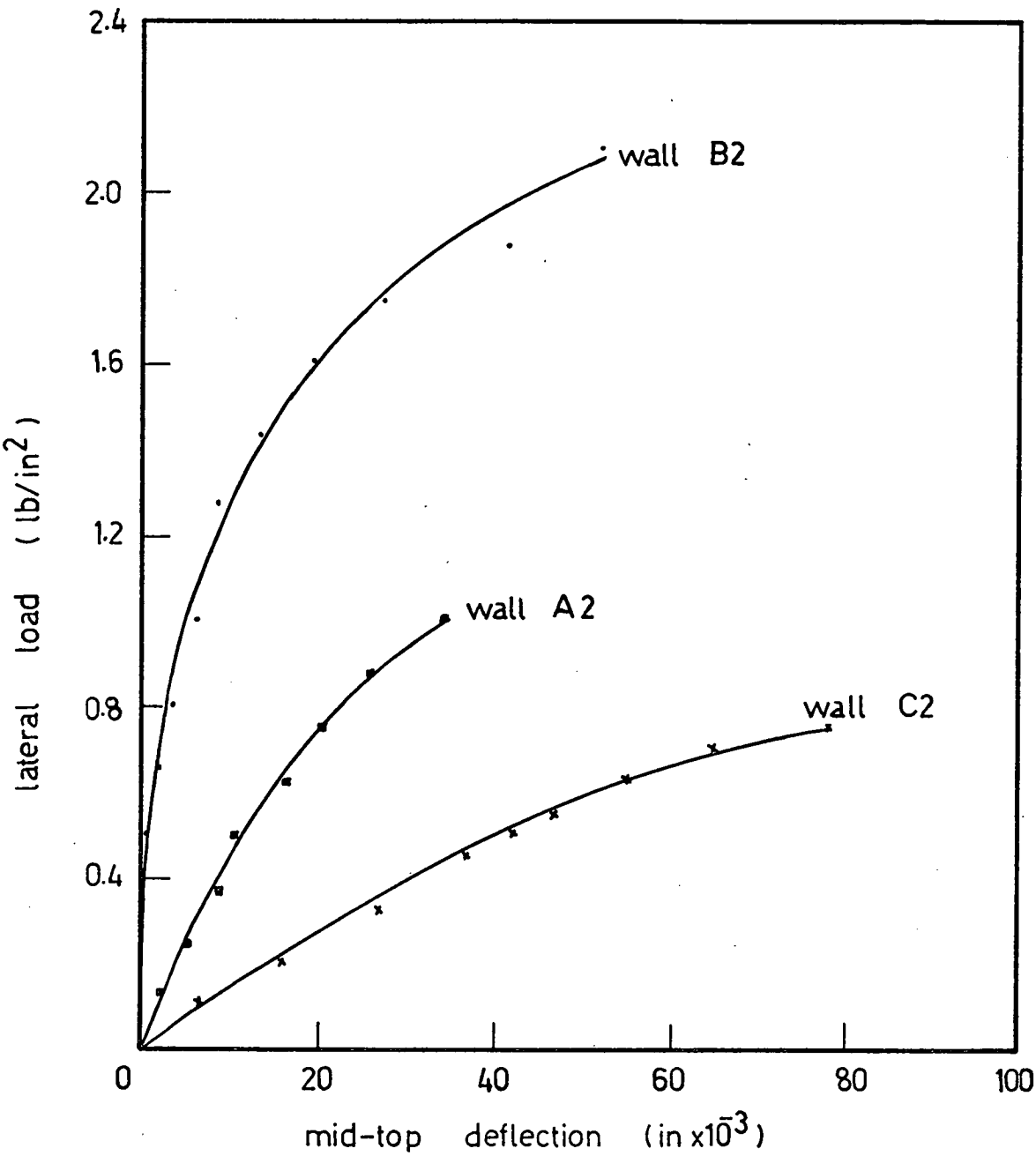

FIG. 5.20 VARIATION OF DEFLECTION WITH LATERAL LOAD

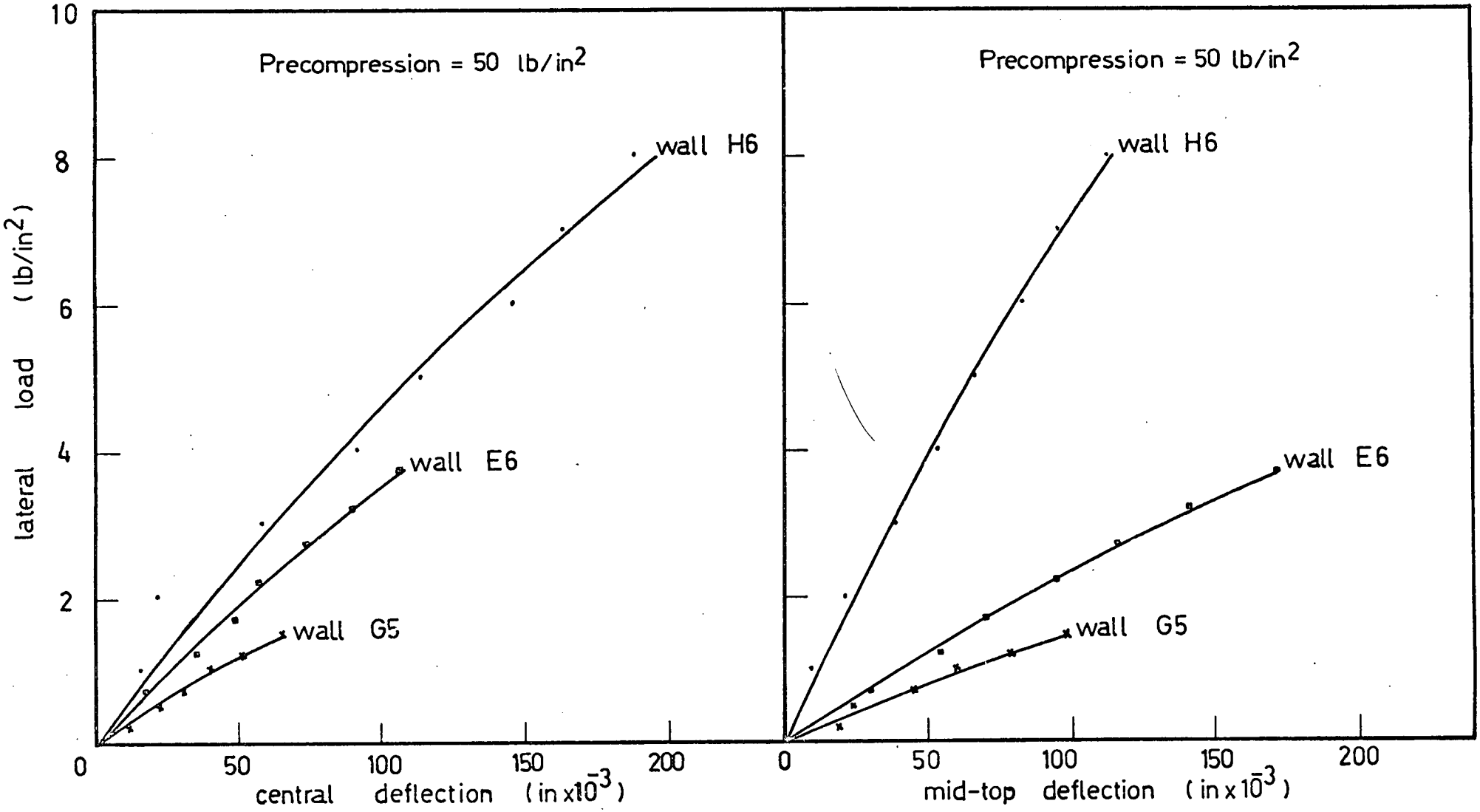

FIG. 5.21 VARIATION OF DEFLECTION WITH LATERAL LOAD FOR AXIALLY PRECOMPRESSED WALLS

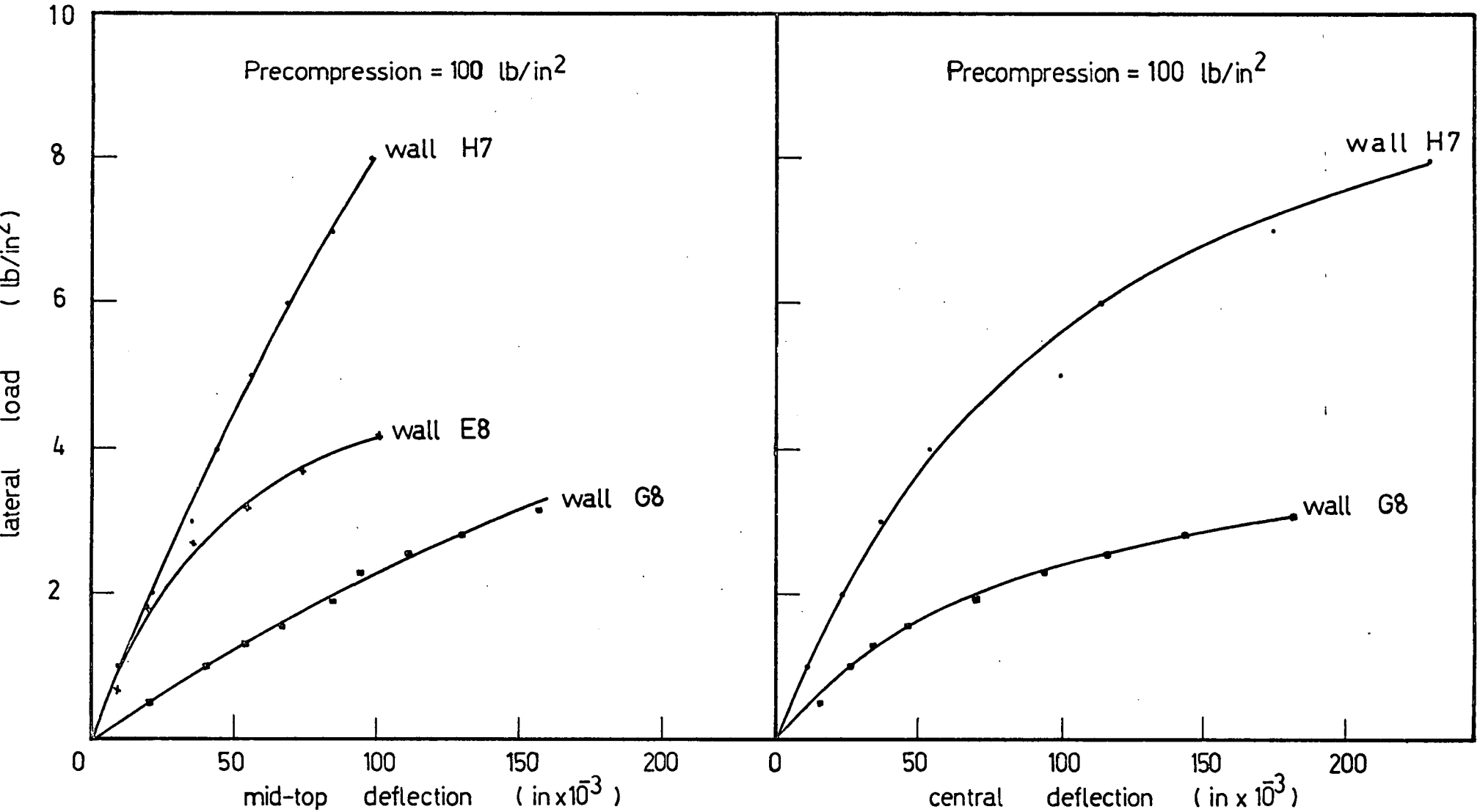

FIG. 5.22 VARIATION OF DEFLECTION WITH LATERAL LOAD FOR AXIALLY PRECOMPRESSED WALLS

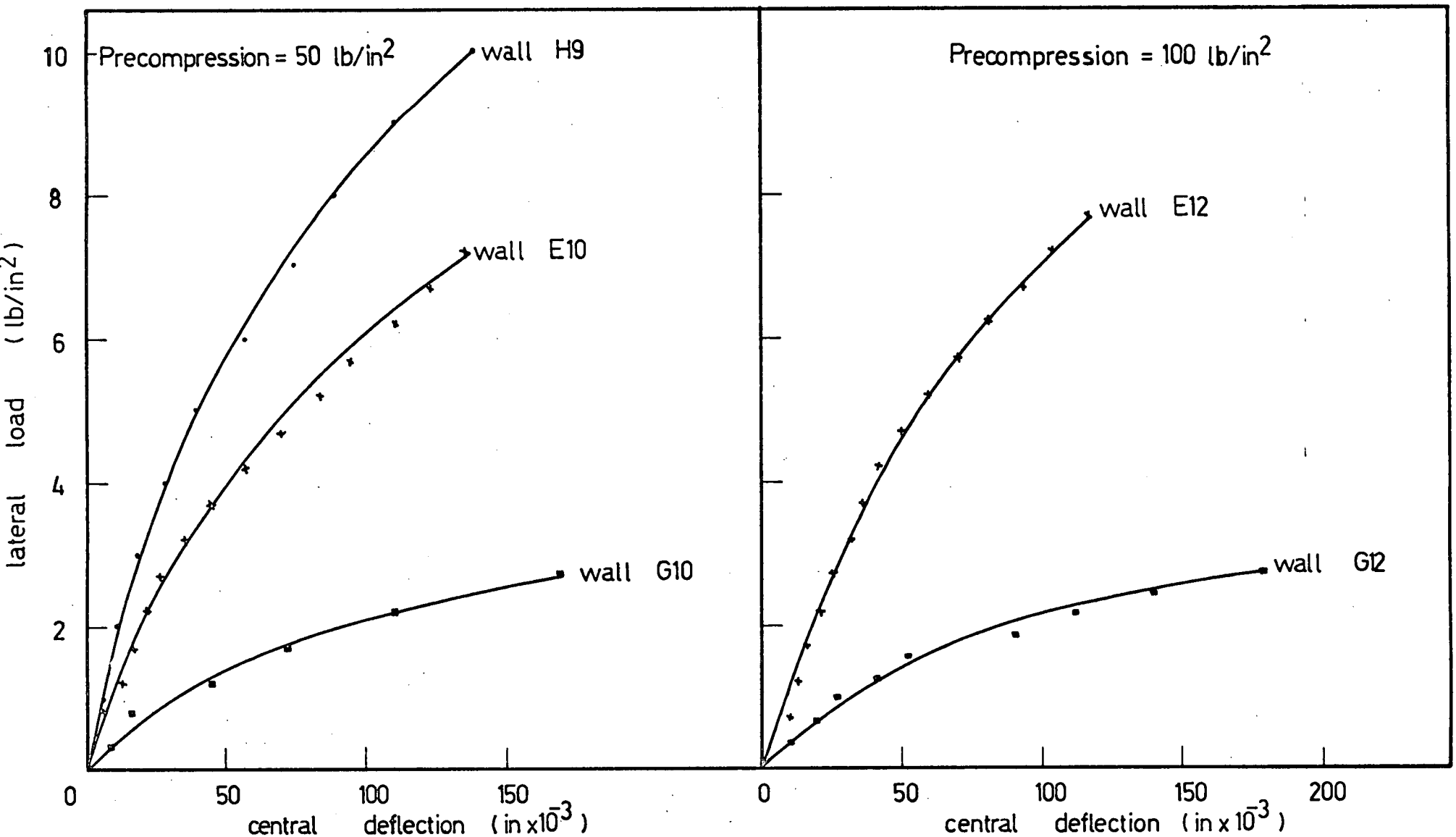

FIG. 5.23 VARIATION OF DEFLECTION WITH LATERAL LOAD FOR AXIALLY PRECOMPRESSED WALLS

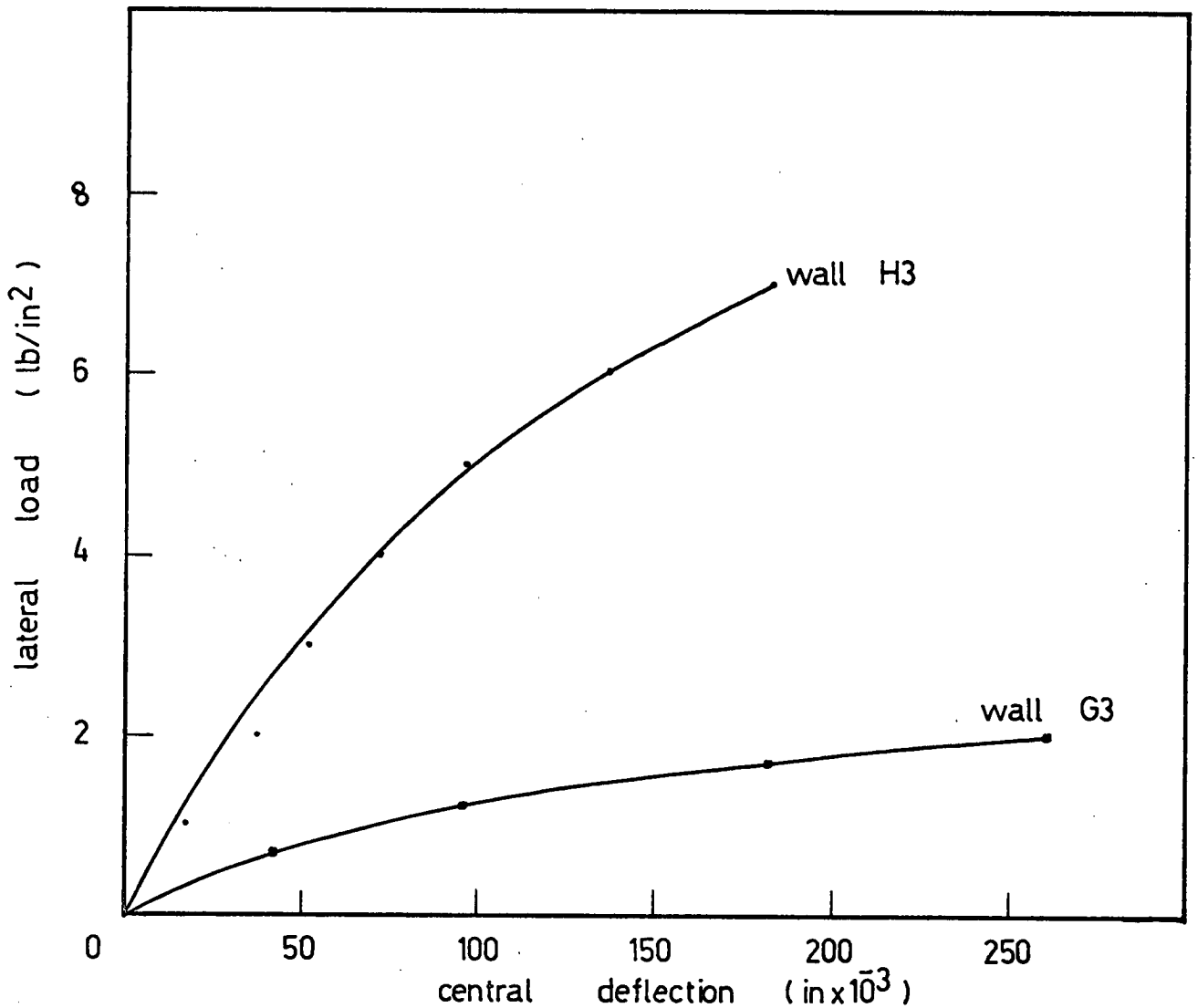

FIG. 5.24 VARIATION OF DEFLECTION WITH LATERAL LOAD

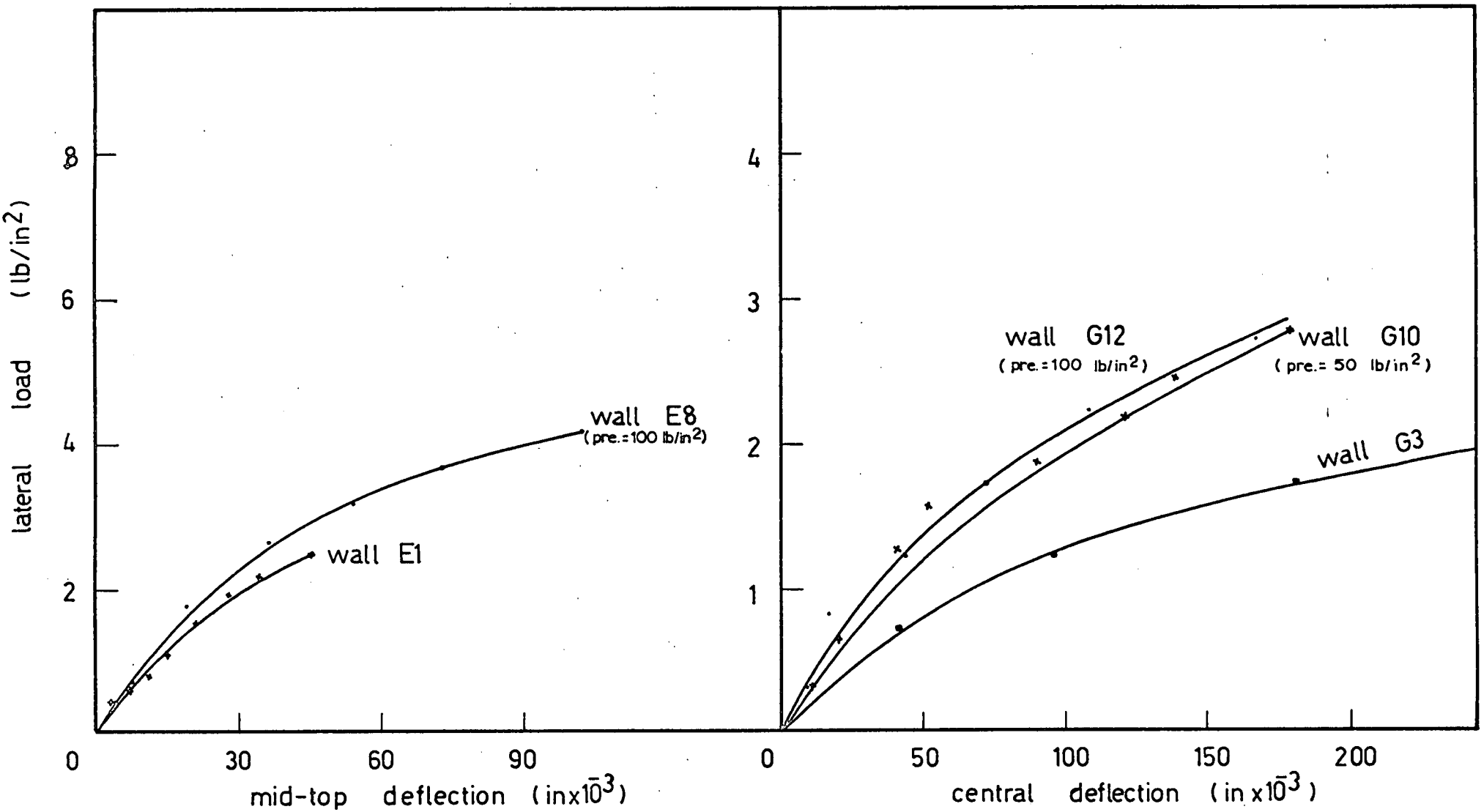

FIG. 5.25 VARIATION OF DEFLECTION WITH LATERAL LOAD FOR IDENTICAL WALLS UNDER DIFFERENT PRECOMPRESSION

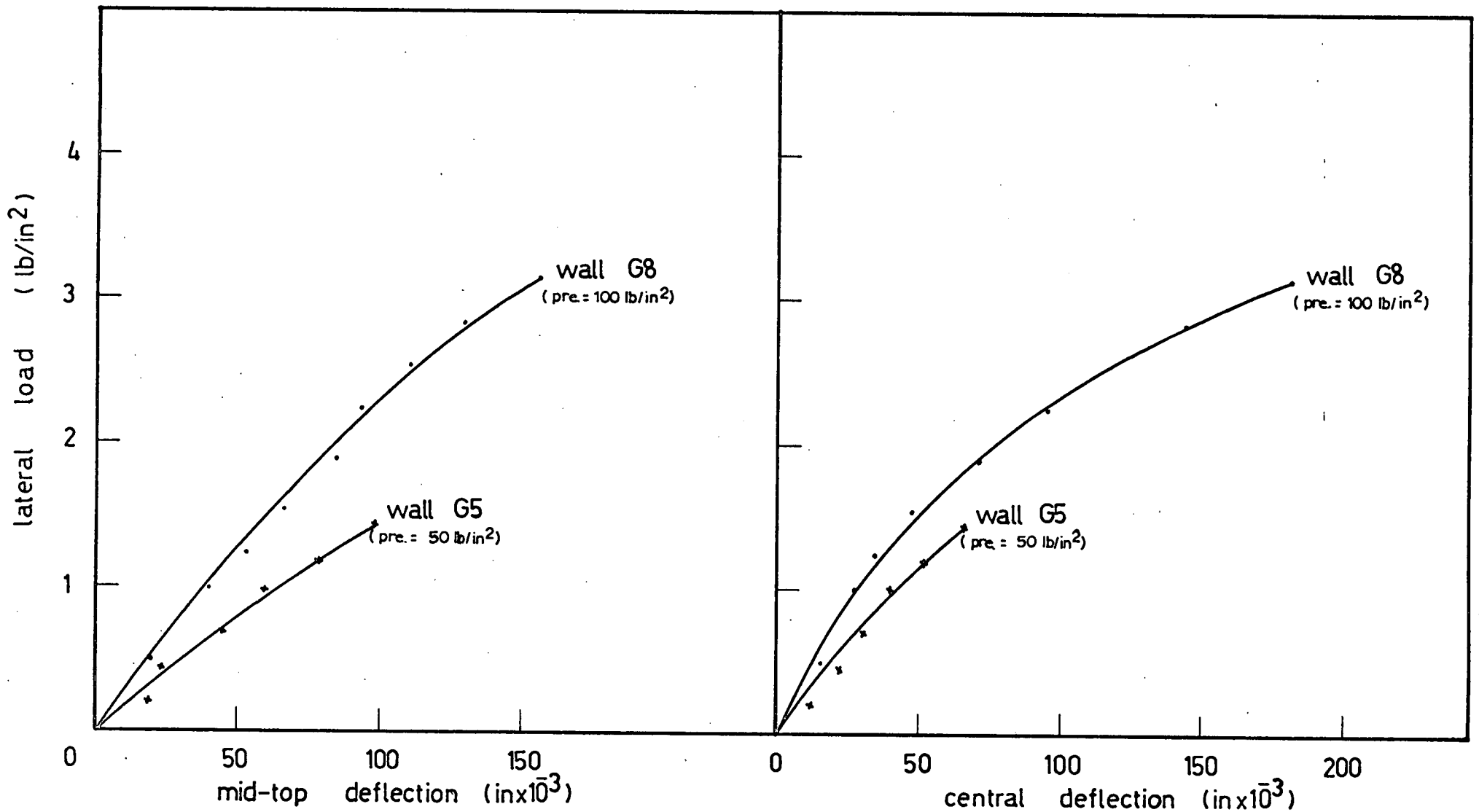

G.5.26 VARIATION OF DEFLECTION WITH LATERAL LOAD FOR IDENTICAL WALLS UNDER DIFFERENT PRECOMPRESSIONS

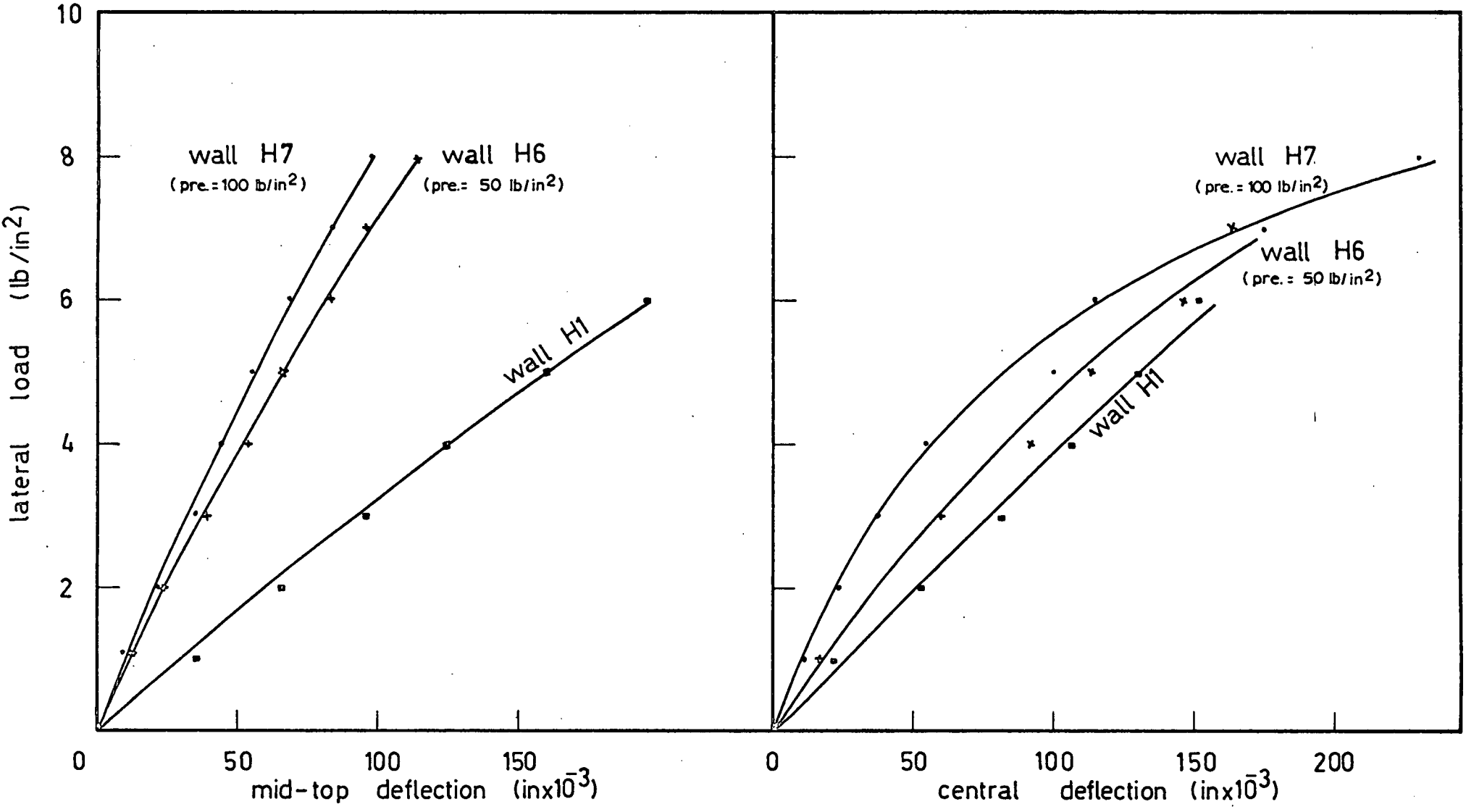

FIG 5.27 VARIATION OF DEFLECTION WITH LATERAL LOAD FOR IDENTICAL WALLS UNDER DIFFERENT PRECOMPRESSIONS

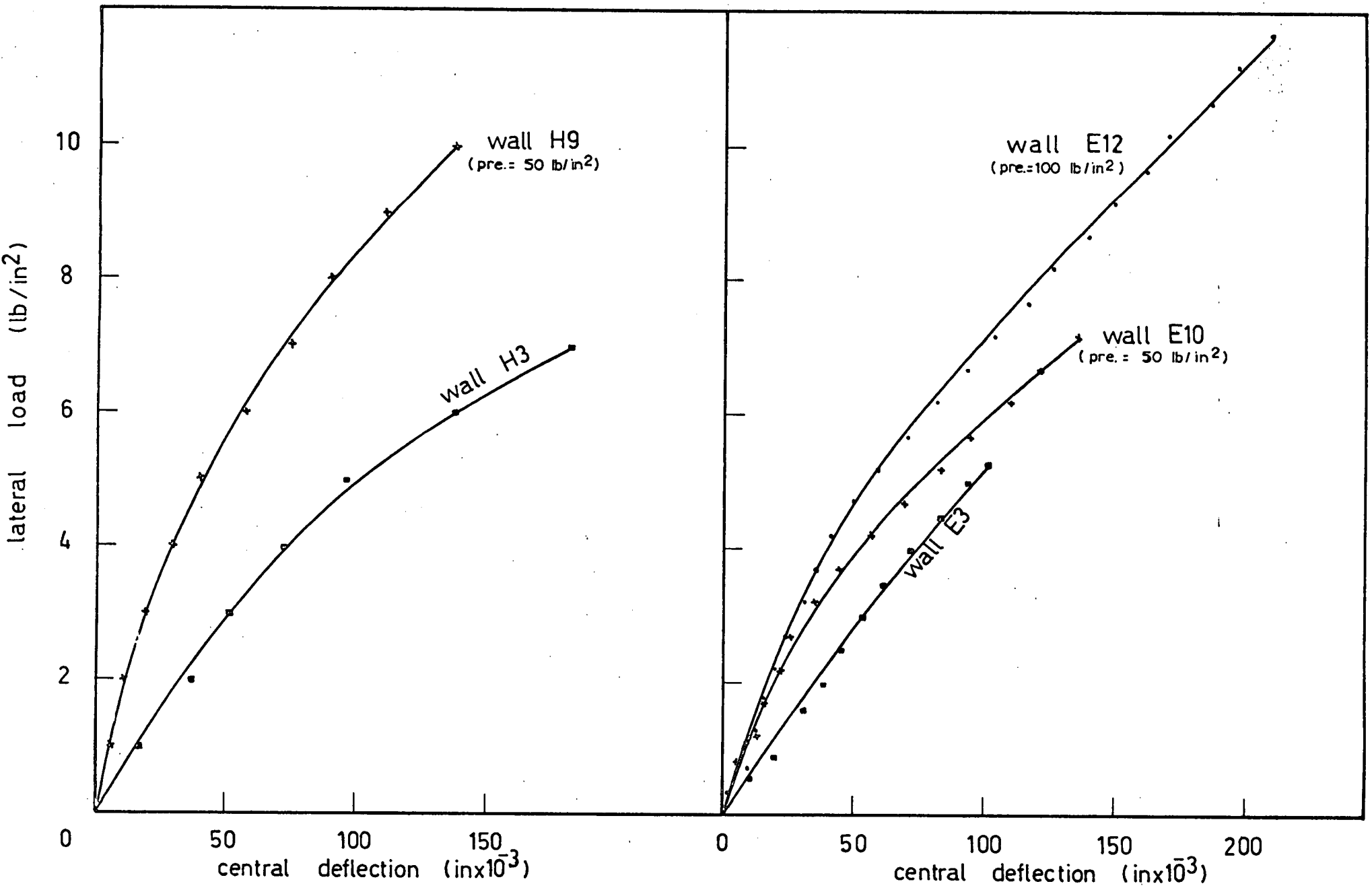

FIG. 5.28 VARIATION OF DEFLECTION WITH LATERAL LOAD FOR IDENTICAL WALLS UNDER DIFFERENT PRECOMPRESSIONS

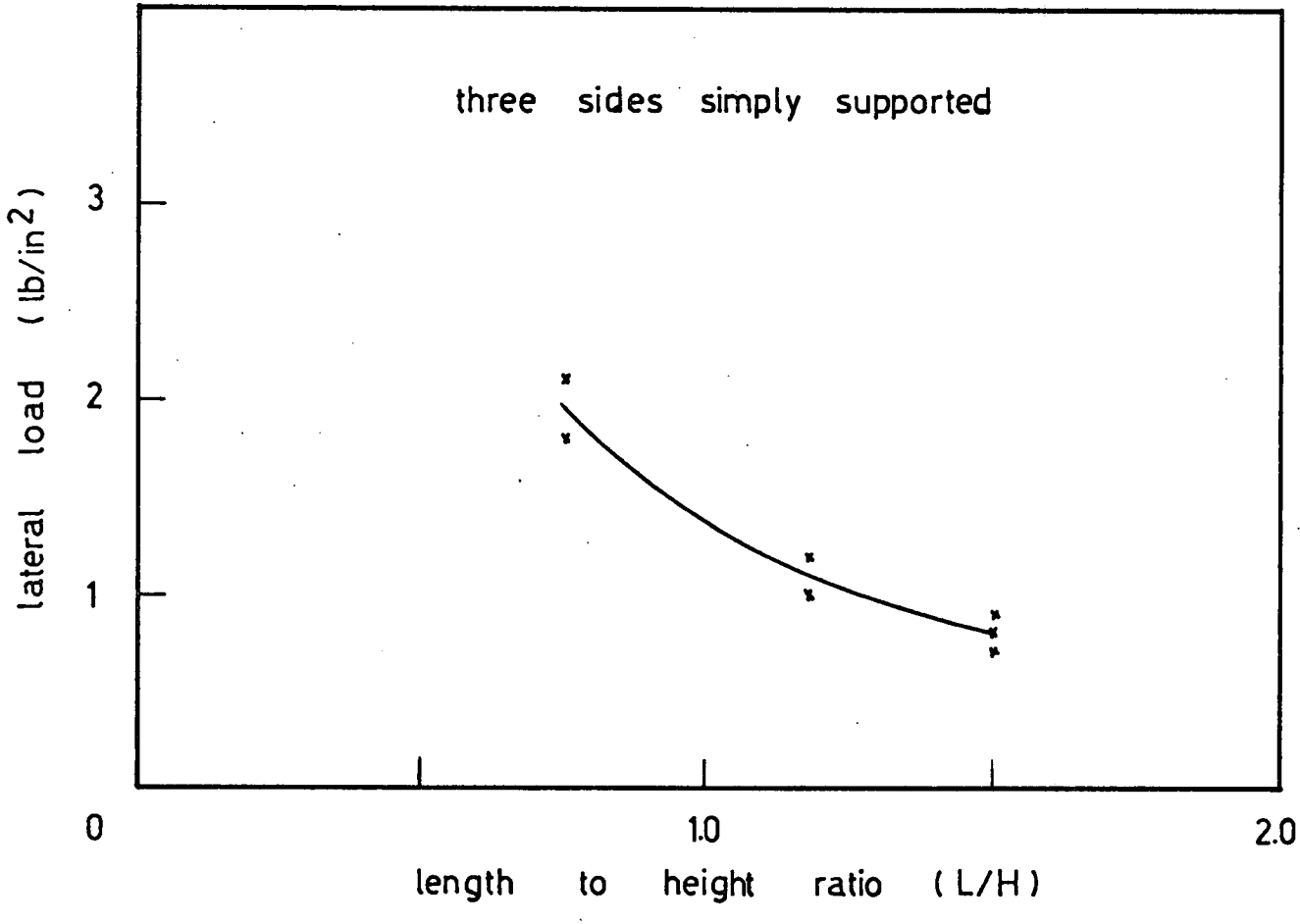

FIG. 5.29 VARIATION OF LATERAL LOAD WITH (L/H) FOR HALF - BRICK WALLS

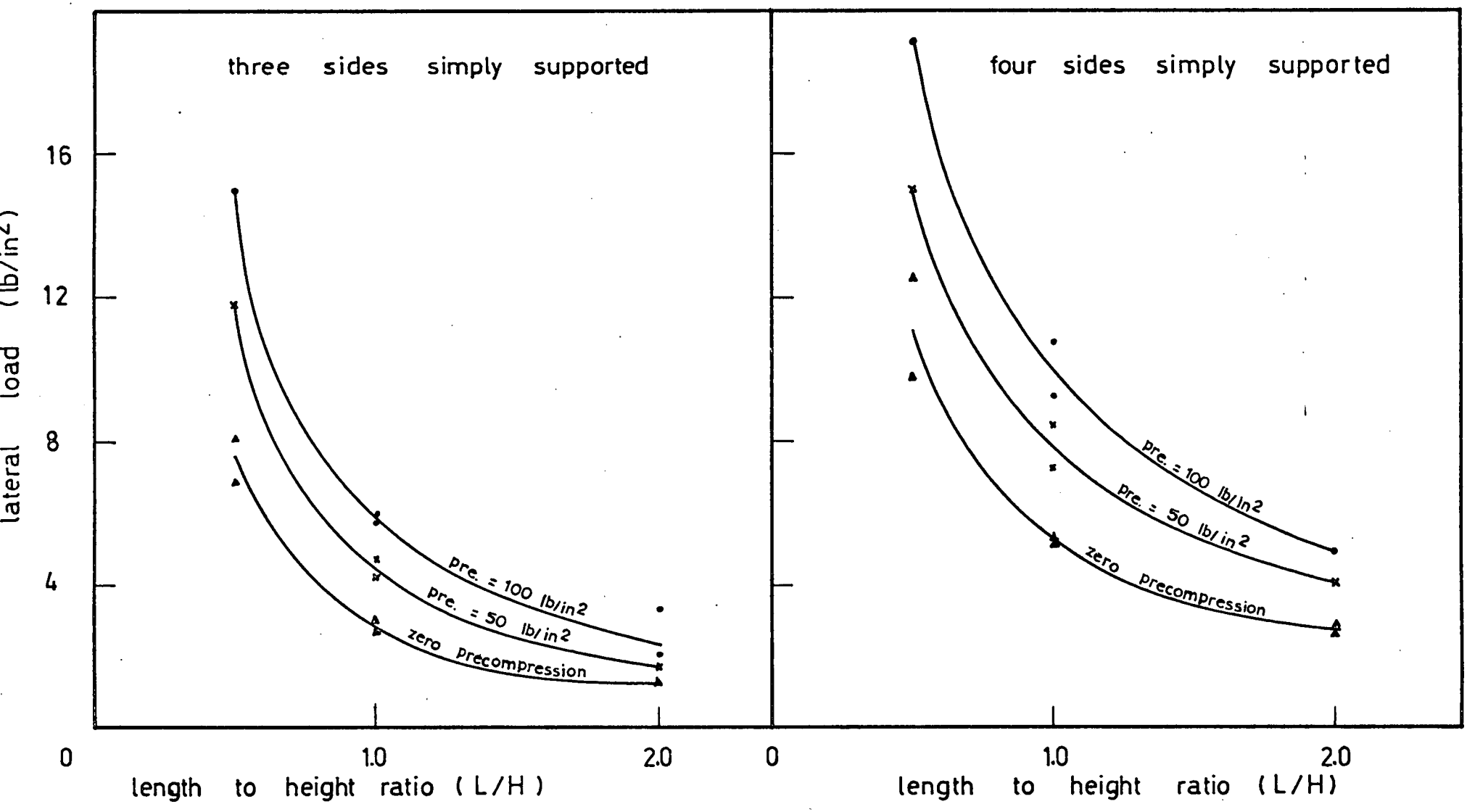

FIG. 5.30 VARIATION OF LATERAL LOAD WITH (L/H) FOR ONE - BRICK WALLS

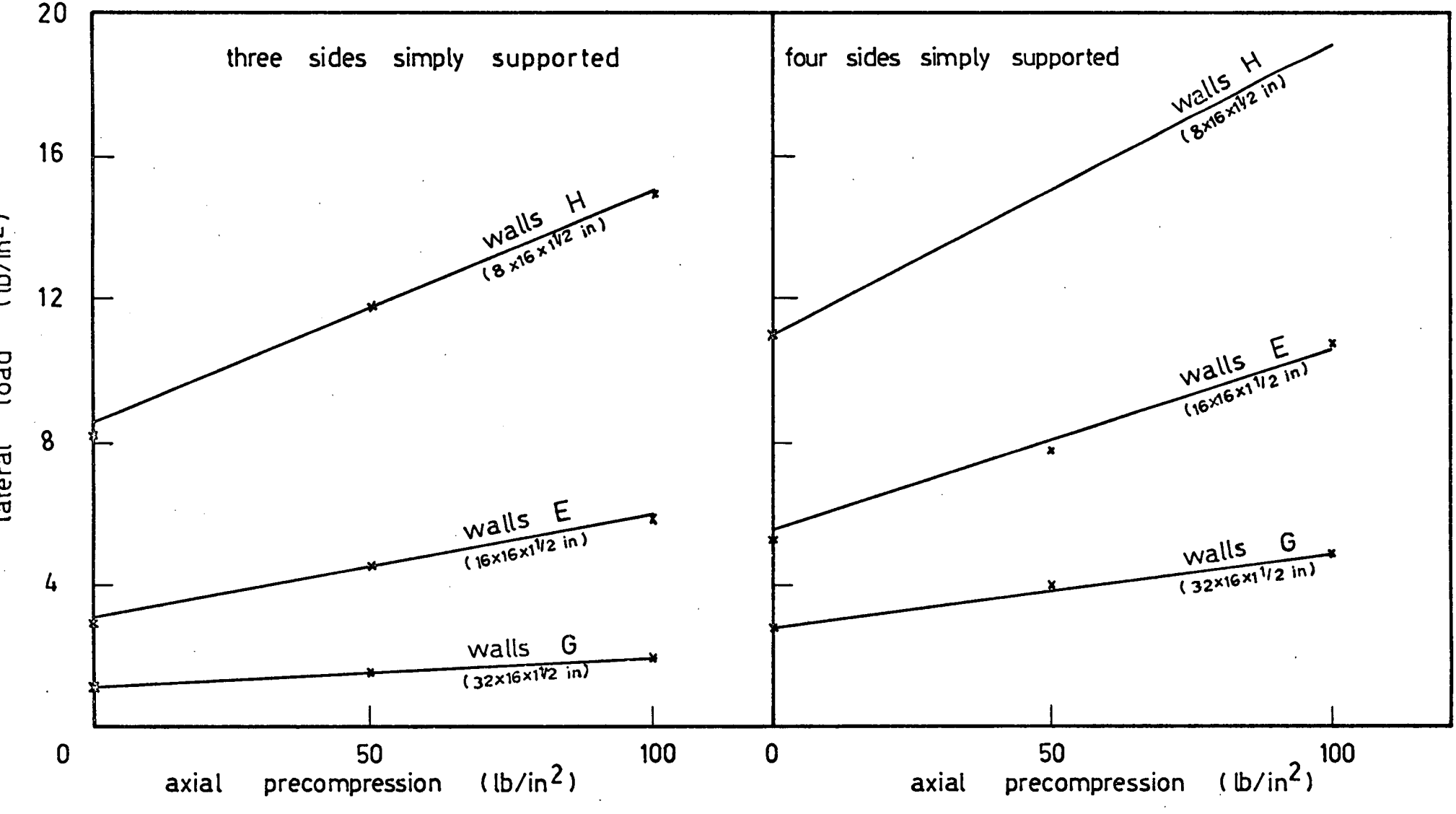

FIG. 5.31 VARIATION OF LATERAL LOAD WITH AXIAL PRECOMPRESSION FOR ONE-BRICK WALLS

CHAPTER 6

COMPARISON OF EXPERIMENTAL AND THEORETICAL RESULTS

6.1 YIELD-LINE METHOD AND EXPERIMENTAL RESULTS

6.1.1 Half-Brick Model Walls.

Except for wall (A1) mentioned earlier (5.3.1), reasonable agreement has been obtained between test results of this series and the analysis done using the yield-line method, Table (4.2). It was clear that failure was according to the predicted yield-line pattern, but sometimes failure lines reached somewhere above the corners of the panel. This is due to these failure lines following the weak sections at the mortar joints; but in some cases failure lines can jump across a brick and change their route to the edge of the wall. Also failure lines can reach the edge as one or many lines. The distance from a corner where a yield line finishes depends upon the length of the vertical and horizontal failure lines for walls supported from three or four sides respectively, workmanship, and variations of bond strength as these will affect the route which the failure lines would take to reach the boundary of the wall.

As the modulus of rupture of the test walls was measured using beams prepared from the same materials and cured under similar conditions, then any variations in values of the modulus of rupture of one wall could be reflected on its estimated failure load as these values/

values of the modulus of rupture were used to estimate the bending moments of resistance for the model walls. These bending moments were used in the yield-line method to estimate the failure load, and so variations in the modulus of rupture values are reflected on the resulting theoretical failure loads. In fact the coefficient of variation of the modulus of rupture for single-brick model walls varies between 8% and 29% as shown in Table (5.3). It is noted that the experimental failure load varies directly with the modulus of rupture, for walls of the same dimensions and support conditions as shown in Table (6.1)

(i) $\frac{pL^2}{m}$ from Yield-Line Theory and Tests

Using the Yield-Line Theory, the expression for (m) for a panel supported from three sides is given by

$$m = \frac{pL^2}{24}\left(\sqrt{3 + {}^1/_4\alpha^2} - {}^1/_2\alpha\right)^2$$

from which

$$\frac{pL^2}{m} = \frac{24}{\left(\sqrt{3 + {}^1/_4\alpha^2} - {}^1/_2\alpha\right)^2} \qquad \ldots\ldots(6.1)$$

Now calculation of $\frac{pL^2}{m}$ for half-brick walls can be carried out using equation (6.1) as follows:

(a) Model walls (A); $\alpha = 0.85$, $\alpha^2 = 0.72$ and $\frac{pL^2}{m} = 15.58$

(b) Model/

(b) Model walls (B); $\alpha = 4/3$, $\alpha^2 = 16/9$ and $pL^2/m = 12.3$

(c) Model walls (C); $\alpha = 2/3$, $\alpha^2 = 4/9$ and $pL^2/m = 18.75$

Also the experimental results were used to calculate the corresponding pL^2/m values for the model walls A, B and C. The Results of these calculations together with the above theoretical values and the length to height ratio (L/H) appear in Table (6.2). These results are also presented in a graphic form in Fig. (6.1), where the reasonable agreement achieved demonstrates the usefulness of the Yield-Line Method in estimating the load capacity of these walls.

6.1.2 One-Brick Model Walls

What was mentioned earlier, (6.1.1), about single brick walls could be repeated here. That includes failure in a yield-line pattern and the effect of the modulus of rupture on the estimated wall capacity.

(i) Laterally Loaded Walls

pL^2/m from Yield-Line Theory and Tests:-

Using the expression given in equation (6.1) values of pL^2/m for these walls can be calculated. These are given, together with the respective values obtained from experimental results and L/H ratios, in Table (6.3).Fig. (6.2) presents a plot of these results. For walls (G) the following expression was used to calculate pL^2/m instead of equation/

equation (6.1) as these walls assume a different collapse pattern

$$pL^2/m = \frac{24}{\alpha^2 \left(\sqrt{4 + 9/\alpha^2} - 2 \right)} \qquad \ldots\ldots(6.2)$$

For walls supported from four sides the Yield-Line Theory predicts the relationship

$$m = \frac{p(\alpha L)^2}{24} \left(\sqrt{3 + \alpha^2} - \alpha \right)^2$$

for the bending moment per unit length; from which

$$pL^2/m = \frac{24}{\alpha^2 \left(\sqrt{3 + \alpha^2} - \alpha \right)^2} \qquad \ldots\ldots(6.3)$$

Values for pL^2/m can be obtained for walls of different dimensions using equation (6.3) as follows:

Model walls (E); $\alpha = \alpha^2 = 1.0$ and $pL^2/m = 24$

Model walls (G); $\alpha = 0.5$, $\alpha^2 = 0.25$ and $pL^2/m = 56.58$

Model walls (H); $\alpha = 2.0$, $\alpha^2 = 4.$ and $pL^2/m = 14.39$

Again the resulting theoretical and experimental calculations are listed in Table (6.4) and plotted in Fig. (6.3)

(ii) Walls under Combined Axial and Lateral Loadings

Tables (6.5) and (6.6) give experimental values of pL^2/m and Figs./

Figs (6.2) and (6.3) compare these values with the curve from Yield-Line Theory for walls of varying dimensions, boundary conditions and axial precompression.

As indicated by the graphs the variation of pL^2/m with L/H for wall supported from three sides is quite different from that for walls supported on all four sides. This could be due to the ever increasing load capacities of four-sides supported walls compared with their equals supported from three sides: At lower values of L/H ratio the difference between pL^2/m values is not much, but it increases very fast with increasing values of L/H ratio, and a sharp difference in variation results. Reference to Fig. (6.4), which compares the variations of pL^2/m with L/H ratio for the two types of supports, shows that pL^2/m for three-sides supported walls varies with L/H ratio in somewhat regular intervals showing the matching between the increase in (L^2) and decrease in (p). For four-sides-supported walls it seems that the increase in (L^2) cannot be matched by the decrease in (p) and therefore the variation of pL^2/m with L/h ratio shoots up every time there is an increase in L/H ratio.

6.2 FINITE ELEMENT METHOD AND EXPERIMENTAL RESULTS

6.2.1 Half-Brick Model Walls

Results of the analysis of the model walls by The Finite Element Method are compared with the experimental results in three ways. The loads producing failure of the walls analysed are compared with the experimental/

experimental ones as well as those obtained by The Yield-Line Theory.

Fig. (6.5) shows the variation of these lateral loads with $^{L}/_{H}$ ratio, and it would be seen that The Finite Element Method could give a good guidance as to the load capacity of these model walls.

Next the measured deflections are compared with those obtained from the analysis by The Finite Element Method as indicated by Figs. (6.6), (6.7), (6.8) and (6.9).

It is obvious that the variation with applied loads of The Finite Element Method deflections is in a linear manner as the method is essentially an elastic one, whereas the experimental deflections tend to shift away from any linearity they had attained in the early stages of loading and assume a different variation with increasing deflections for the same loading intervals at the later stages of loading.

The third comparison carried out is between the experimental modes produced at failure of the walls and the patterns traced through application of The Finite Element Method. Here the agreement achieved could be checked throughout Figs. (4.5), (4.6), (4.7) and (4.8), showing contours of the principal tensile stresses developed at the loads causing failure of the walls analysed, and Figs. (5.2) to (5.7) which assemble a number of photographs taken at failure of the walls. In all these figures distinct yield-line patterns could be noticed.

6.2.2 One-Brick Model Walls

The/

The Finite Element Method was used to analyse selected walls from the one-brick series. Again load capacities, deflections and patterns of failure obtained from these analyses are compared with their corresponding experimental results. Figs. (6.10) and (6.11) give a graphic representation of the variations of these lateral loads, obtained by the three different methods, with $^{L}/_{H}$ ratios for walls supported from three or four sides respectively. By studying these graphs and that of Fig. (6.5) it would be reasonable to suggest that both Finite Element and Yield-Line Methods could be used safely to estimate the lateral load capacities of brick walls in spite of the fact that the results for the walls with $^{L}/_{H}$ ratio equal to 0.5 look more scattered when compared with those of the other walls.

Comparisons of the measured deflections with those obtained from the Finite Element Method analysis for a sample of one-brick walls are given in Figs. (6.12), (6.13) and (6.14)

The patterns of failure traced using the analytical method are shown in Figs. (4.9), (4.10), (4.11), (4.12), (4.13) which could be seen to compare with the actual experimental modes presented in Figs. (5.10), (5.11), (5.12) (5.13) and (5.14)

TABLE 6.1

VARIATION OF FAILURE LOAD WITH MODULUS OF RUPTURE, LB/IN^2

Model Wall No	A1	A2	A3	B1	B2	C1	C2	C3
Exerpimental failure load	1.45	1.0	0.65	1.8	2.1	0.9	0.8	0.7
Modulus of Rupture	180	242	177	192	208	238	214	209

TABLE 6.2

Half-Brick Model Walls: Three Sides Supported

pL^2/m and L/H

Model Wall No.	A1	A2	A3	B1	B2	C1	C2	C3
pL^2/m from theory	15.58	15.58	15.58	12.3	12.3	18.75	18.75	18.75
pL^2/m from tests	28.4	17.3	15.6	14.4	15.5	23.2	23.0	20.6
L/H	1.175	1.175	1.175	0.75	0.75	1.5	1.5	1.5

TABLE 6.3

One-Brick Model Walls: Three sides supported

Model Wall No.	E1	E2	G1	G2	H1	H2
pL^2/m from theory	14.2	14.2	22.5	22.5	10.67	10.67
pL^2/m from tests	13.0	14.4	18.4	22.2	8.75	10.4
L/H	1.0	1.0	2.0	2.0	0.5	0.5

TABLE 6.4

One-Brick Model Walls: Four Sides Supported

pL^2/m and L/H

Model Wall No	E3	E4	G3	G4	H3	H4
pL^2/m from theory	24.0	24.0	56.58	56.58	14.39	14.39
$pL^2/$ from tests	26.2	25.7	59.2	53.1	12.4	16.0
L/H	1.0	1.0	2.0	2.0	0.5	0.5

TABLE 6.5

One-Brick Model Walls

Precompression = 50 lb/in^2

pL^2/m and L/H

Boundary Conditions	Three sides supported				Four sides supported			
Model Wall No.	E5	E6	G5	H6	E9	E10	G10	H9
pL^2/m experimental	23.3	20.8	33.7	15.1	35.8	41.8	81.4	20
L/H	1.0	1.0	2.0	0.5	1.0	1.0	2.0	0.5

TABLE 6.6

One-Brick Model Walls

Precompression = 100 lb/in^2

pL^2/m and L/H

Boundary Conditions	Three sides supported					Four sides supported			
Model Wall No	E7	E8	G7	G8	H7	E11	E12	G12	H12
pL^2/m experimental	29.3	28.4	43	68.3	19.1	45.8	53.2	99	27
L/H	1.0	1.0	2.0	2.0	0.5	1.0	1.0	2.0	0.5

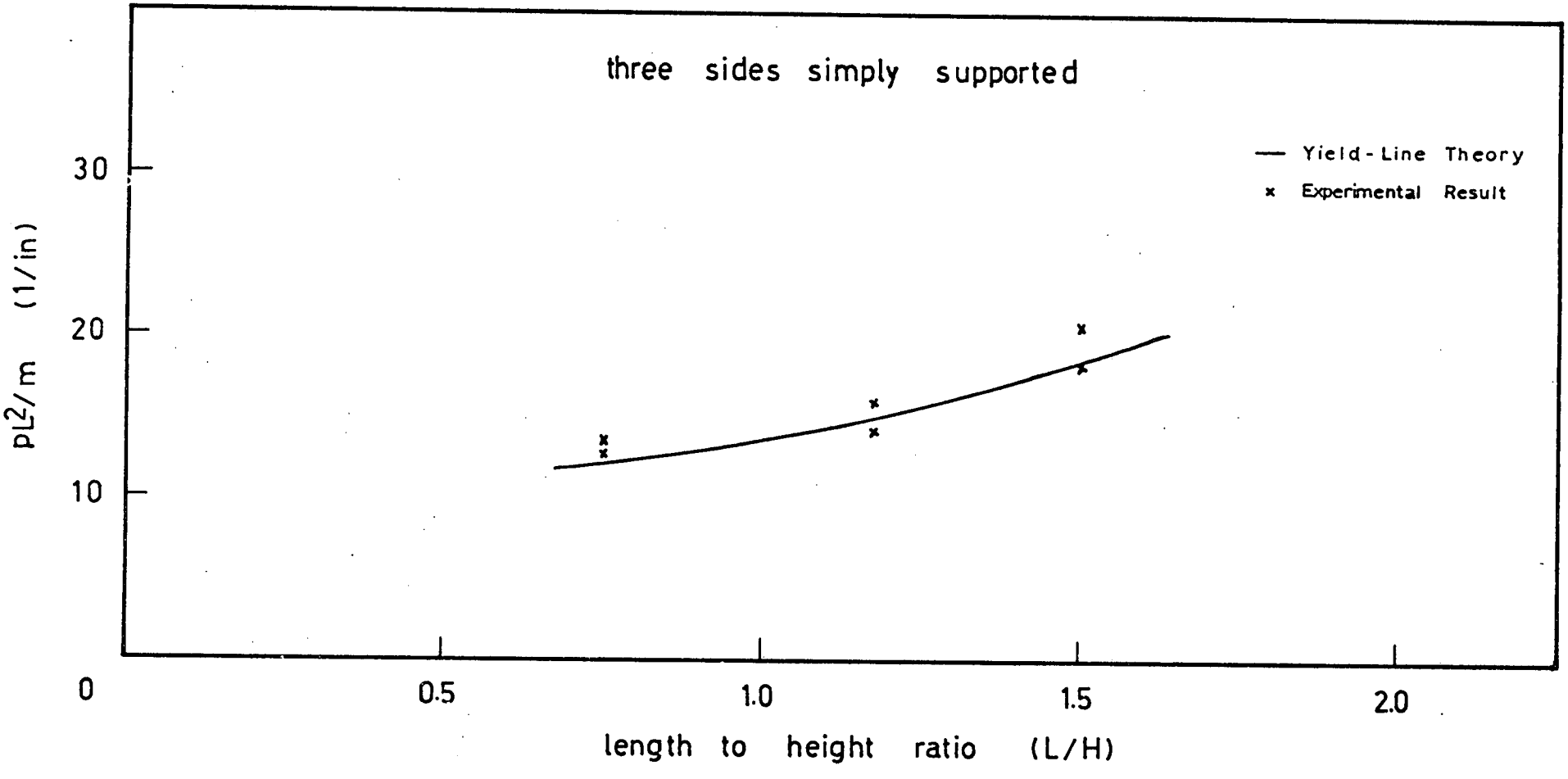

FIG. 6.1: VARIATION OF (pL^2/m) WITH (L/H) FOR HALF - BRICK WALLS

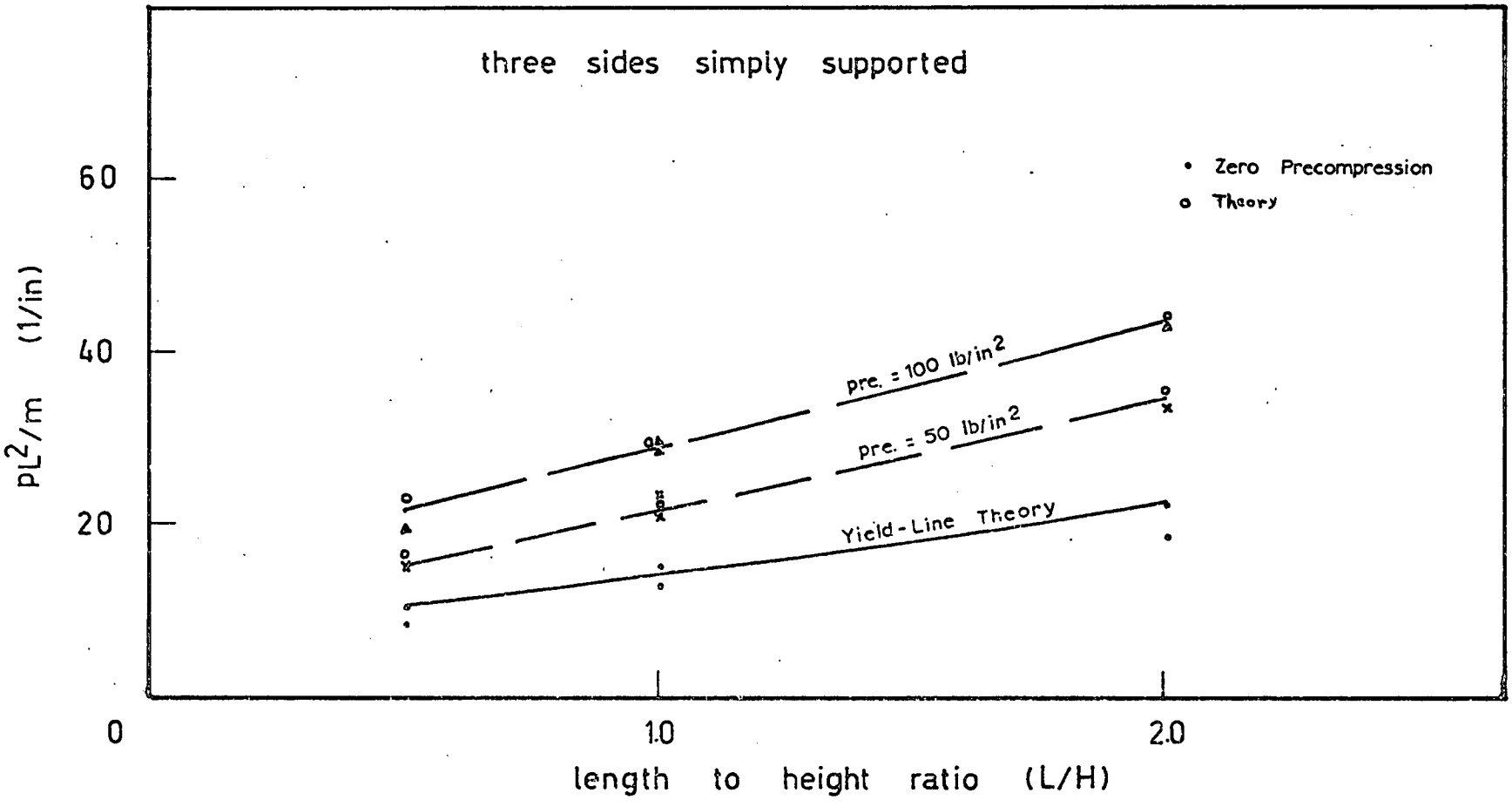

FIG. 6.2: VARIATION OF (pL^2/m) WITH (L/H) FOR ONE – BRICK WALLS

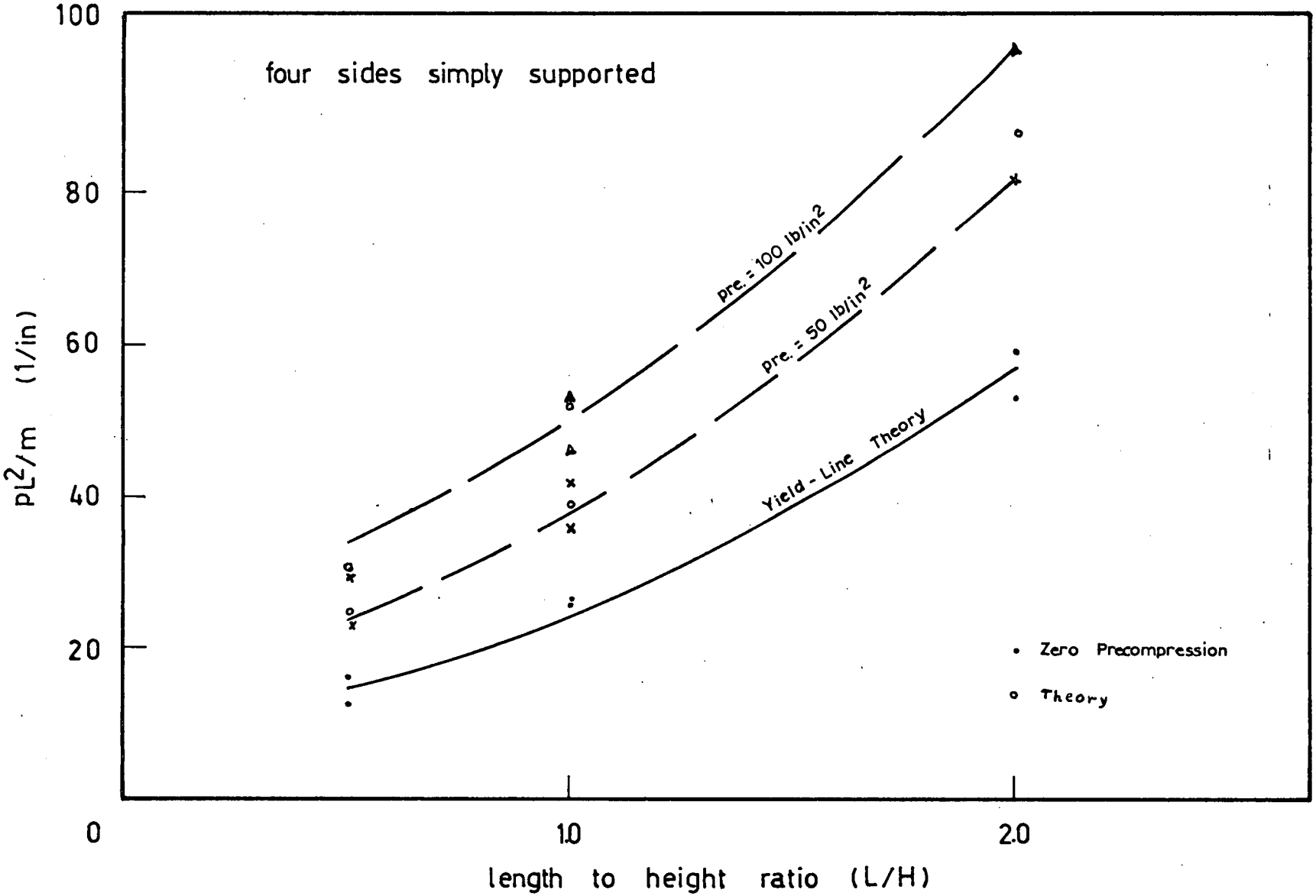

FIG. 6.3: VARIATION OF (PL^2/m) WITH (L/H) FOR ONE – BRICK WALLS

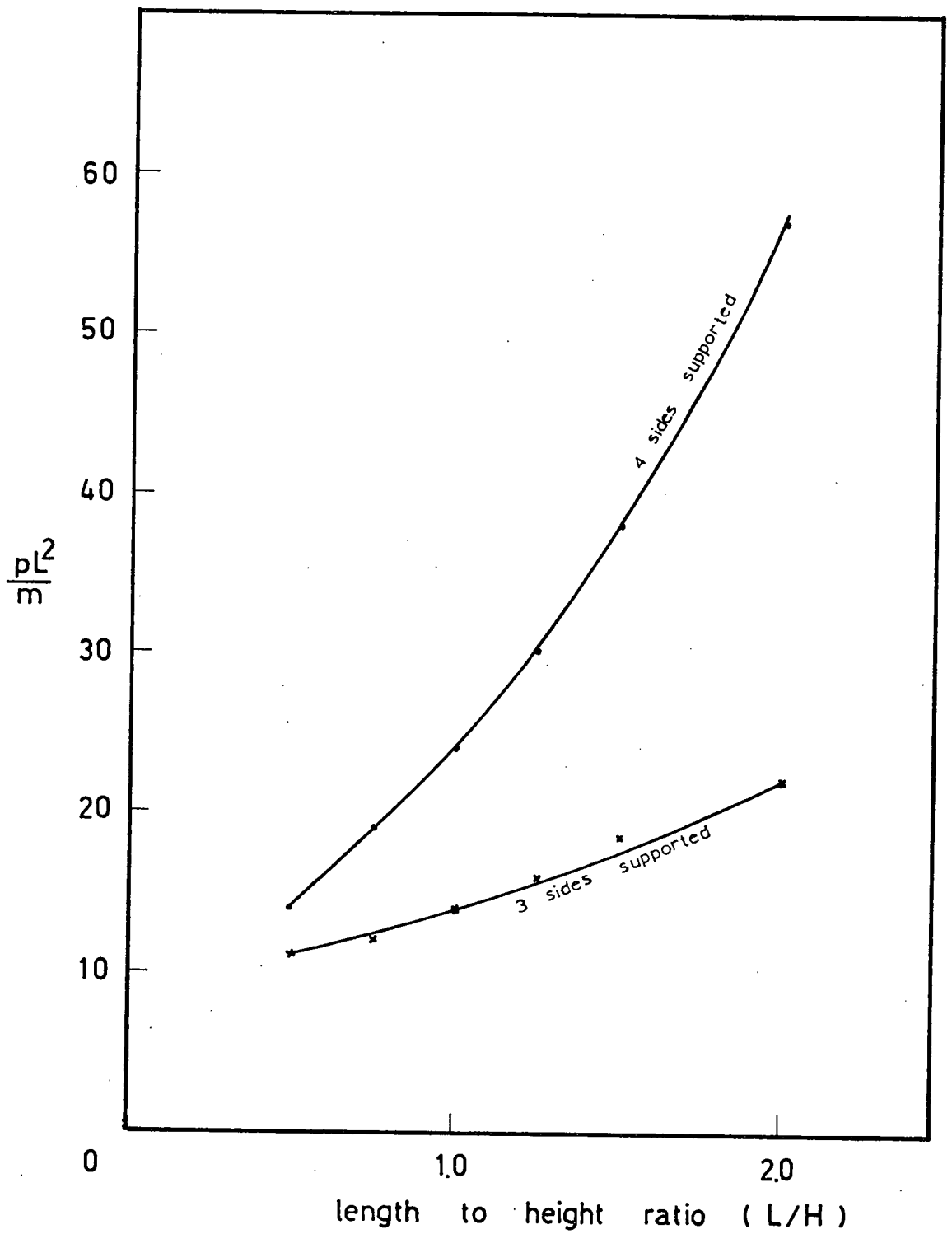
60
50
40
30
20
10
0
$\frac{pL^2}{m}$
4 sides supported
3 sides supported
1.0
2.0
length to height ratio (L/H)

FIG. 6.4

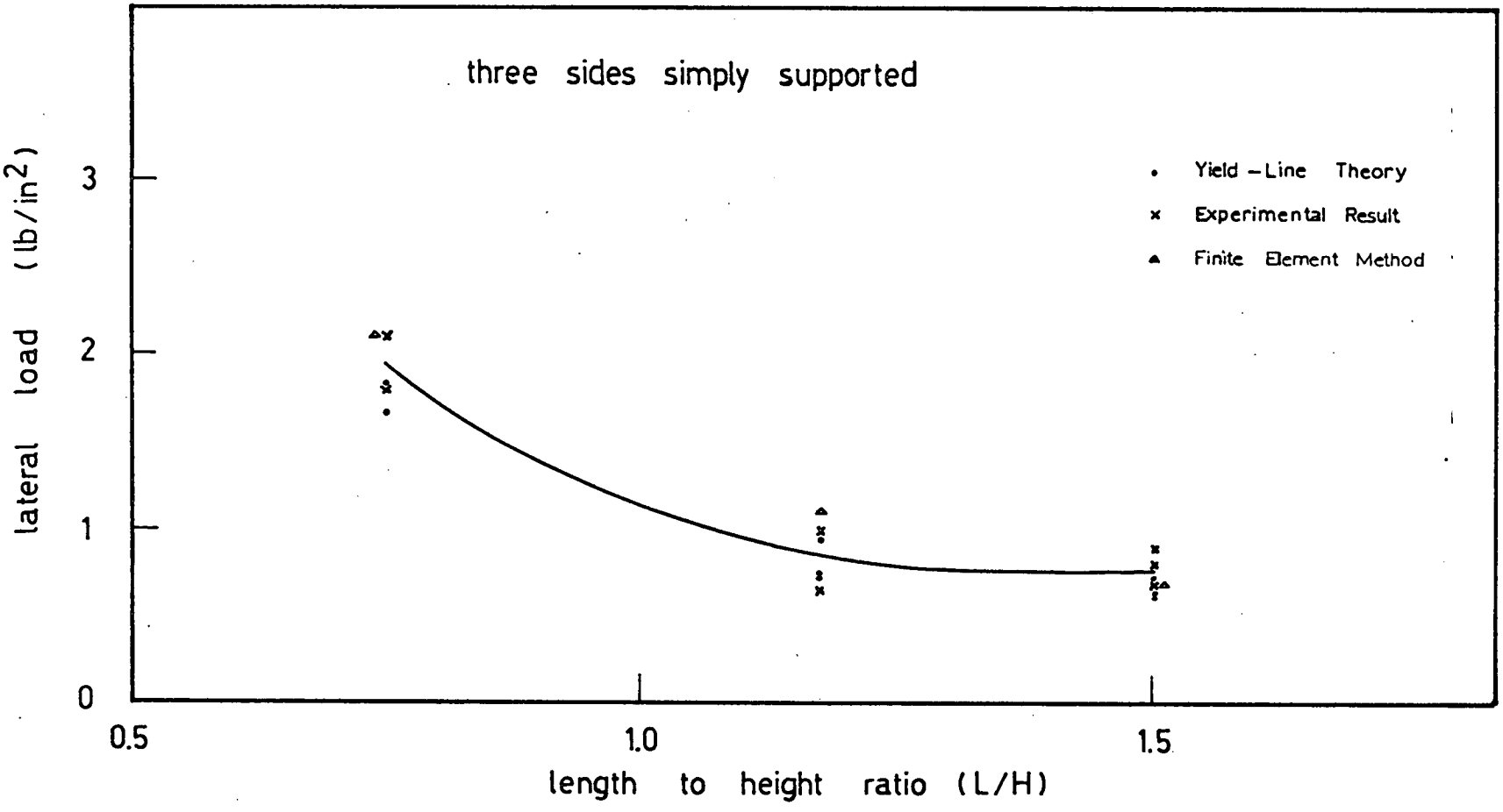

FIG. 6.5: VARIATION OF LATERAL LOAD WITH (L/H) FOR HALF-BRICK WALLS

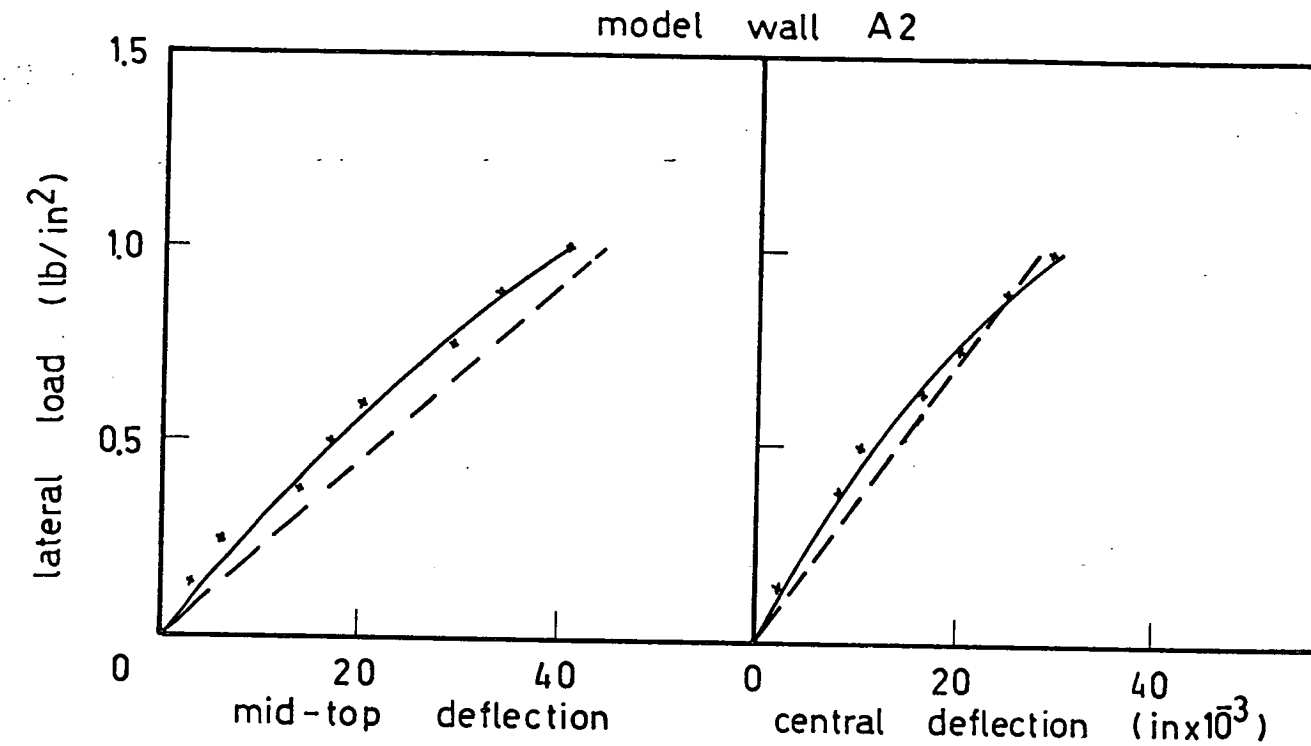

FIG. 6.6

TESTS

F. E.M.

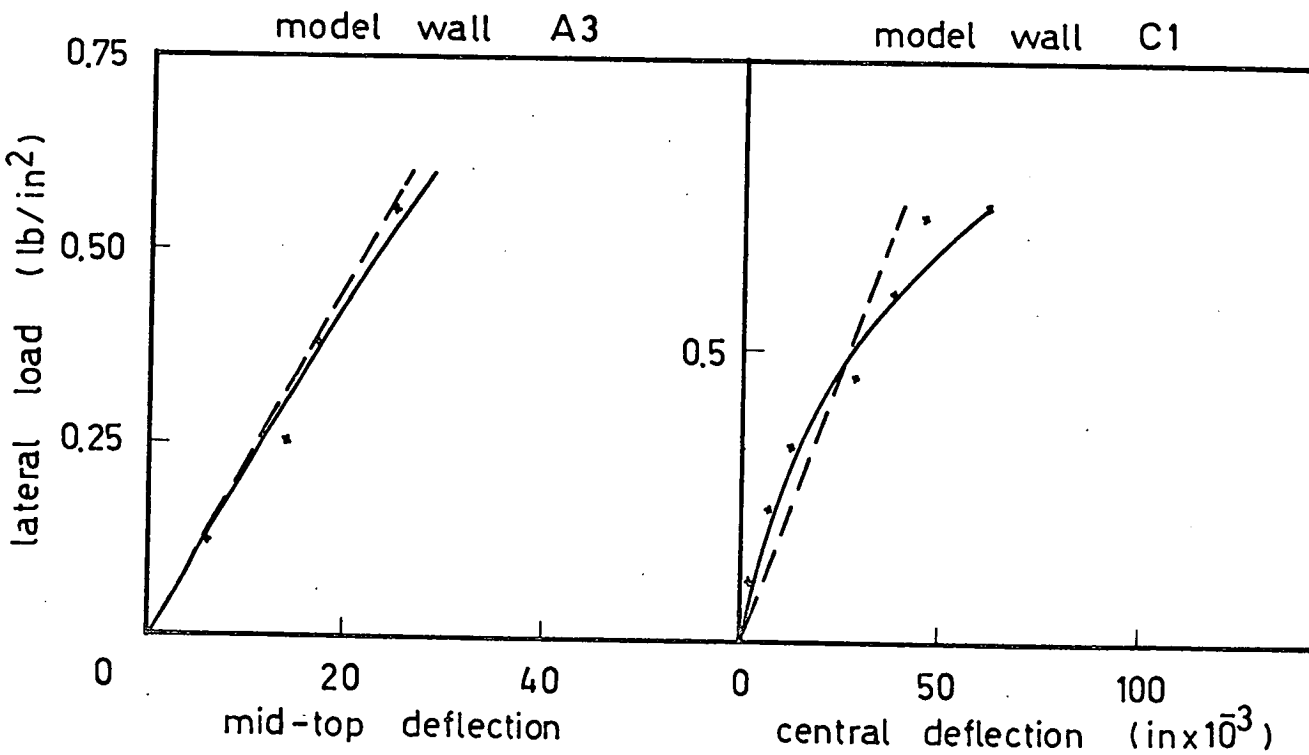

FIG 6.7

FIG 6.8

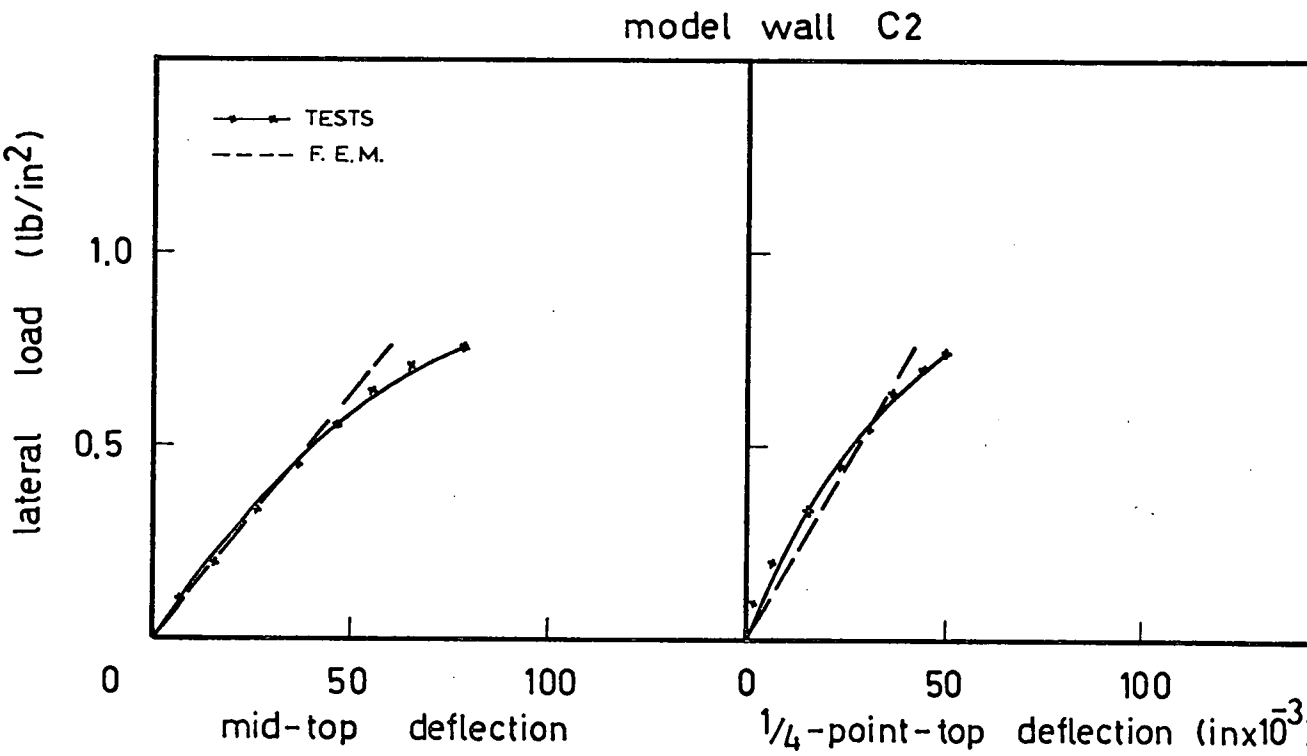
model wall C2
TESTS
F. E.M.
lateral load (lb/in²)
1.0
0.5
0
50
100
mid-top deflection
0
50
100
¼-point-top deflection (in x 10⁻³

FIG. 6.9

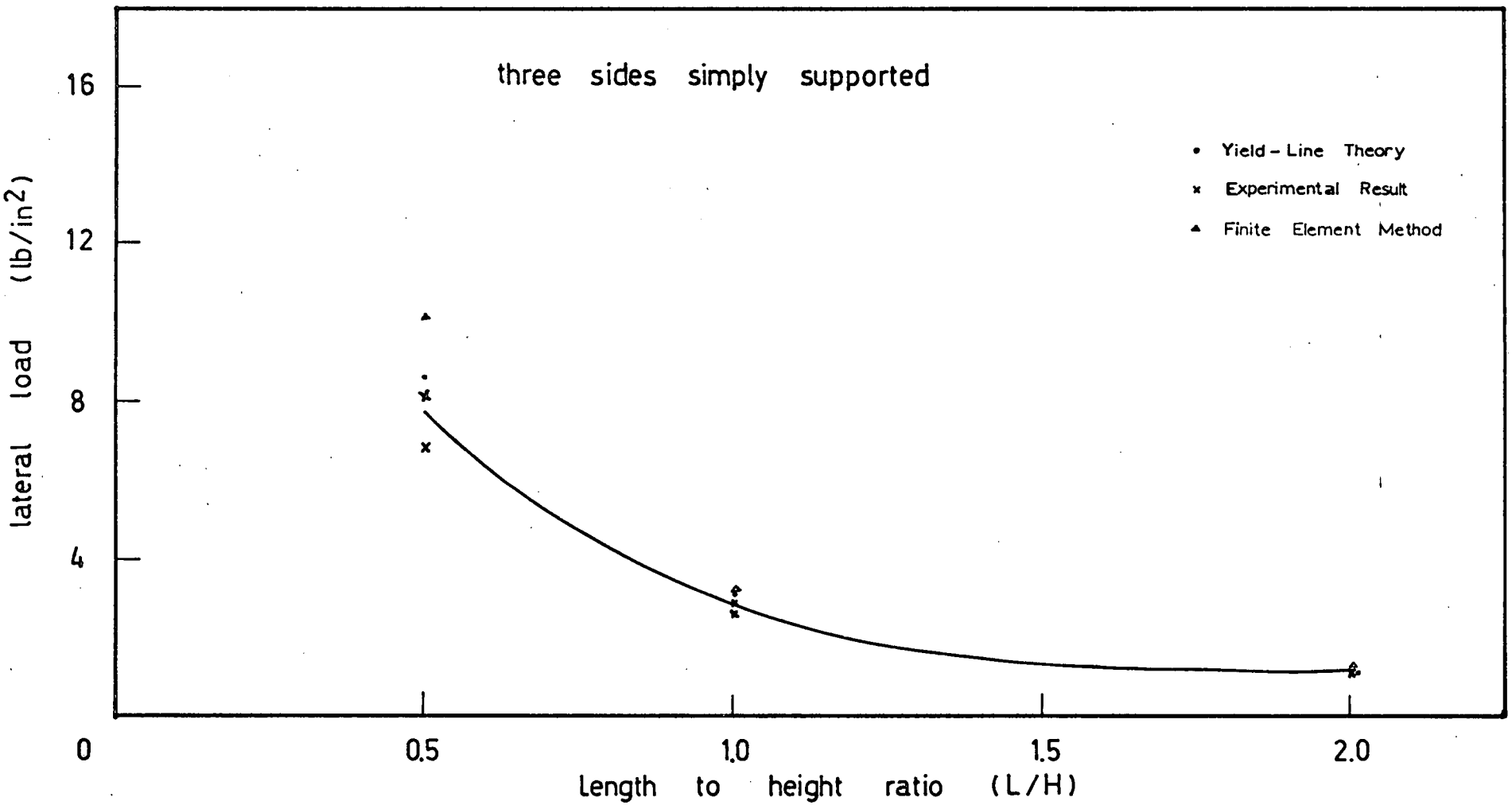

FIG. 6.10 VARIATION OF LATERAL LOAD WITH (L/H) FOR ONE-BRICK WALLS

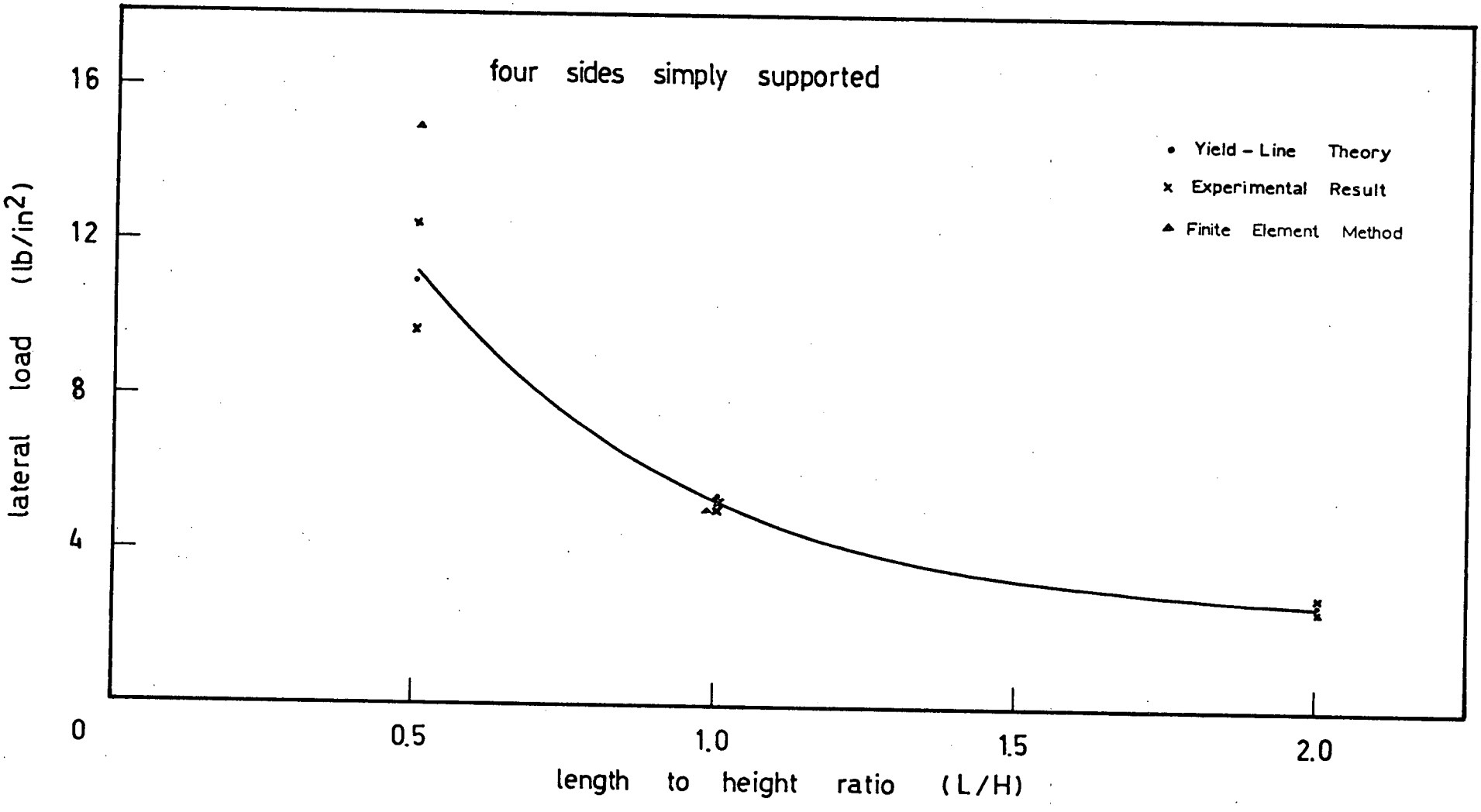

FIG. 6.11 VARIATION OF LATERAL LOAD WITH (L/H) FOR ONE-BRICK WALLS

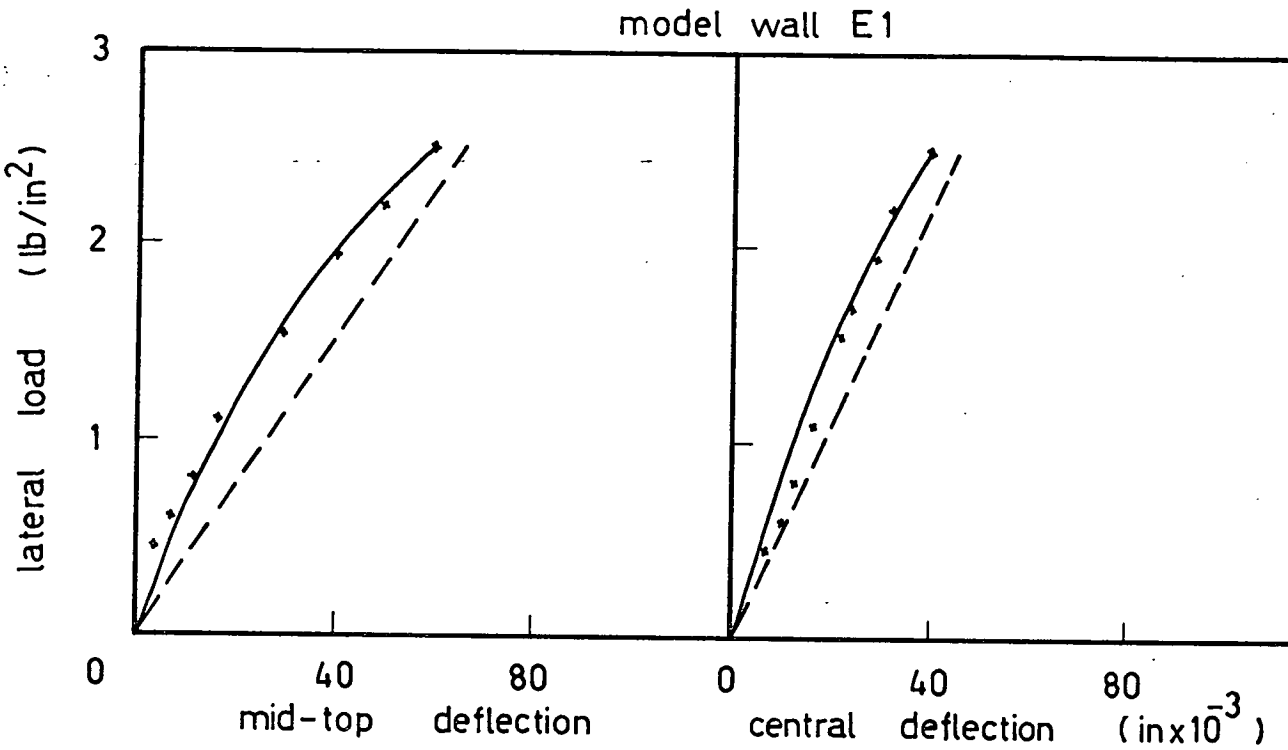

FIG. 6.12

TESTS
F. E. M.

FIG. 6.13

FIG. 6.14

CHAPTER 7

MODULUS OF RUPTURE OF BRICKWORK

7.1 INTRODUCTION

As the yield-line theory has been used for the analysis of the brick walls tested, and the bending moment used in the theory was based on modulus of rupture of brickwork beams it was felt necessary to include in this study a more detailed examination of the modulus of rupture of brickwork for typical brick-mortar combinations and the degree of variability to be expected. The modulus of rupture is a measure of the bond strength between the mortar and units. The ability of mortars to bond firmly to building units is important, because lateral strength and water-tightness of walls are largely dependent on this property. This definition is valid when failure is by break of bond and not the units.

Although shear strength and tensile strength of the brickwork have been regarded as minor properties the increasing interest in load-bearing masonry for non-framed multi-storey construction and in the use of masonry infill to reduce sway of tall steel-framed structures and the need for designing for wind pressures has underlined the importance of these properties.

Experience with various masonry bond tests has shown that most of them give inconsistent results. The magnitude of the deviations in the bond test results reported by Pearson[31] is evidence of the presence of uncontrolled variables of considerable importance. The indeterminate pressure or tapping applied in making specimens has been found[31] to be a major factor affecting bond strength. Also the degree of control of mortar consistency could have some effect. Mortar squeezing out more or less unevenly would leave an indefinite

zone/

zone of little or no bond around the perimeter of the brick faces as verified by McBurney[32]. The effect of these zones upon the flexural strength would be obvious.

7.2 REVIEW OF EXISTING WORK

7.2.1 Factors Affecting The Modulus of Rupture of Brickwork

1 - Effect of mortar tensile strength and bond.

Since a masonry wall spanning vertically may fail in the mortar joint (tensile failure in mortar) or in the interface between the mortar bed joint and the brick (bond failure) or sometimes partly in the mortar, partly at the interface and partly in the brick (Mortar, bond, brick failure), it is to be expected that the mortar and brick tensile strengths and the bond strength are important factors for the modulus of rupture of masonry.

Tests by SCPRF[9] show that the tensile strength of the mortar influenced the modulus of rupture of brick masonry as shown in Fig (7.1). Since the tensile strength of mortar varies with its compressive strength, then it could be stated that the modulus of rupture of brick masonry would vary with mortar compressive strength as is given in Fig. (7.2).

Since the variation between the modulus of rupture of the masonry and mortar tensile strength is not even nearly constant, there must be also other important factors changing with the mortar tensile and bond/

bond strength.

2. - Effect of brick suction and mortar flow.
The modulus of rupture of brick masonry was tested at SCPRF[9] for bricks with different suctions using the same mortar. As can be seen from Table (7.1), the highest modulus of rupture is obtained for a suction of 5 to 30 g/min. The decrease in modulus of rupture for high suction probably does not show up in full magnitude in these tests since bricks with suction higher than 20 g/min per 30 sq. in. were wetted before being laid. The tensile bond strength decreases rapidly with high suction of the bricks as can be seen from Fig. (7.3)[33]. However, the influence of brick suction on the tensile strength of masonry is not only varying with mortar strength or cement content, but also with the mortar flow as shown by Fig (7.4) composed by Plummer and Reardon[33]. This figure must, however, be read with caution since other mortar properties were not held constant for all the points.

3 - Effect of type of mortar.
The effect of type of mortar on the flexural strength of brick masonry was investigated by SCPRF[9]. Results of these tests are given in Table (7.2). Five like specimens were built with each of four types of cement-lime mortars, but with the same type of brick and $^{3}/8$ in joints. These data indicate that transverse strength increases with the tensile strength of the mortar

4 - Effect of mortar bed joint thickness
A series of panels were built, at SCPRF[9], using the same type of brick, but with varying bed joint thickness. Five specimens each were built with joint thicknesses from $\frac{1}{4}$ to $\frac{3}{4}$ in., $in^{1}/8$ in increments for a total of 25 specimens. The results of the flexural tests of these panels are summarised in Table(7.3) and Fig. (7.5). The strength ratios were related to the flexural strength of panels built with $^{3}/8$ in joints. The data indicate that flexural or transverse strength of brick masonry varies inversely as the thickness of the bed joints.

The variation of modulus of rupture with the inverse of thickness of/

of the bed joint is not easily related to one single variable. However, the curing conditions and workmanship could be influenced by a change of bed joint thickness. When the joint thickness increases the chances for a weak spot being enclosed in the joint also increases and thus the statistical effect could be a part of the cause.

5 - Effect of brick strength

As failure of masonry in bending often takes place in the mortar or the interface between mortar and brick, it would be reasonable to assume that brick strength has little effect on the modulus of rupture of masonry. But tests at SCPRF[9] and by Davies reported by Plummer and Reardon[33], show a strong influence of the brick strength on the modulus of rupture of the masonry, (Fig. (7.6). The relationship, however, is different for different mortar mixes, and probably varies with wall thickness. The modulus of rupture is influenced by the brick strength only indirectly because of the change in suction with the change in brick strength. Hallquist[34] reports bending tests on 10-brick wallettes built with cement-lime mortar and two types of bricks; one medium and one hard burned. The modulus of rupture was 33 lb/in^2 for the medium burned (high suction), and 103 lb/in^2 for the hard burned (low suction) bricks.

6 - Effect of masonry compressive strength

Since the compressive strength of masonry is influenced by many of the/

the factors which determine the modulus of rupture, it is conceivable that a relation between the two could exist. Fig (7.7) present data compiled from SCPRF [9] tests. In this case the modulus of rupture is about 4% of the compressive strength. This percentage was a little higher for some tests on concrete block masonry reported by Hedstrom[35]. Tests by Fishburn[36] gave a modulus of rupture between 3% and 5% of the compressive strength depending on the type of mortar.

In a review of the available literature on the adhesion of brick/mortar combinations, Youl and Coats[37] refer to three methods which have been used for testing bond;

(1) Moisture-penetration tests on panels

(2) Tension tests on two brick specimens

(3) Bending or flexural tests on wall panels.

Method (1) does not give any measurement of bond, although it may sometimes reveal a defective bond.

Workers using method (2) have found that the bond strength varies considerably with small changes in the method of making the joint between the two bricks, that is with changes in the degree of compaction of this joint and in the time taken to complete it. Since it is difficult to devise a method of jointing such a small specimen that is reasonably close to a bricklayer's normal method of jointing brickwork/

brickwork, it therefore seems preferable that bond tests should be carried out by method (3) - by bending or flexural tests on wall panels built by normal methods of bricklaying. However, the preparation, storage and testing of these panels will be facilitated if they are kept as small as is consistent with the use of such methods of construction.

Experience at the Building Research Station[38] with the use of small panels of $4\frac{1}{2}$ in brickwork, 12 in high and 27 in wide, has shown that these can be built by normal bricklaying methods and enable the bricklayer to judge the working properties of the mortar in relation to the suction of the bricks.

Compressive tests on concrete cubes made from batches of concrete used on building sites are used to control the quality of concrete. Should it be considered desirable to control the quality of brickwork similarly, it appears that this type of test panel could be built by site bricklayers from sample batches of bricks and mortar, and then transported to the testing laboratory.

The use of such panels to study the effect on bond strength of the water retentivity of the mortar and the suction of the bricks was reported by Ryder[38]. A number of panels were prepared using mortars of different types and compositions where the bricklayer was allowed to control the water content. The results of the transverse strength tests are reproduced in Table (7.4), and in Fig (7.8) where the average transverse strength of the four panels built with each mortar/

mortar mix is plotted against the water retentivity of the mortar. It is apparent that with these high suction bricks the flexural strength is approximately proportional to the water retentivity of the mortar.

To examine the effect of brick suction on the transverse strength, a second series of test panels was built with similar bricks which had been immersed in water for various periods before being laid with two of the mortar mixes of poor water retentivity - the normal 1:1:6 cement=lime=sand mortar and the normal aerated 1:6 cement: sand mortar (mixes No. 1 and No. 3 of Table 7.4). Two of the highly water retentive mortars (mixes No. 2 and No. 4 of Table (7.4) were also used to build test panels with the bricks that had been immersed in water for the longest times. Three panels were built with each variation of mortar composition or brick suction.

The results of the transverse strength tests on these panels, the details of the mortar mixes and the absorption of the bricks at the time of building the panels, are reproduced in Table (7.5).

Comparison of the transverse strengths in Table (7.4) and Table (7.5) for the panels built with mortars No. 2 and No. 4 shows that, with such highly water retentive mortars, wetting the bricks to reduce their suction may cause a slight drop in transverse strength. However, with mortars of poor water retentivity and high-suction bricks, there is a progressive increase in transverse strength as the absorption of the bricks is decreased by wetting (Fig. 7.9).

The/

The effect of mortar strength on the deflection of panels built with soaked wire-cut facing-bricks, and the good agreement between measurements on triplicate panels which was usually obtained in such tests on well-bonded brickwork is shown in Fig. (7.10)[38].

Deflection measurements on panels which failed in bond tended to show greater variation between triplicate panels, and more acute changes in the slope of the load/deflection curve.

7.3 MEASUREMENT OF MODULUS OF RUPTURE OF BRICKWORK

7.3.1 Purpose and Scope of Tests

It is felt that more tests were needed to supplement those already available so that a firm idea could be established about the factors affecting modulus of rupture of brickwork. For this purpose five different types of bricks and two of mortars were used to prepare wallettes and prisms tested with their axes of bending parallel to or at 45° or 90° to the bed joints.

7.3.2. Materials

(i) Bricks

Five types of bricks, Fig. (7.11), of varying properties have been used to conduct this study. Suction rate as determined according to/

to The British Ceramic Research Association recommendations[39], was found to be within the stated limit of 2 kg/m^2/min. A shallow tray was placed on a level table. Two metal rods of equal size were placed a few inches apart, in the bottom of the tray and the tray filled with water until the metal rods were covered to a depth of about 3mm. The brick to be tested, which was dry, was weighted to the nearest gramme and then placed, bed face downwards, on the metal rods and left in position for 60 $\pm$ 2 seconds. It was then removed, surplus water quickly wiped off with a damp cloth and reweighed.

The modulus of rupture of the brick on edge and the crushing strength were also determined[40]. Fig. (7.12) presents the type of failure for bricks tested on edge, and results of bricks properties are listed in Table (7.6)

(ii) Mortar

Cement was rapid hardening "Ferrocrete". Two types of mortar were used with each brick type:

(a) 1:1:6 cement = lime = sand by volume,

(b) 1:$\frac{1}{4}$:3 cement = lime = sand by volume.

4 x 4 x 4 in. mortar cubes and briquettes were tested for crushing and tensile strength respectively. Results of these tests are given/

given in Table (7.7).

7.3.3 Preparation of Samples

Five wallettes four courses high and four bricks long together with five prisms six bricks high were prepared from each brick and mortar type. Every batch of ten specimens was prepared using the same mortar mix obtained by a mixer in which the quantity of water added was controlled by the bricklayer to give a workable mix for the bricks used (Figs (7.14) and (7.15) give views of a sample of wallettes and prisms.

Another series of wallettes six courses high and two bricks long was constructed using four brick types and the two types of mortar above. Three wallettes were built using the same brick and mortar type. One mortar mix was used for all twelve specimens corresponding to the four brick types.

7.3.4 Testing of Samples

At the end of a two-weeks curing period under plastic sheets outdoors, the brickwork samples were subjected to a transverse loading test. The wallettes belonging to the first series were supported on a span of 30 in. by two roller bearers 2 in. diameter, and the load was applied centrally at a rate of 200 lb/min, until failure occurred. Mid-span deflections were measured by dial gauges/

gauges at reasonable load intervals. Fig (7.16) shows one wallette placed in position ready to be tested.

The prisms were tested by means of weights hung from mid-span after they had been simply supported along brick length.

Wallettes of the second series were tested to determine the modulus of rupture on axis at 45^{o} to the bedding plane. A rig was made up of two members each of which was composed of two channel sections welded at right angles. The horizontal channel sections were bolted to the floor of the laboratory through two bolts and the two vertical sections tied together at top and bottom. The two members were placed so that the test sample could be put between them and become supported from the bottom and one vertical edge. Loading was applied at a distance from the corner of the free edges by means of a hydraulically operated jack and a 3-ton load cell through a spreader beam and was recorded by a digital voltmeter. Fig (7.17) gives a general view of the whole set-up. Any clearance between the test specimen and the channel supports was properly packed to prevent any rotation of the specimen when the load was applied.

7.3.5 Results

Three types of failure were noticed when testing wallettes of the first series. Most of the wallettes built with $1:\frac{1}{4}:3$ cement = lime = sand mortar failed either by breaking two bricks and two vertical joints or by combination of break of bond and splitting of a brick. Whereas/

Whereas wallettes prepared using 1:1:6 cement = lime = sand mortar, with a few exceptions, failed in the mortar joints without any bricks breaking. The type of failure of each wallette was therefore recorded, in addition to the load at failure and deflections at various stages of loading. Table (7.8) gives experimental results and Figs. (7.18) and (7.19) show the failure of two wallettes. Figs. (7.20) (7.21), (7.22), (7.23) and (7.24) give plots of mid-span deflections against mid-span loads for some of the wallettes.

All prisms failed by the breaking of bond between brick and mortar. Tables (7.9) and (7.10) present the calculated modulus of rupture for both prisms and wallettes prepared from the five types of bricks and the two mortars. Figs. (7.25), (7.26), (7.27),(7.28), (7.29) and (7.30) indicate the variation of the modulus of rupture of wallettes with suction rate of the bricks, modulus of rupture of prisms and bricks, and crushing strength of bricks and the brick-work. Variation of modulus of rupture of bricks with their suction rate is also given.

Wallettes of the second series failed by the break of bond between mortar and bricks in variable ways in a stepping manner as shown in Figs. (7.31), (7.32), (7.33), (7.34) and (7.35). Measurements were taken for the failure load, the distance of its point of application from the cracked section and the length of the crack. Modulus of rupture was then calculated using these measurements from which the maximum bending moment and section modulus were obtained. Results of these tests are listed in Table (7.11).

7.3.6 Discussion

Information on the transverse strength of brick structures is not as extensive as that available on the compressive strength of walls and piers. Transverse tests of specimens prepared from materials representative of those used in construction, provide data from which it is possible to estimate the expected transverse strength of brickwork if the type of workmanship and curing conditions are maintained the same.

The resistance of brick walls to lateral loads applied normal to the face of the wall depends primarily upon the bond strength of the mortar joints through which failures normally occur. Bond between mortar and brick is affected by mortar composition and flow, suction of the bricks when laid and the method of forming the mortar joint.

The Brick property that appears to have the greatest influence on the transverse strength of brickwork is the suction rate of the unit at the time of laying, since it greatly affects the bond developed between the brick and mortar. This is shown in Fig. (7.25) for the two types of mortar indicated although there is considerable scatter of test results. This scatter could be due, in part , to another variable that can affect the bond developed at the brick-mortar interface. This is the character of the bedding surface and the extent to which mechanical inter-locking of the mortar with brick is/

is achieved.

A look at Tables (7.9), (7.10) and (7.11) would show the variation of the values obtained for the modulus of rupture using two different types of mortar. Higher values of modulus of rupture are associated with the stronger mortar in all three types of test carried out.

The degree of scatter experienced with the variation of the modulus of rupture of brickwork with that of the units makes it difficult to draw any correlation although the results obtained with the 1:$\frac{1}{4}$:3 mortar are more convincing in that direction.

The same could be said about the variation of the modulus of rupture with the crushing strength of the brick or brickwork; Figs (7.29), (7.30). As the failure of brickwork in bending often takes place in the mortar or in the interface between brick and mortar, it would be reasonable to assume that the brick strength has only an indirect effect on the modulus of rupture of brickwork because of the change in suction rate with the change in brick strength.

A direct relation between the modulus of rupture of wallettes with that of prisms was found from the test results as given in Fig (7.26). The/

The relation also depends on the type of mortar used.

From the test results of wallettes with axis of bending at 45^{o} to the bed joints, it has been confirmed that the modulus of rupture of brickwork is gradually increased with increasing angle between the bed joints and the axis of bending up to 90^{o}; Figs (7.36), (7.37).

Based on the results obtained for the modulus of rupture when using $1:\frac{1}{4}:3$ mortar and for suction rates of the bricks below 2 $kg/m^2/min$, its value has been estimated as 100 lb/in^2 in a direction normal to the perpend joints. This value proves that the permissible tensile stress given by CP 111[1] is on the safe side as the resulting factor of safety will be equal to 5. If higher values of modulus of rupture than those specified in CP 111[1] are to be used, tests should be conducted using the same materials and workmanship as those in construction. The estimated value of modulus of rupture obtained using 1:1:6 mortar was about 80 lb/in^2, (Fig (7.25).

Too low values to give a reasonable factor of safety over the permissible stress of CP 111[1] were obtained in the direction normal to bed joints, Fig (7.25)

TABLE 7.1

Effect of Brick Suction on Transverse Strength of 4 in. Brick Wallettes

Suction of Brick, g per min per 30 sq. in.	Wallette strength		
	N	Modulus of Rupture lb/in^2	Strength Ratio
Less than 5	30	113	0.84
5 to 30	80	135	1.00
Over 30	25	98	0.73

16 x 16 in. wallettes built with $1:\frac{1}{2}:4\frac{1}{2}$ mortar.

N: number of specimens tested.

TABLE 7.2

Effect of Mortar Tensile Strength on Transverse Strength of 4-in Brick Masonry Panels

MORTAR			PANELS		
Type	Proportions by Volume	Tensile Strength, lb/in^2	n	Modulus of Rupture lb/in^2	Relative strength
M	$1:\frac{1}{4}:3$	278	5	137	1.10
S	$1:\frac{1}{2}:4\ \frac{1}{2}$	200	5	125	1.00
N	1:1:6	128	5	96	0.77
O	1:2:9	48	5	85	0.68

TABLE 7.3

Effect of Mortar Bed Joint Thickness on Transverse Strength of 4 - in. Brick Masonry Panels

Bed Joint Thickness in	PANELS		
	n	Modulus of Rupture lb/in^2	Strength Ratio
$\frac{1}{4}$	5	154	1.23
3/8	5	125	1.00
1/2	5	104	0.83
5/8	5	83	0.66
3/4	5	64	0.51

TABLE 7.4

Transverse strength tests on panels built with dry bricks

Mix No	Sand	Mortar type and composition (a) by wt. (b) by vol. (cement=lime=sand)	Water Content (% of dry mix)	Air Content (%)	Consistence (mm penetration)	Water retention (%)	M of R at 28 days (lb/in^2)	Panel strength at 28 days	
								Failing load (t) and type of failure (1)	Average M of R (lb/in^2)
1	B	Normal (a) 1:0.4:6.6 (b) 1:1:6	17.4	-	12.0	45	386	0.11 B 0.18 B 0.23 B 0.23 B	70
2	B	Activated (a) 1:0.4:6.6 (b) 1:1:6	20.9	-	12.2	63	345	0.65 A 0.72 B 0.45 B 0.43 A	210
3	B	Normal aerated (a) 1: 0:6.6 (b) 1: 0:6	14.4	19	9.8	51	322	0.20 B 0.16 B 0.17 B 0.29 B	75
4	B	Special aerated (a) 1: 0:6.6 (b) 1: 0:6	16.2	17	11.6	65	337	0.86 A 0.65 A 0.56 A 0.74 A	260
5	B	Masonry cement (a) 1: 0:5.25 (b) 1: 0:4½	14.9	18	10.6	44	340	0.23 B 0.22 B 0.22 B 0.19 B	80

TABLE 7.4 (contd.....)

Mix No	Sand	Mortar type and composition (a) by wt. (b) by vol. (cement=lime=sand)	Water Content (% of dry mix)	Air Content (%)	Consist-ence (mm penetrat-ion	Water retention (%)	M of R at 28 days (lb/in^2)	Panel strength at 28 days	
								Failing load (t) and type of failure (1)	Average M of R (lb/in^2)
6	C	Normal (a) 1:0.4:6.6 (b) 1:1:6	21.5	-	11.8	54	321	0.50 B 0.40 B 0.61 B 0.44 B	180
7	C	Activated (a) 1:0.4:6.6 (b) 1:1:6	23.2	-	11.1	69	296	0.62 A 0.68 B 0.58 B 0.36 B	210
8	C	Normal aerated (a) 1: 0:6.6 (b) 1: 0:6	18.9	15	11.3	50	348	0.46 AB 0.49 B 0.25 B 0.51 B	160
9	C	Special aerated (a) 1: 0:6.6 (b) 1: 0:6	18.9	15	8.0	62	369	0.64 B 0.51 B 0.61 B 0.62 B	220
10	C	Masonry cement (a) 1: 0:5.25 (b) 1: 0:4$\frac{1}{2}$	16.9	17	11.7	53	320	0.35 B 0.35 B 0.31 B 0.35 B	125

NOTE - The suffix A to the failing load indicates a straight fracture of the panel in the transverse test, breaking two bricks and two vertical joints. The suffix B indicates a bond failure, with no broken bricks, whereas AB indicates a partial bond failure, normally in the top course only.

TABLE 7.5

Transverse Strength Tests on Panels Built with Bricks of Varying Suction

Brick Condition		I.R.A. gm/min/ 30 sq in	Mortar Mix (1)	Water content (% of dry mix)	Air content (%)	Consist-ence (mm penetrat-ion)	Water retention (%)	M of R at 28 days (lb/in^2)	Panel Strength at 28 days	
Soaked	Drained								Failing load (t) and type of failure (2)	Aver-age M of R (lb/in^2)
DRY		48	No. 1	18.6	-	12.3	35	550	0.36 B 0.21 B 0.26 B	100
DRY		48	No. 3	14.4	20	9.4	43	400	Nil B Nil B Nil B	Nil
1Min	½ h	27	No. 1	18.2	-	9.9	37	470	0.48 AB 0.46 B 0.54 AB	185
1Min	½ h	27	No. 3	14.5	19	9.0	42	430	0.35 B 0.18 B 0.21 B	90
1Min	24 h	34	No. 1	18.5	-	10.8	39	515	0.47 B 0.48 AB 0.51 AB	180

TABLE 7.5 (contd.....)

Brick Condition		I.R.A. gm/min/ 30 sq in	Mortar Mix (1)	Water content (% of dry mix)	Air content (%)	Consist-ence (mm penetrat-ion)	Water Retention (%)	M of R at 28 days (lb/in^2)	Panel Strength at 28 days	
Soaked	Drained								Failing load (t) and type of failure (2)	Aver-age M of R (lb/in^2)
1 Min	24 H	34	No. 3	14.5	20	10.0	42	440	0.11 B 0.20 B 0.15 B	55
24 h	24 h	18	No. 1	18.2	-	9.5	40	460	0.56 A 0.51 A 0.64 A	210
24 h	24 h	18	No. 3	14.5	20	9.3	40	450	0.59 AB 0.55 A 0.56 B	210
24 h	24 h	18	No. 2	20.2	-	11.0	65	390	0.45 A 0.60 A 0.60 A	205
24 h	24 h	18	No. 4	16.9	18	10.3	68	320	0.55 A 0.59 A 0.60 A	220

NOTE 1 - The mortar mixes are numbered to correspond with the mix compositions shown in Table 7.4

NOTE 2 - The suffix A indicates a straight fracture of the panel, breaking two bricks and two vertical joints. B indicates bond failure, with no bricks broken, whereas AB indicates a partial bond failure, normally in the top course only.

TABLE 7.6

Properties of The Bricks In Present Investigation

Type of Brick	Modulus of Rupture (lb/in^2)	Crushing Strength (lb/in^2)	Suction Rate $kg/m^2/min$
5-Hole[1]	726	5393	1.90
	649	4425	1.82
	693	5116	1.80
		4978	1.96
		3180	1.70
			1.96
Average =	689	4618	1.86
Avonbridge[2]	378	1871	1.95
	254	2227	2.10
	497	1603	2.58
	311	1663	1.30
	233	2257	
Average =	335	1924	1.98
Deep-frog[3]	717	3270	2.0
	698	3211	1.3
	557	2692	2.0
	486	3671	1.9
	640	3231	1.4
Average =	620	3215	1.7
3-Hole[4]	885	4440	1.93
	939	5766	1.01
	975	4043	1.93
	518	5302	1.61
	723	4308	
Average =	808	4772	1.62
NCB Roslin[5]	390	3724	1.2
	311	2706	0.7
	1021	3600	0.7
	474	2799	1.5
	353	2917	0.9
	653		0.7
Average =	534	3149	0.95

TABLE 7.6 (contd.....)

(1)	Brick with five rectangular holes.
(2)	Two rounded shallow frogs on both faces of the brick
(3)	A deep frog on one face, the other face being flat.
(4)	Two circular and one square hole in between.
(5)	A rounded and a right-angled shallow frogs on the faces of the brick.

TABLE 7.7

MORTAR PROPERTIES

Proportions by Volume	Compressive strength (lb/in^2)	Tensile strength (lb/in^2)
1:1:6 cement: lime: sand	960 1008 1078 834 990 1039	150 155 170 168 165 170
1:$\frac{1}{4}$:3 cement: lime: sand	2500 2960 2408 2310 2600 2408	273 284 248

TABLE 7.8

Type of brick	Type of Mortar	Wallettes Dimensions (in)	Test No	Mid-span Load (tons)	Mid-span deflection (in x 10^{-3})
5-hole	1:1:6 cement: lime: sand: (by volume)	$35 \times 12\frac{7}{8} \times 4\frac{1}{8}$	1	0	0
				0.05	5
				0.10	7
				0.15	9
				0.20	14
				0.23	
			2	0	0
				0.05	9
				0.10	12
				0.15	16
				0.20	19
				0.23	
			3	0	0
				0.05	4
				0.10	6
				0.15	7
				0.20	9
				0.25	11
				0.26	

Table 7.8 (contd....)

Type of brick	Type of Mortar	Wallettes Dimensions (in)	Test No	Mid-span Load (tons)	Mid-span Deflection (in x 10^{-3})
5 - hole	1:1:6	35 x $12\frac{7}{8}$x$4\frac{1}{8}$	4	0 0.05 0.10 0.15 0.20 0.205	0 2 4 6 8
			5	0 0.05 0.10 0.12	0 2 7 16
	1:$\frac{1}{4}$:3	35 x $12\frac{7}{8}$x$4\frac{1}{8}$	1	0 0.05 0.10 0.15 0.20 0.25 0.30	0 2 4 5 7 8 15
			2	0 0.05 0.10 0.15 0.195	0 6 8 11 15
			3	0 0.05 0.10 0.15 0.20 0.25 0.29	0 2 4 6 8 11
5-hole	1:$\frac{1}{4}$:3	35 x $12\frac{7}{8}$x$4\frac{1}{8}$	4	0 0.05 0.10 0.14	0 1 5 8

TABLE 7.8 (contd.....)

Type of Brick	Type of Mortar	Wallettes Dimensions (in)	Test No	Mid-span Load (tons)	Mid-span Deflection (in x 10^{-3})
			5	0 0.05 0.10 0.15 0.20	0 1 2 3 5
Deep frog	1:1:6	$34 \times 11\frac{5}{8} \times 4\frac{1}{8}$	1	0 0.05 0.10 0.15 0.18	0 7 11 15 21
			2	0 0.05 0.10 0.15 0.18	0 7 11 15 21
			3	0 0.05 0.10 0.15 0.20 0.25 0.27	0 3 4 5 7 9 11
Deep frog	1:1:6	$34 \times 11\frac{5}{8} \times 4\frac{1}{8}$	4	0 0.05 0.10 0.15 0.20 0.22	0 5 8 11 14 17
			5	0 0.05 0.10 0.15 0.175	0 3 7 12 18

TABLE 7.8 (contd.....)

Type of Brick	Type of Mortar	Wallettes Dimensions (in)	Test No.	Mid-span Load (tons)	Mid-span Deflection (in x 10^{-3})
Deep frog	1:$\frac{1}{4}$:3	34x11$\frac{5}{8}$x4$\frac{1}{8}$	1	0 0.05 0.10 0.15 0.20 0.25 0.28	0 2 4 6 8 10 12
			2	0 0.05 0.10 0.15 0.20 0.25 0.30 0.31	0 7 9 12 15 18 20
			3	0 0.05 0.10 0.15 0.20 0.25 0.30 0.35	0 9 13 16 18 20 21 24
			4	0 0.05 0.10 0.15 0.20 0.25 0.30 0.335	0 5 7 9 12 15 18
Deep frog	1:$\frac{1}{4}$:3	34x11$\frac{5}{8}$x4$\frac{1}{8}$	5	0 0.05 0.10 0.15 0.20 0.25 0.28	0 4 6 8 11 14

TABLE 7.8 (contd....)

Type of Brick	Type of Mortar	Wallettes Dimensions (in)	Test No	Mid-span Load (tons)	Mid-span Deflection (in x 10^{-3})
Avon-bridge	1:1:6	$36\frac{5}{8}$ x $13\frac{1}{2}$ x $4\frac{1}{4}$	1	0 0.05 0.10 0.115	0 8 13
			2	0 0.05 0.10 0.15 0.18	0 6 9 12 19
			3	0 0.05 0.10 0.15 0.20 0.22	0 6 7 9 12
	1:1:6	$36\frac{5}{8}$ x $13\frac{1}{2}$ x $4\frac{1}{4}$	4	0.225	failure
			5	0.175	failure
Avon-bridge	1:$\frac{1}{4}$:3	$36\frac{5}{8}$ x $13\frac{1}{2}$ x $4\frac{1}{4}$	1	0 0.05 0.10 0.15 0.20 0.25 0.405	0 - 1 2 3 4
			2	0 0.05 0.10 0.15 0.20 0.25 0.285	0 3 7 10 14 18 25

TABLE 7.8 (contd.....)

Type of Brick	Type of Mortar	Wallettes Dimensions (in)	Test No	Mid-span load (tons)	Mid-span deflection (in x 10^{-3})
Avon-bridge	1:$\frac{1}{4}$:3	$36\frac{5}{8}$ x $13\frac{1}{2}$ x $4\frac{1}{4}$	3	0 0.05 0.10 0.15 0.20 0.25 0.30 0.32	0 4 5 7 8 9 11 15
			4	0 0.05 0.10 0.15 0.20 0.25 0.30	0 3 5 8 12 15 20
			5	0 0.05 0.10 0.15 0.17	0 4 6 7 11
NCB Roslin	1:1:6	36 x 13 x $4\frac{1}{8}$	1	0 0.05 0.10 0.15 0.19	0 4 6 8 12
			2	0 0.05 0.10 0.15 0.20 0.225	0 6 14 19 25 34
NCB Roslin	1:1:6	36 x 13 x $4\frac{1}{8}$		0 0.05 0.10	0 9 11

TABLE 7.8 (contd.....)

Type of Brick	Type of Mortar	Wallettes Dimensions (in)	Test No	Mid-span load (tons)	Mid-span deflection (in x 10^{-3})
NCB Roslin	1:1:6	36 x 13 x $4\frac{1}{8}$	3	0.15 0.20 0.236	13 17 23
			4	0 0.05 0.10 0.15 0.20 0.25 0.255	0 3 4 6 9 13
			5	0 0.05 0.10 0.15 0.20 0.25 0.28	0 8 9 13 16 20 28
	1:$\frac{1}{4}$:3	36 x 13 x $4\frac{1}{8}$	1	0 0.05 0.10 0.15 0.20 0.25 0.30 0.36	0 2 3 5 7 9 13 16
			2	0 0.05 0.10 0.15 0.20 0.25 0.26	0 2 4 6 9 14 20
				0 0.05 0.10	0 3 5

TABLE 7.8 (contd....)

Type of Brick	Type of Mortar	Walletes Dimensions (in)	Test No	Mid-span load (tons)	Mid-span deflection (in x 10^{-3})
NCB Roslin	1:$\frac{1}{4}$:3	36 x 13 x $4\frac{1}{8}$	3	0.15 0.20 0.25	8 12 17
			4	0 0.05 0.10 0.15 0.20 0.25 0.29	0 1 2 5 8 13 32
			5	0 0.05 0.10 0.15 0.20 0.25 0.30	0 1 3 5 6 8 10
3-hole	1:1:6	35 x 12 x $4\frac{1}{4}$	1	0.10	failure
			2	0 0.05 0.10 0.15 0.20	0 2 4 6 9
3-hole	1:1:6	35 x 12 x $4\frac{1}{4}$	3	0 0.05 0.10 0.15	0 1 4 9
			4	0.117	failure
			5	0.18	failure
				0	0

TABLE 7.8 (contd.....)

Type of Brick	Type of Mortar	Wallettes Dimensions (in)	Test No	Mid-span load (tons)	Mid-span deflection (in x 10^{-3})
3 -hole	1:$\frac{1}{4}$:3	35 x 12 x 4$\frac{1}{4}$	1	0.05 0.10 0.15 0.20 0.25 0.30 0.35	2 3 6 7 8 9 13
			2	0 0.05 0.10 0.15 0.20 0.25 0.28	0 1 3 5 11 16 22
			3	0 0.05 0.10 0.15 0.20 0.25 0.30 0.35 0.376	0 2 3 5 7 9 12 15
			4	0 0.05 0.10 0.15 0.20 0.25 0.28	0 3 4 6 7 9 11
3-hole	1:$\frac{1}{4}$:3	35 x 12 x 4$\frac{1}{4}$	5	0 0.05 0.10 0.15 0.20 0.25 0.30 0.345	0 1 2 2.5 3 4 6 9

TABLE 7.9

MORTAR 1:1:6

Type of Brick	MODULUS OF RUPTURE LB/IN^2					
	Wallettes	Standard deviation 's'	Coefficient of variation %	Prisms	Standard deviation 's'	Coefficient of variation %
5-Hole	105 105C 118 93 55 Av.= 95	24	25	8 13 8 11 Av.=10	2.5	24
Deep-Frog	92C 59 138 112 89C Av.= 98	29	30	10 9 15 17 Av.=13	3.9	30
Avon-bridge	91 48 74 93 72 Av.= 76	18	24	25 11 11 8 Av.=14	7.6	55
NCB Roslin	87 103C 108C 116 128 Av.= 108	15	14	2 25 8 20 Av.=14	10.6	76
3-Hole	47 92 69 54 84 Av.= 69	19	28	10 11 8 4 Av.= 8	3.1	39

C: Failure by combination of break of bond and splitting of a brick

TABLE 7.10

MORTAR 1:$\frac{1}{4}$:3

Type of brick	MODULUS OF RUPTURE, LB/IN^2					
	Wallettes	Standard deviation 's'	Coefficient of variation %	Prisms	Standard deviation 's'	Coefficient of variation %
5 - hole	138 90 133 64 92 Ave=103	31	30	18 24 16 36 20 Ave=23	7.9	35
Deep-frog	147 B 163 B 184 B 176 C 147 Ave=163	17	10	26 18 30 33 Ave=30	6.5	24
Avon-bridge	167 B 118 C 132 B 124 C 70 Ave=122	35	29	42 56 32 37 49 Ave=43	9.5	22
NCB Roslin	164 B 118 C 114 C 132 C 137 C Ave=133	20	15	22 27 30 25 26 Ave=26	8.5	33
3-hole	173 138 C 186 138 170 Ave=161	22	14	42 13 17 27 25 Ave=25	11.2	45

B = Failure by breaking two bricks and two vertical joints.

C = Failure by combination of break of bond and splitting of a brick

TABLE 7.11.

Type of Brick	Type of Mortar	Failure Load (tons)	Moment Arm (in)	Crack Length (in)	Modulus of Rupture (lb/in^2)
Deep-frog	1:$\frac{1}{4}$:3	0.28	8.4	18.4	101
		0.24	9.2	18.4	95
		0.16	10.8	18.4	74
	Average=				90
	1:1:6	0.16	3.0	18.4	21
		0.11	6.8	18.4	32
		0.16	8.8	18.4	60
	Average=				38
5-Hole	1:$\frac{1}{4}$:3	0.27	6.8	19.6	74
		0.37	6.8	19.2	104
		0.26	4.8	19.2	51
	Average=				76
	1:1:6	0.18	6.0	19.2	44
		0.24	6.4	20.0	61
		0.15	1.8	18.4	12
	Average=				39
	1:$\frac{1}{4}$:3	0.16	8.8	18.4	60
		0.17	6.8	18.4	50

TABLE 7.11 (contd.....)

Type of Brick	Type of Mortar	Failure Load (tons)	Moment Arm (in)	Crack Length (in)	Modulus of Rupture (lb/in^2)
3-Hole		0.22	6.8	18.4	64
	Average=				58
		0.10	7.2	19.6	29
	1:1:6	0.24	2.4	20.0	23
		0.18	2.4	20.0	17
	Average=				23
Avonbridge		0.20	4.8	17.6	40
	1:$\frac{1}{4}$:3	0.38	7.2	22	93
		0.163	7.2	20	44
	Average=				59
		0.26	1.6	18.8	16
	1:1:6	0.29	3.6	22	35
		0.35	2.4	18.8	33
	Average=				28

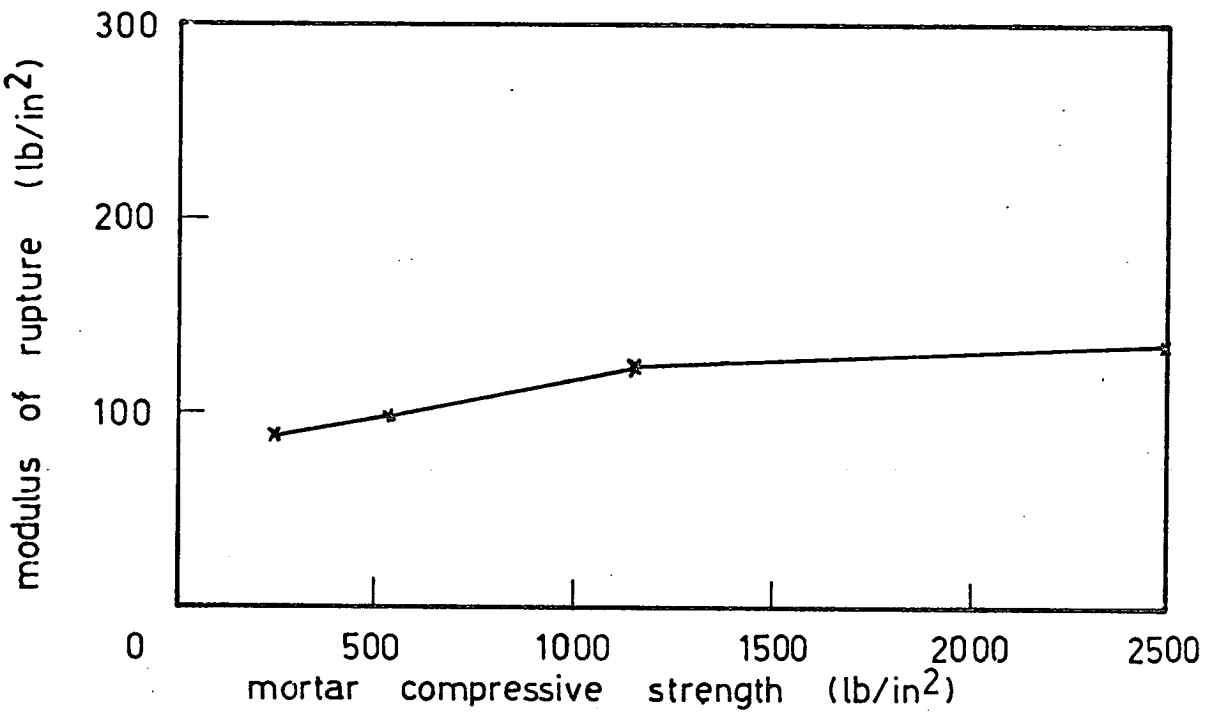

FIG. 7.2: EFFECT OF MORTAR COMPRESSIVE STRENGTH ON TRANSVERSE STRENGTH OF BRICKWORK

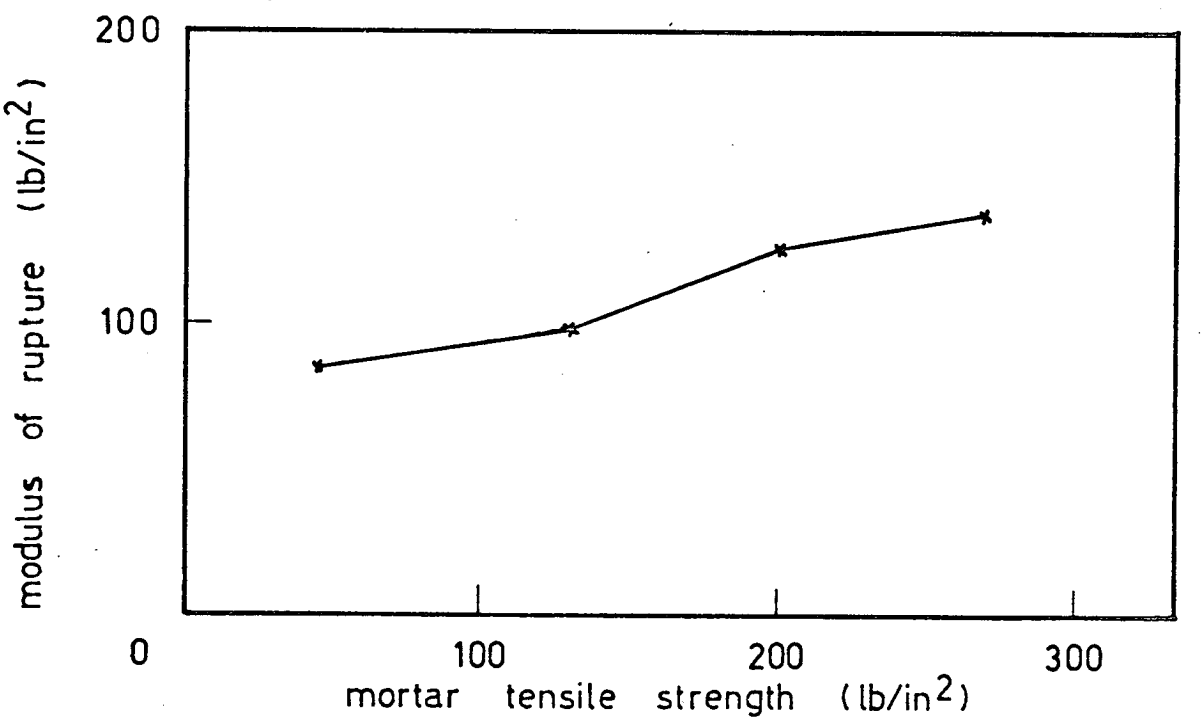

FIG. 7.1: EFFECT OF MORTAR TENSILE STRENGTH ON TRANSVERSE STRENGTH OF BRICK MASONRY

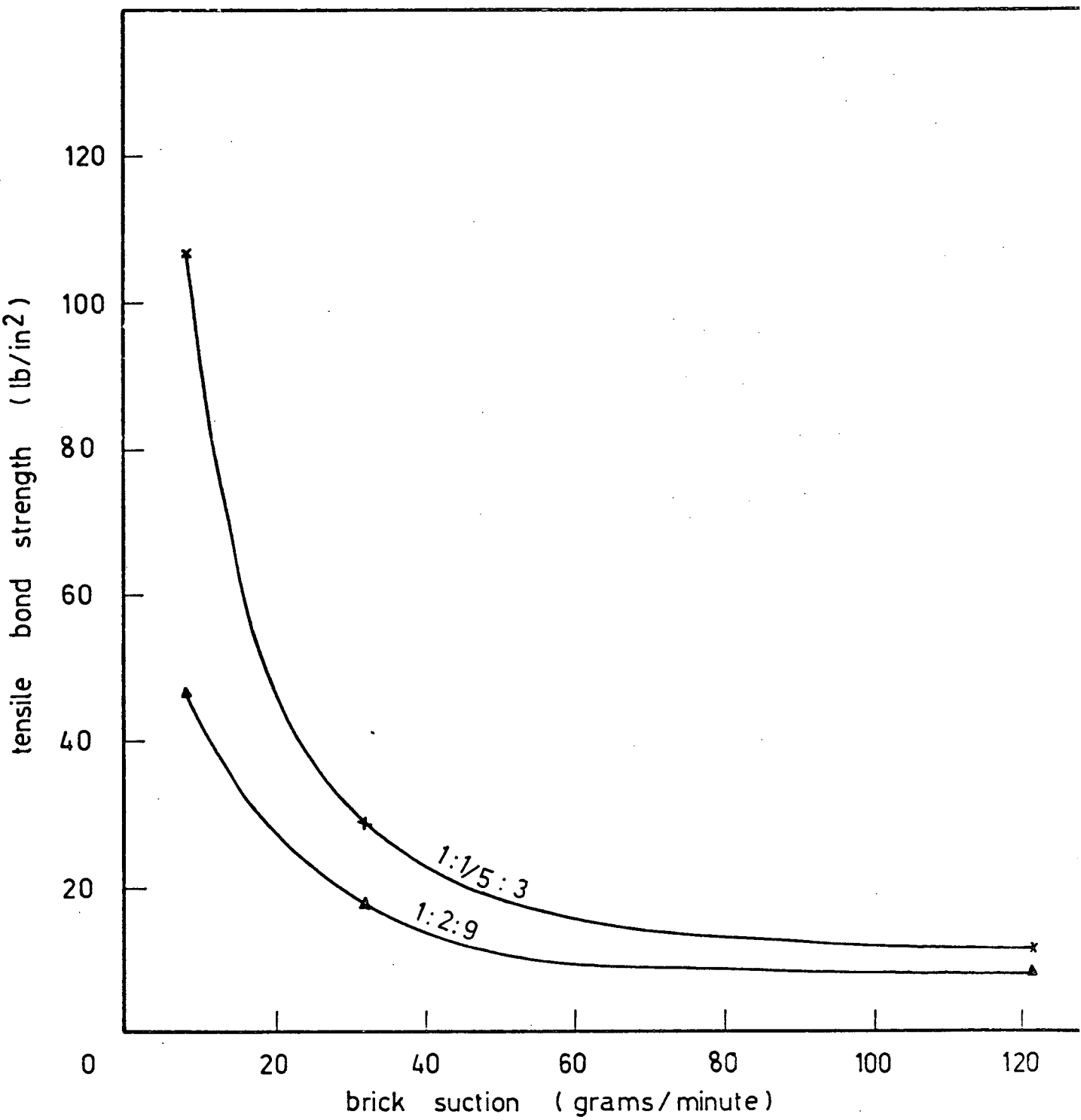

FIG. 7.3: EFFECT OF BRICK SUCTION ON TENSILE BOND STRENGT OF BRICKWORK

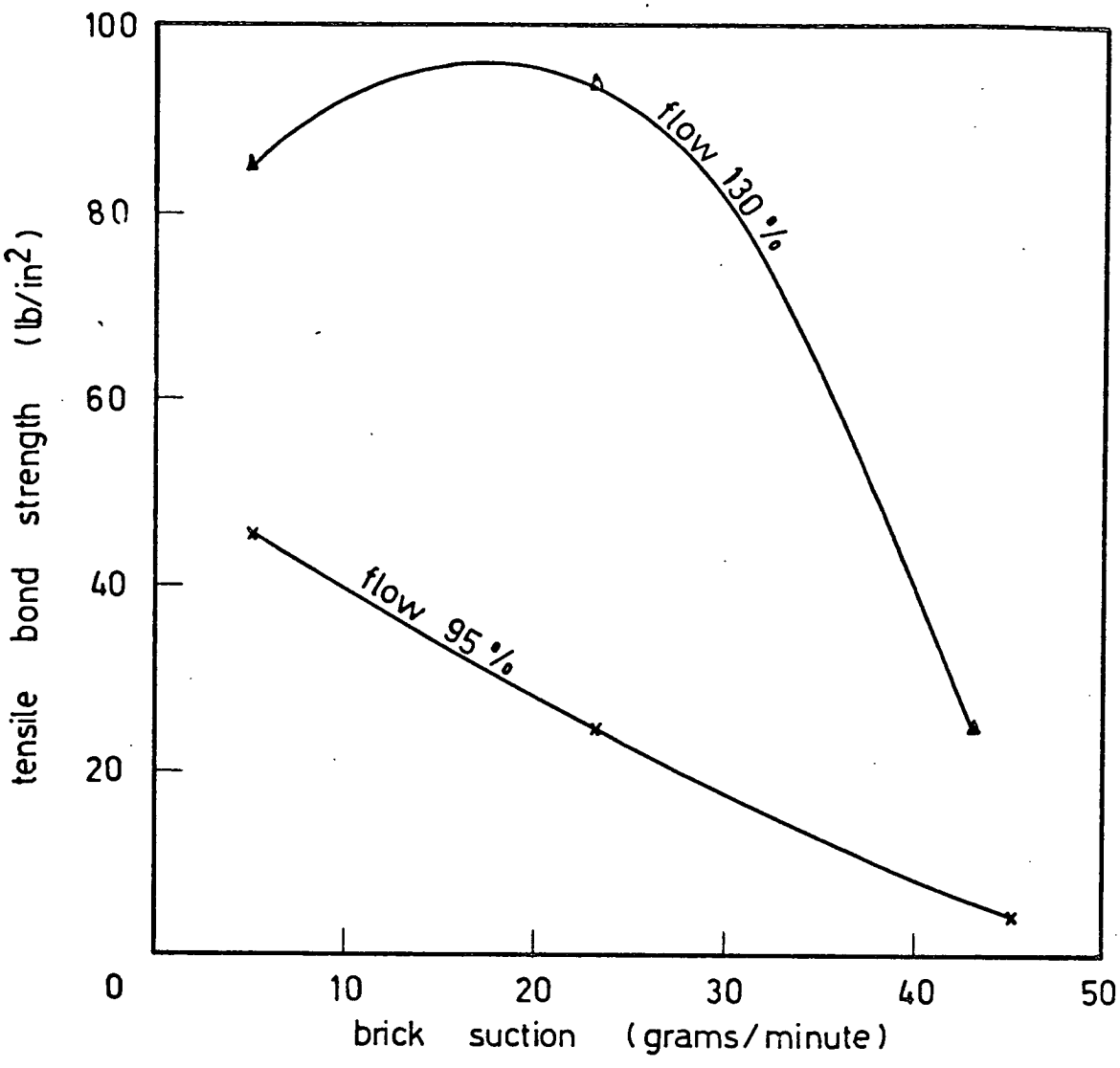
100
80
60
40
20
0
tensile bond strength (lb/in²)
flow 130 %
flow 95 %
10
20
30
40
50
brick suction (grams/minute)

FIG. 7.4

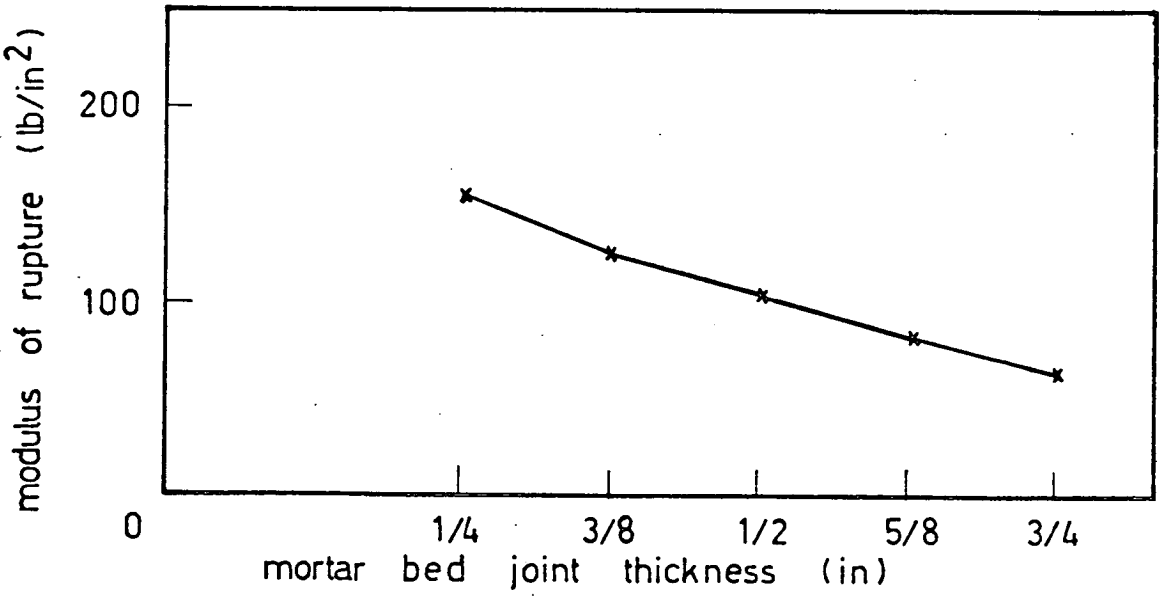
200
100
0
modulus of rupture (lb/in²)
1/4
3/8
1/2
5/8
3/4
mortar bed joint thickness (in)

FIG. 7.5

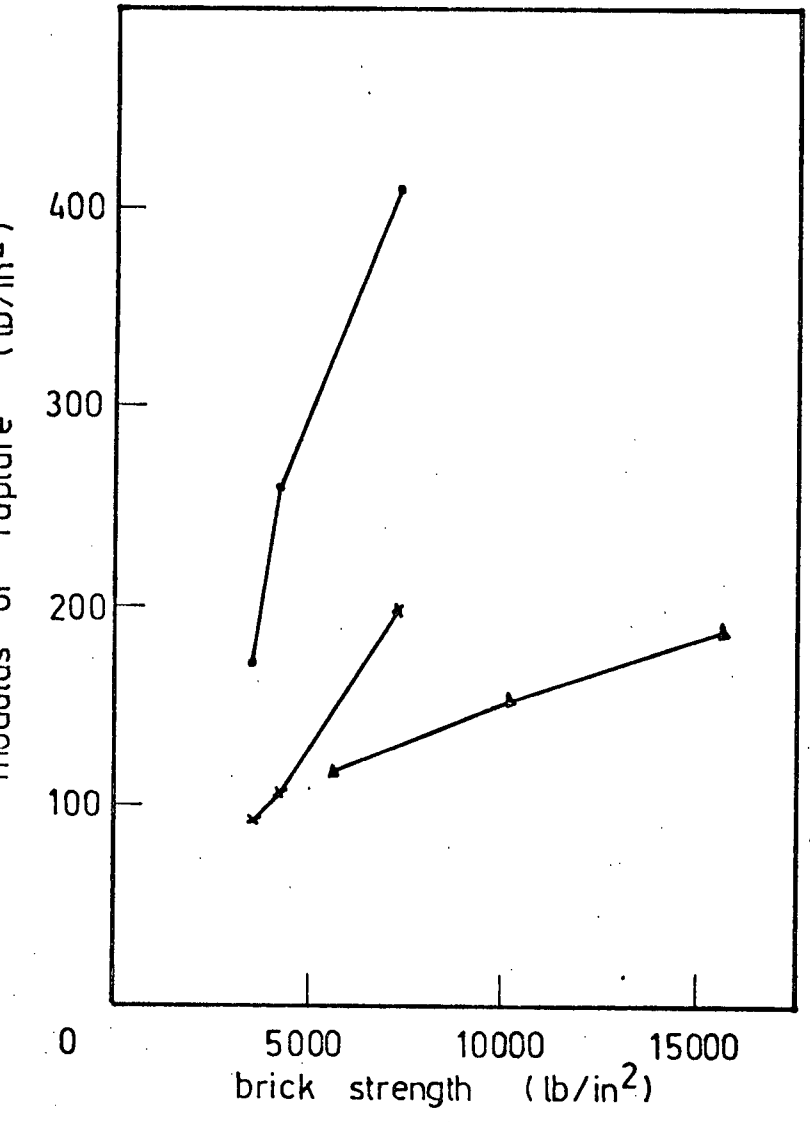

FIG.7.6: EFFECT OF BRICK STRENGTH ON TRANSVERSE STRENGTH OF BRICKWORK

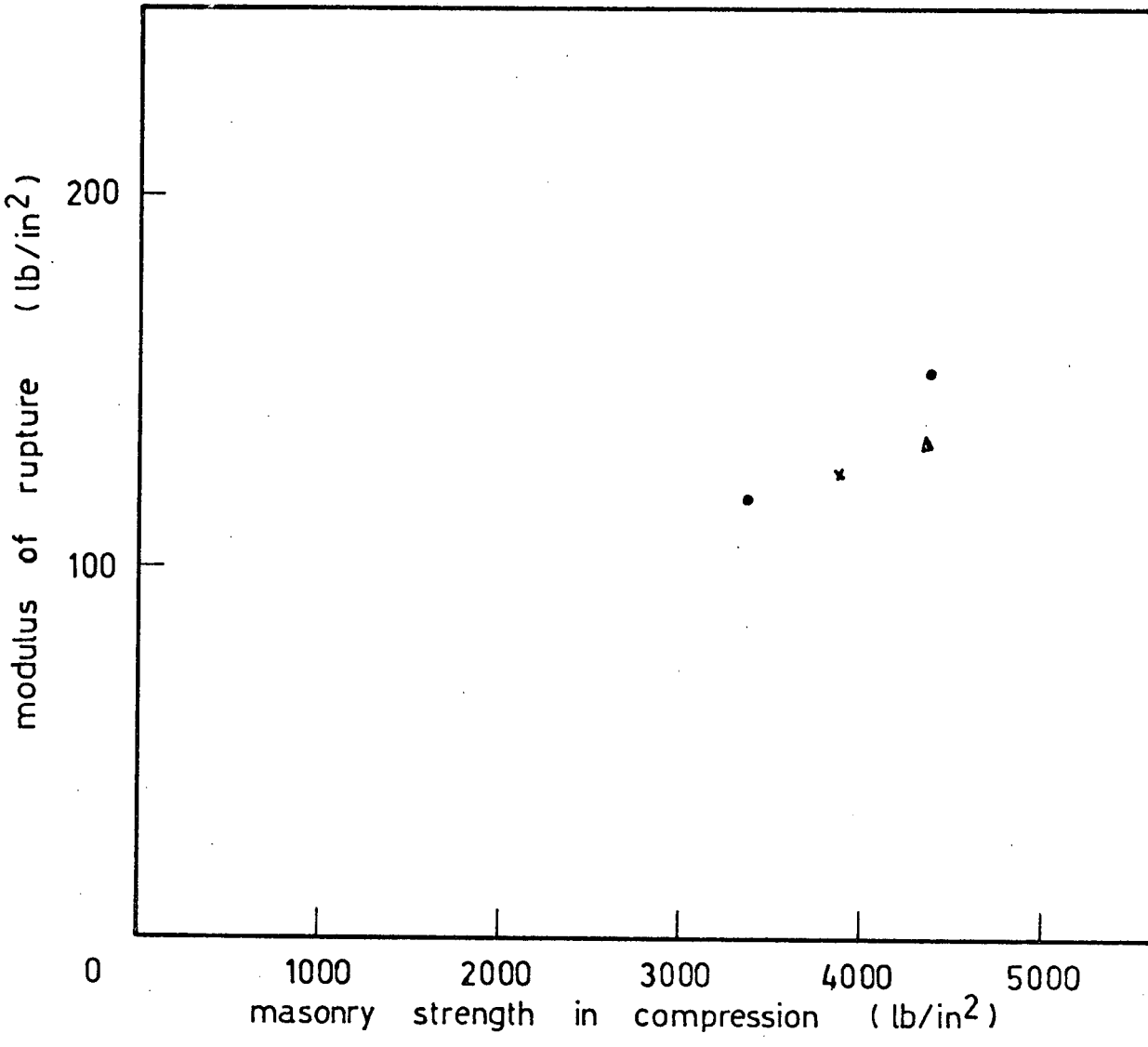

FIG. 7.7: EFFECT OF MASONRY COMPRESSIVE STRENGTH ON TRANSVERSE STRENGTH OF BRICKWORK

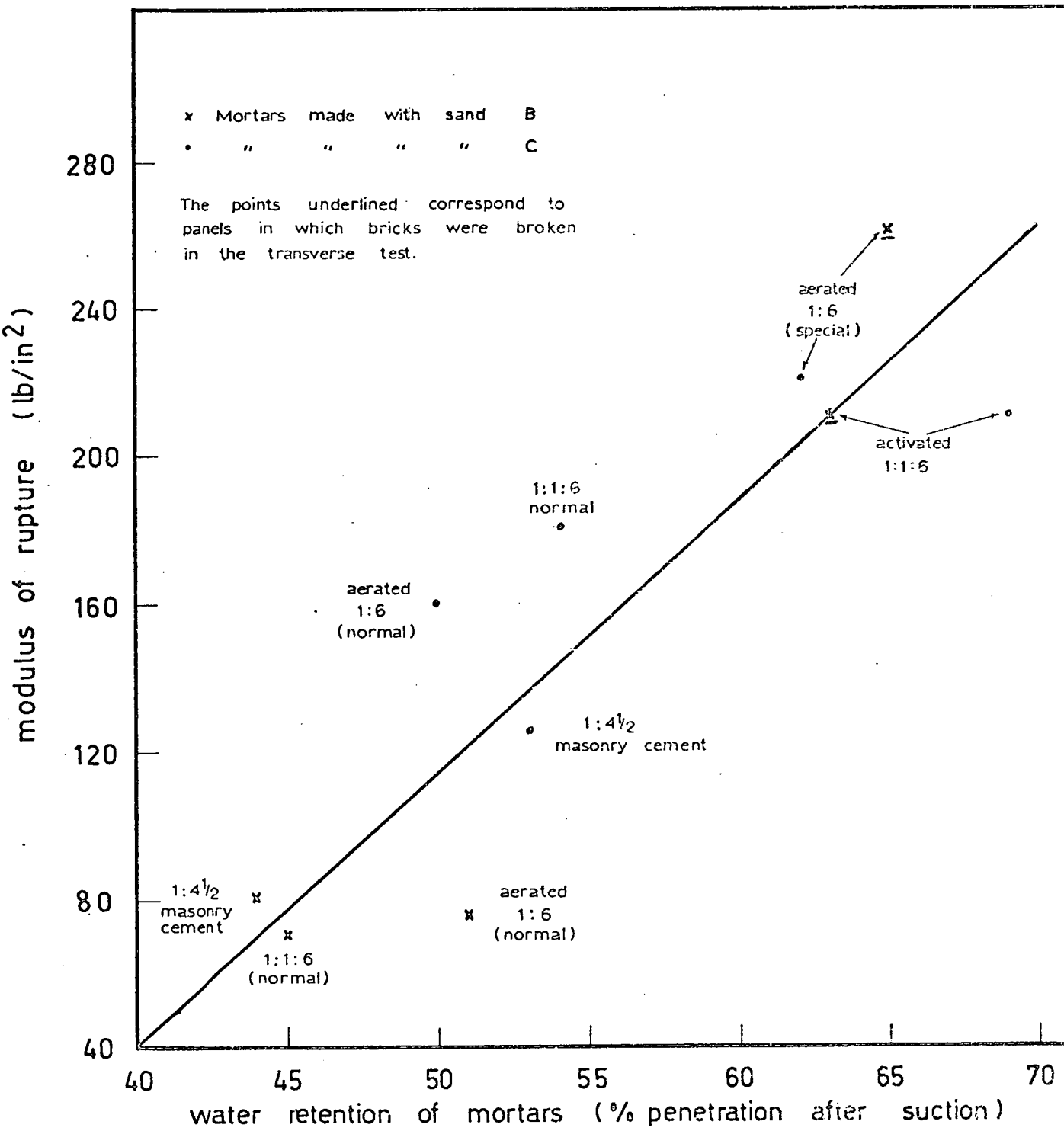

FIG. 7.8: RELATION BETWEEN WATER RETENTION OF MORTARS AND TRANSVERSE STRENGTH OF PANELS BUILT WITH DRY BRICKS OF HIGH SUCTION

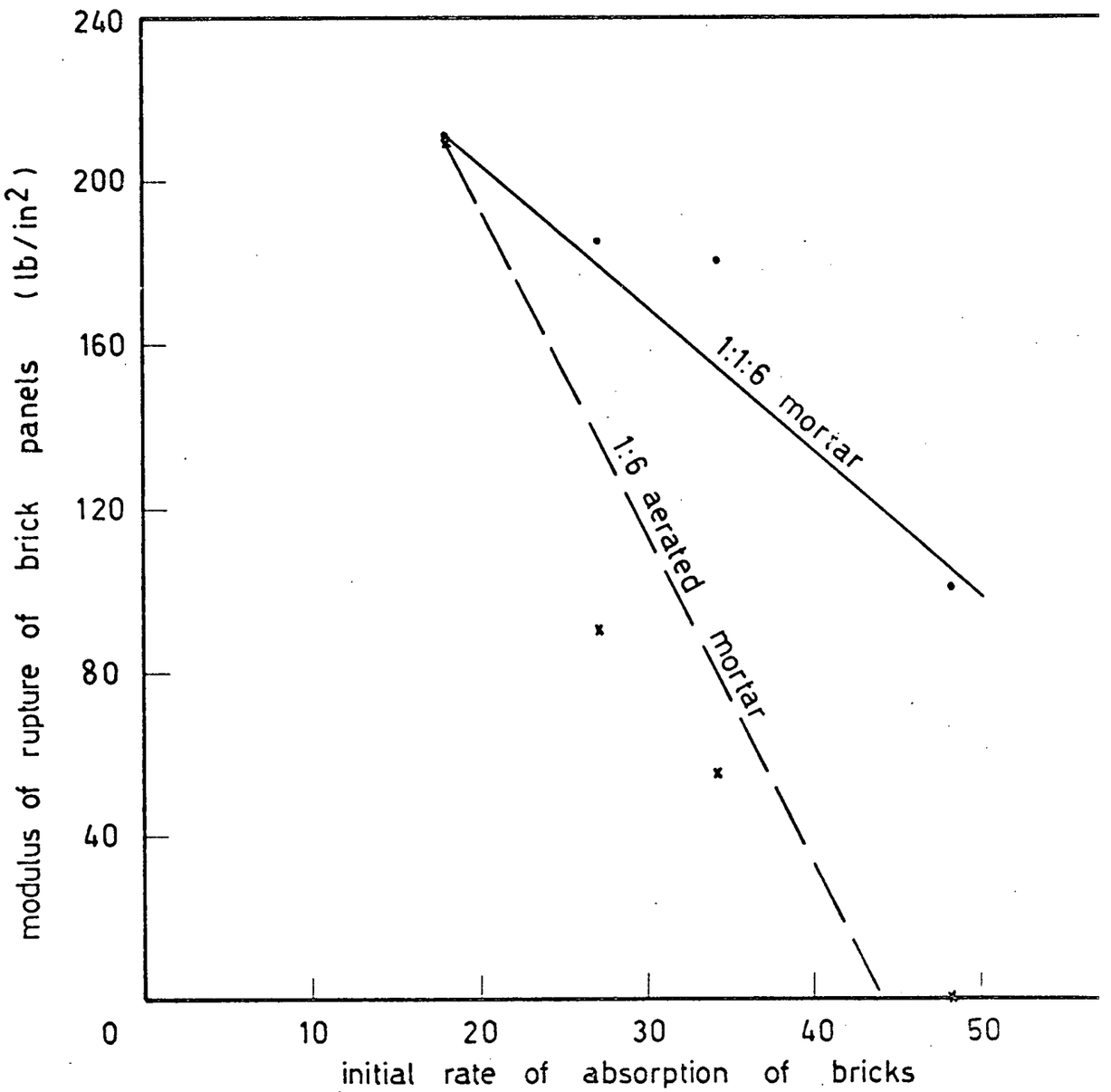

FIG. 7.9: RELATION BETWEEN ABSORPTION OF BRICKS AND TRANSVERSE STRENGTH OF PANELS

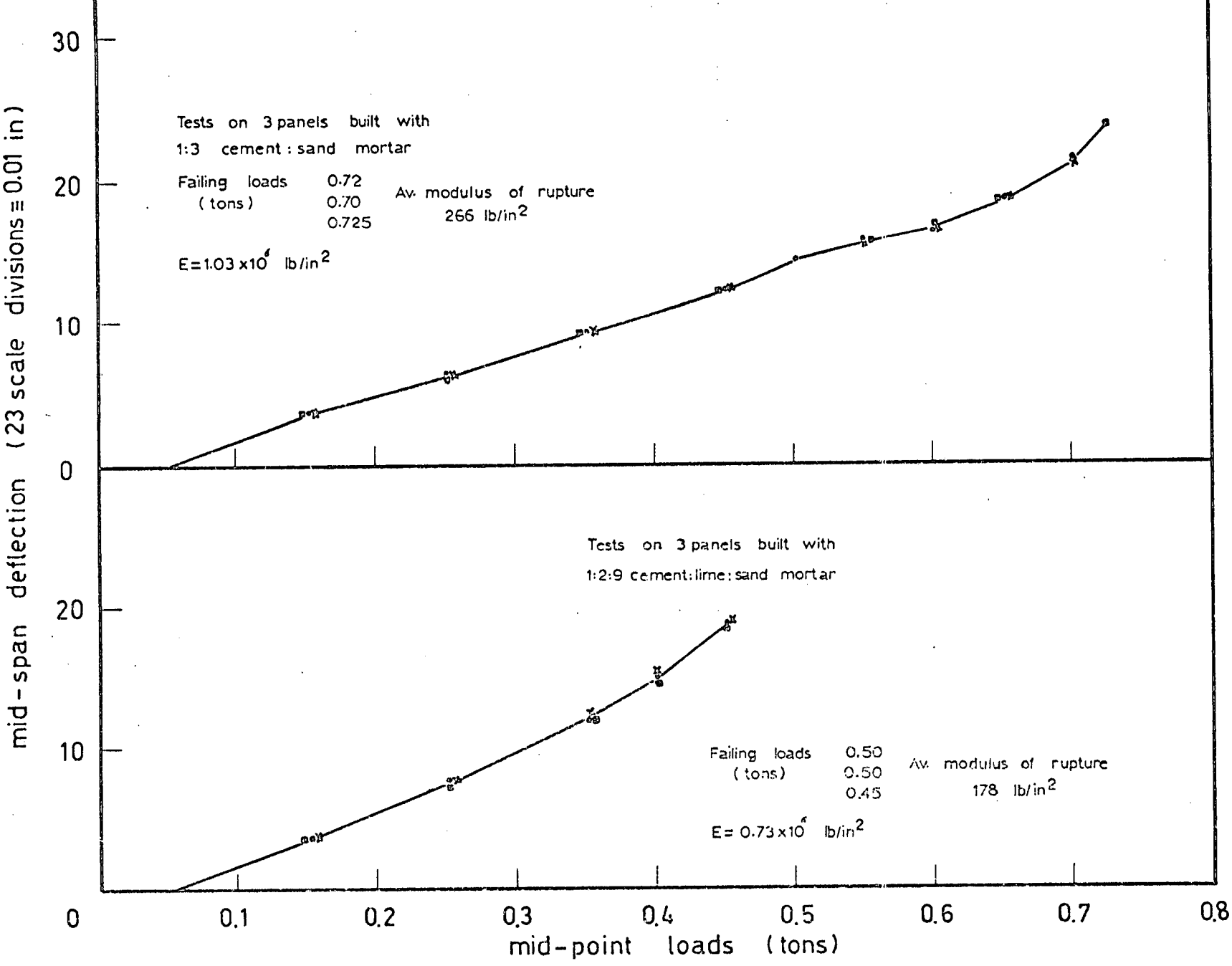

FIG. 7.10: DEFLECTION OF BRICKWORK PANELS UNDER TRANSVERSE LOADING

FIG. 7.11 TYPES OF BRICKS USED IN PRESENT INVESTIGATION

FIG. 7.12 TYPES OF FAILURE OF BRICKS TESTED ON EDGE IN BENDING

FIG. 7.14 WALLETTES READY FOR TEST

FIG. 7.15 PRISMS READY FOR TEST

FIG.7.16 WALLETTE PLACED IN TESTING MACHINE

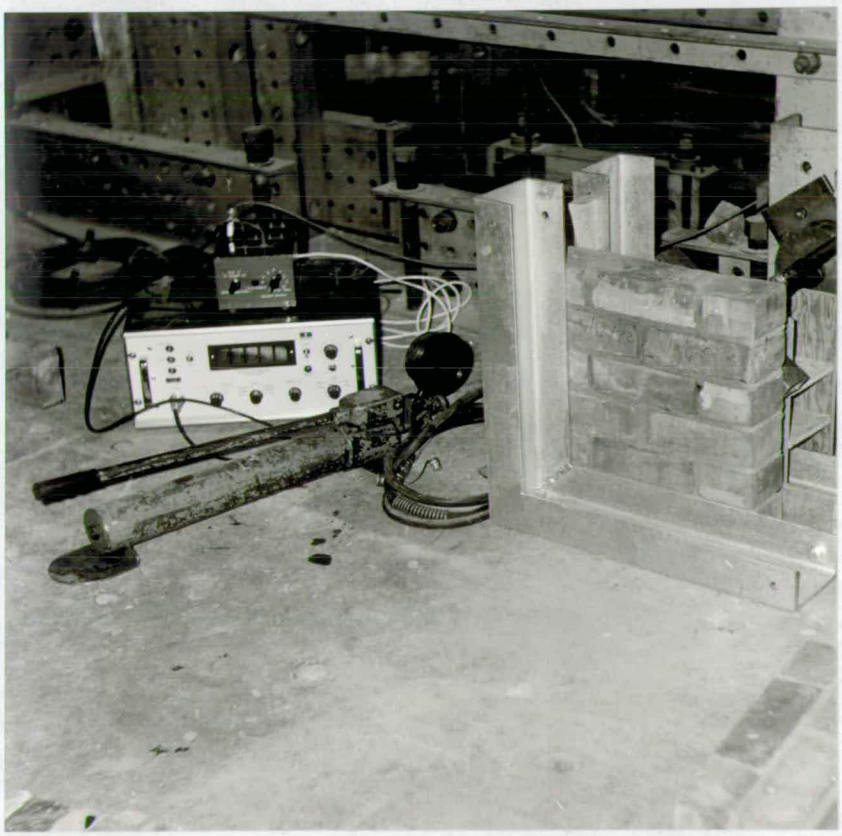

FIG. 7.17 GENERAL VIEW OF TESTING EQUIPMENT OF WALLETTES OF SECOND SERIES

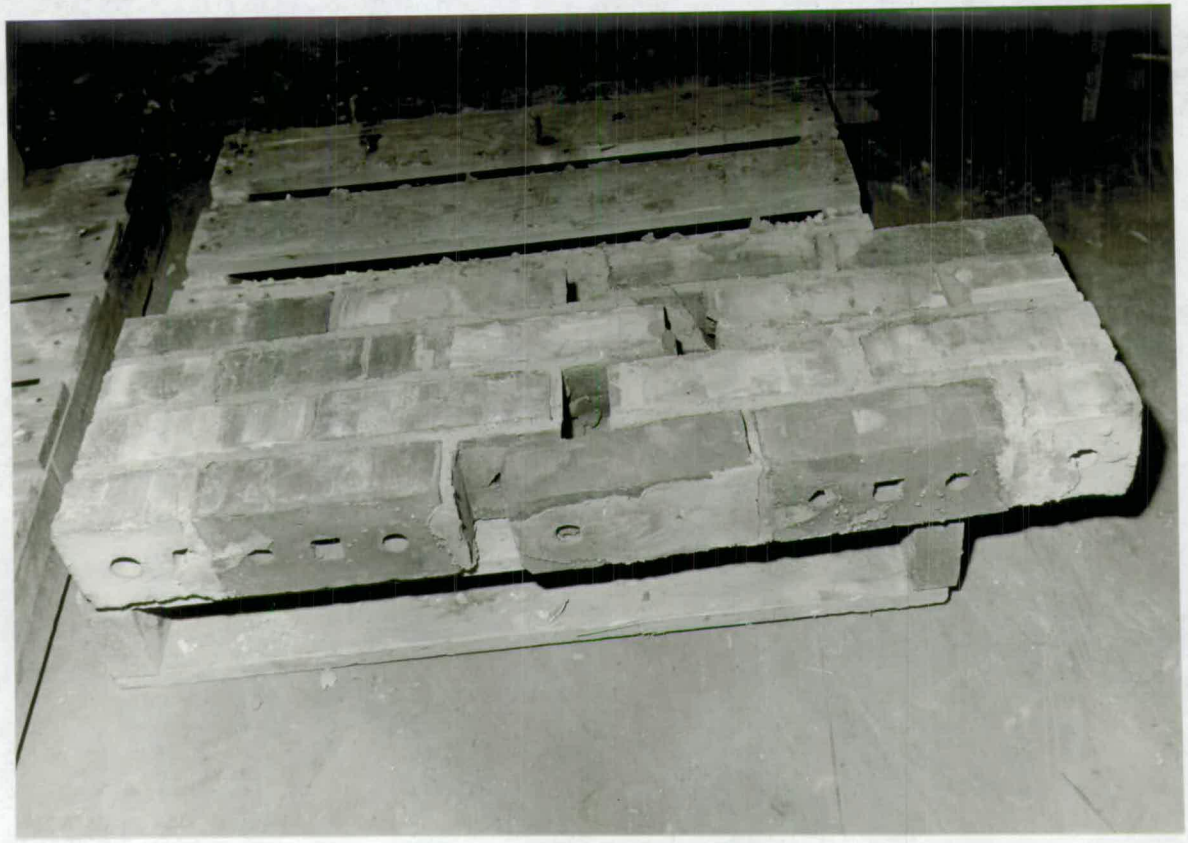

FIG. 7.18 BOND FAILURE OF WALLETTE

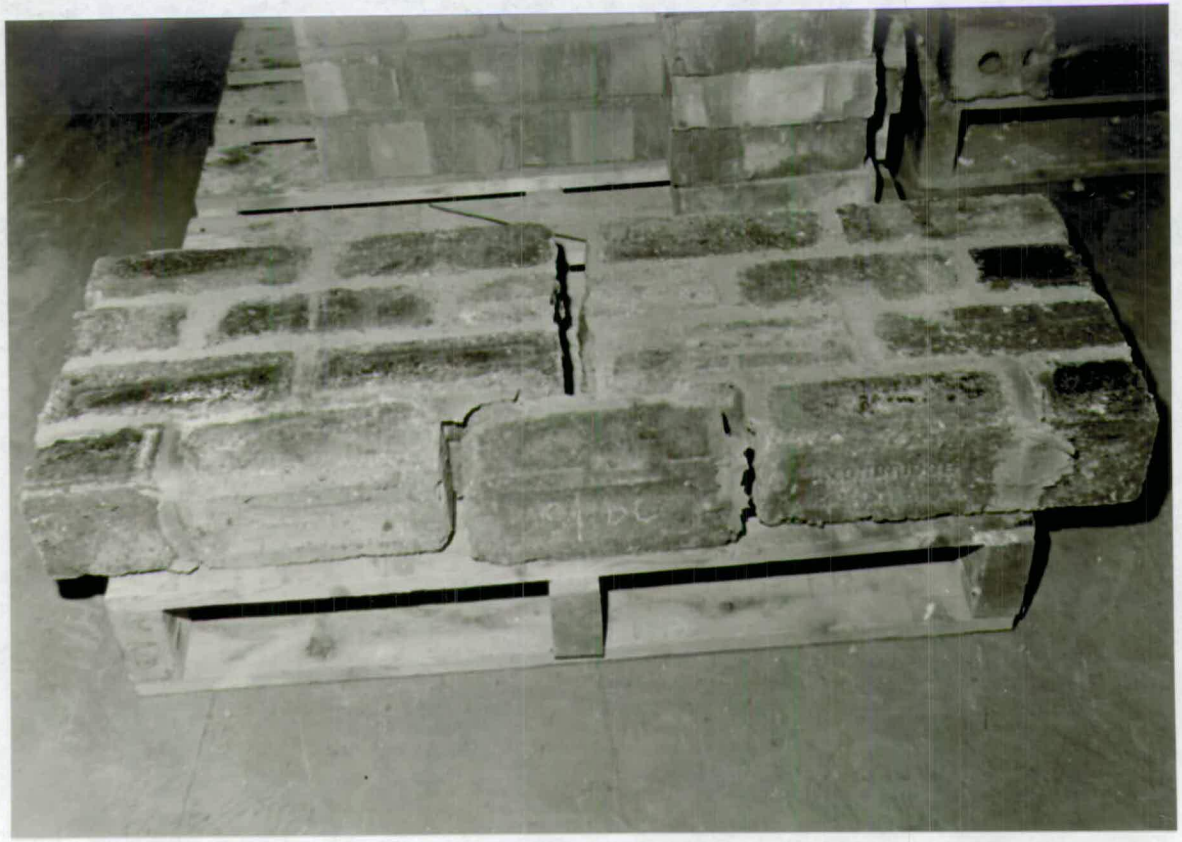

FIG.7.19 COMBINATION OF BOND FAILURE AND SPLITTING OF BRICKS OF A WALLETTE

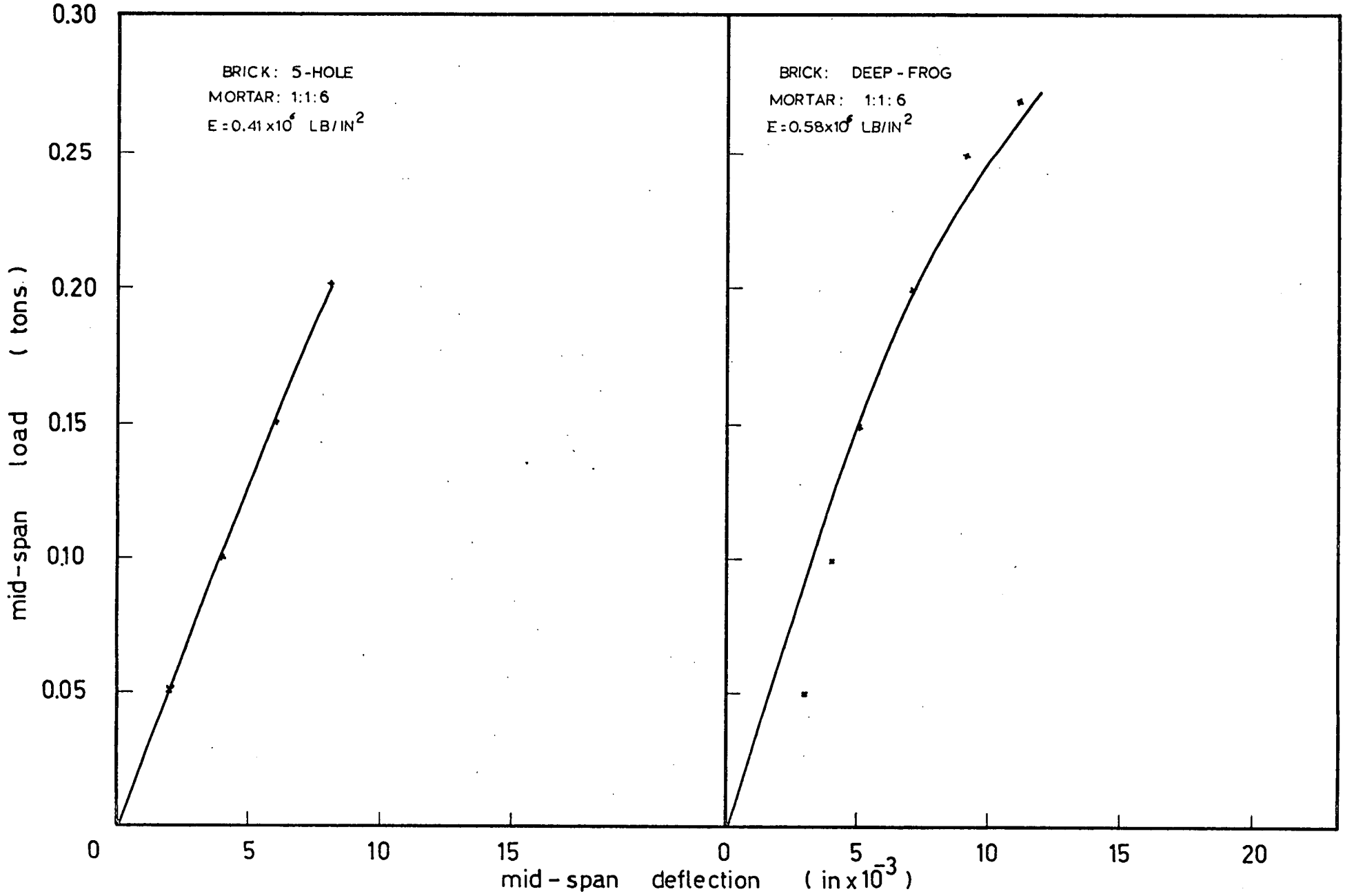
BRICK: 5-HOLE
MORTAR: 1:1:6
E = 0.41 x 10^6 LB/IN^2
BRICK: DEEP - FROG
MORTAR: 1:1:6
E = 0.58 x 10^6 LB/IN^2
mid-span load (tons)
0.30
0.25
0.20
0.15
0.10
0.05
0
5
10
15
0
5
10
15
20
mid - span deflection (in x 10^-3)

FIG 7.20

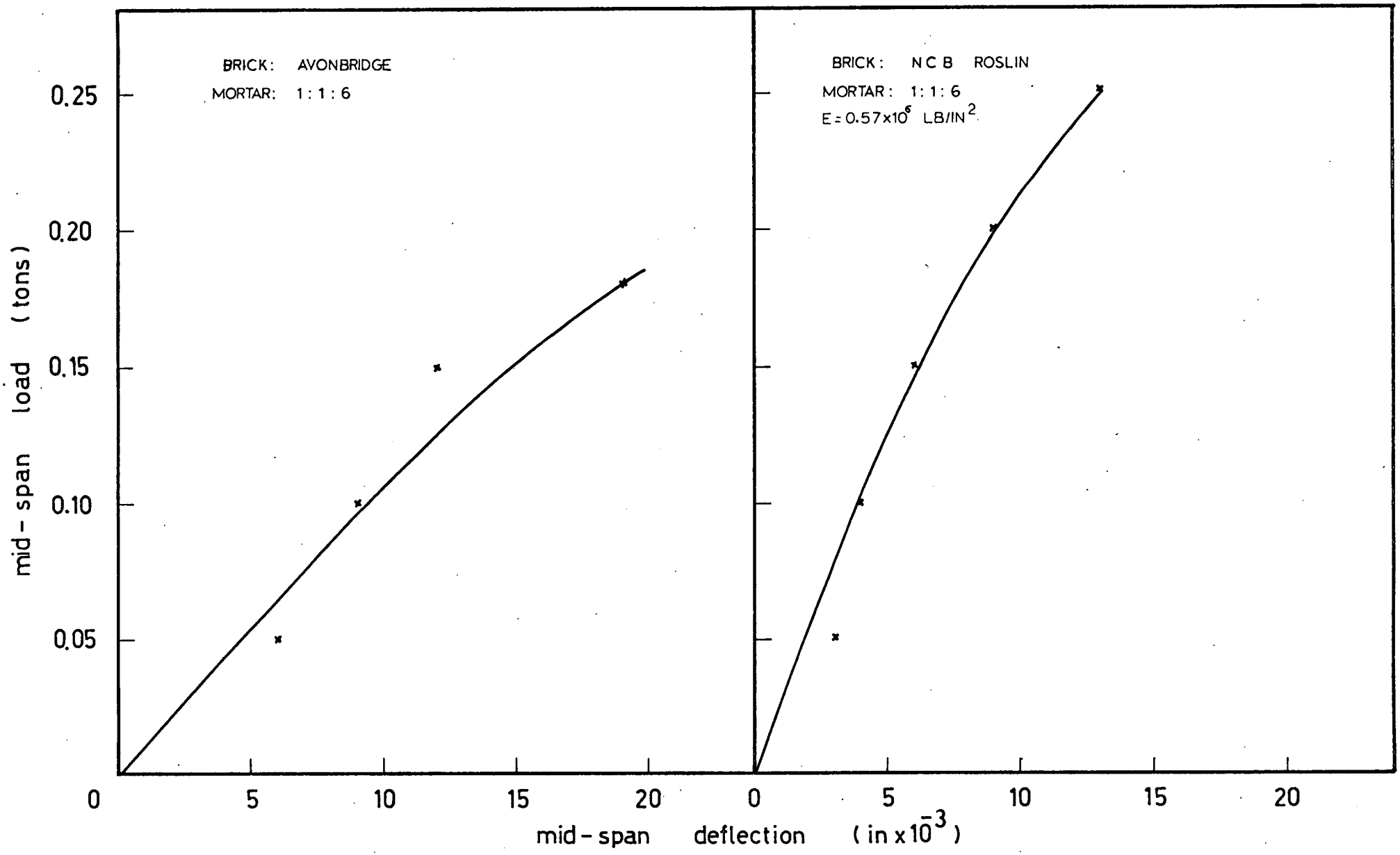
BRICK: AVONBRIDGE
MORTAR: 1 : 1 : 6
BRICK: N C B ROSLIN
MORTAR: 1: 1: 6
E = 0.57x10^6 LB/IN^2
mid - span load (tons)
0.25
0.20
0.15
0.10
0.05
0
5
10
15
20
mid - span deflection (in x10^-3)

FIG. 7.21

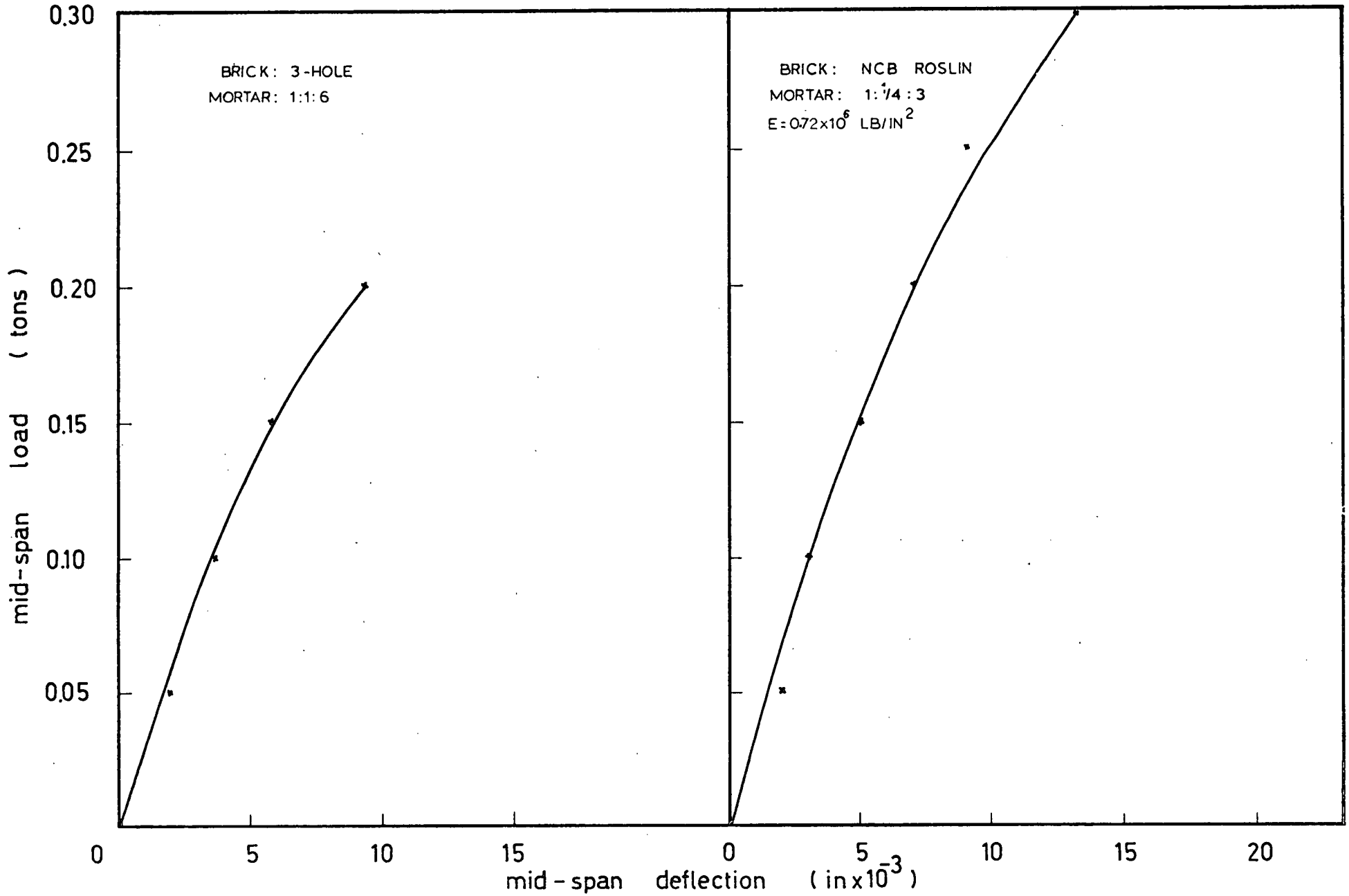
BRICK : 3-HOLE
MORTAR : 1:1:6
BRICK : NCB ROSLIN
MORTAR : 1:¼:3
E = 0.72x10^6 LB/IN^2
0.30
0.25
0.20
0.15
0.10
0.05
mid-span load (tons)
0
5
10
15
0
5
10
15
20
mid - span deflection (in x10^-3)

FIG 7.22

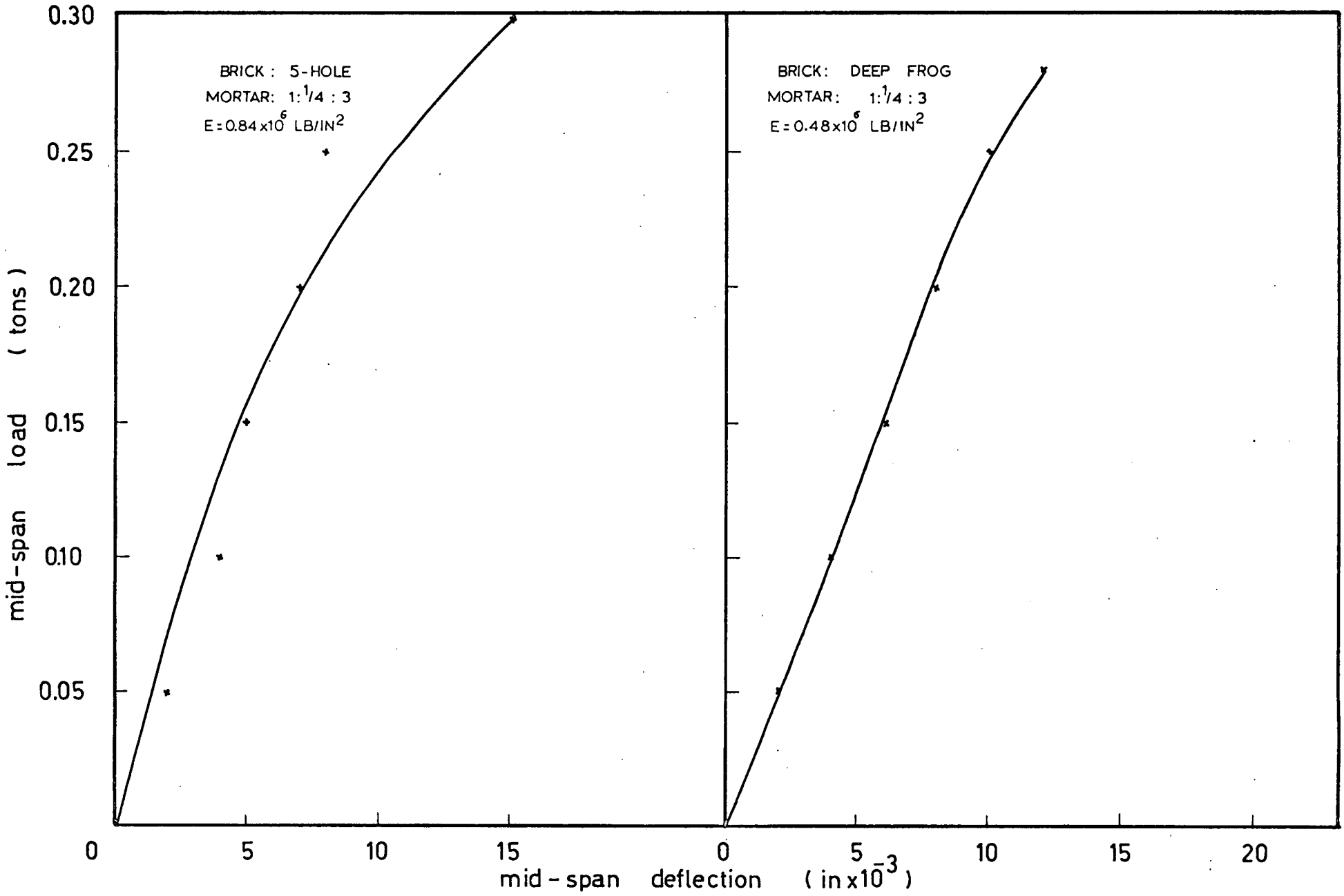
BRICK : 5-HOLE
MORTAR: 1:1/4 : 3
E = 0.84 x 10^6 LB/IN^2
BRICK: DEEP FROG
MORTAR: 1:1/4 : 3
E = 0.48 x 10^6 LB/IN^2
mid-span load (tons)
0.30
0.25
0.20
0.15
0.10
0.05
0
5
10
15
0
5
10
15
20
mid - span deflection (in x 10^-3)

FIG. 7.23

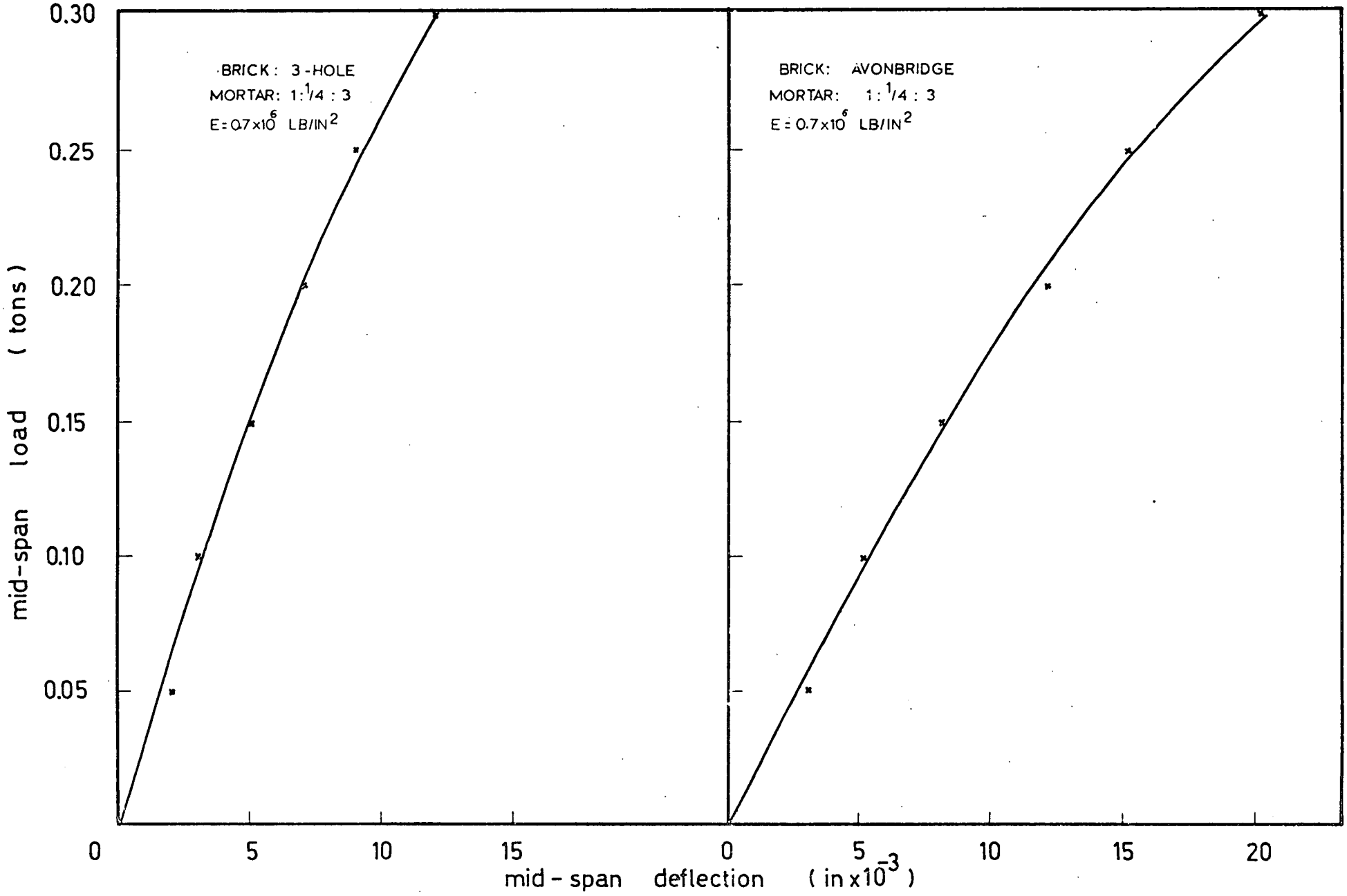
BRICK : 3-HOLE
MORTAR: 1:1/4 : 3
E = 0.7 x 10^6 LB/IN^2
BRICK: AVONBRIDGE
MORTAR: 1 : 1/4 : 3
E = 0.7 x 10^6 LB/IN^2
mid-span load (tons)
0.30
0.25
0.20
0.15
0.10
0.05
0
5
10
15
0
5
10
15
20
mid - span deflection (in x 10^-3)

FIG. 7.24

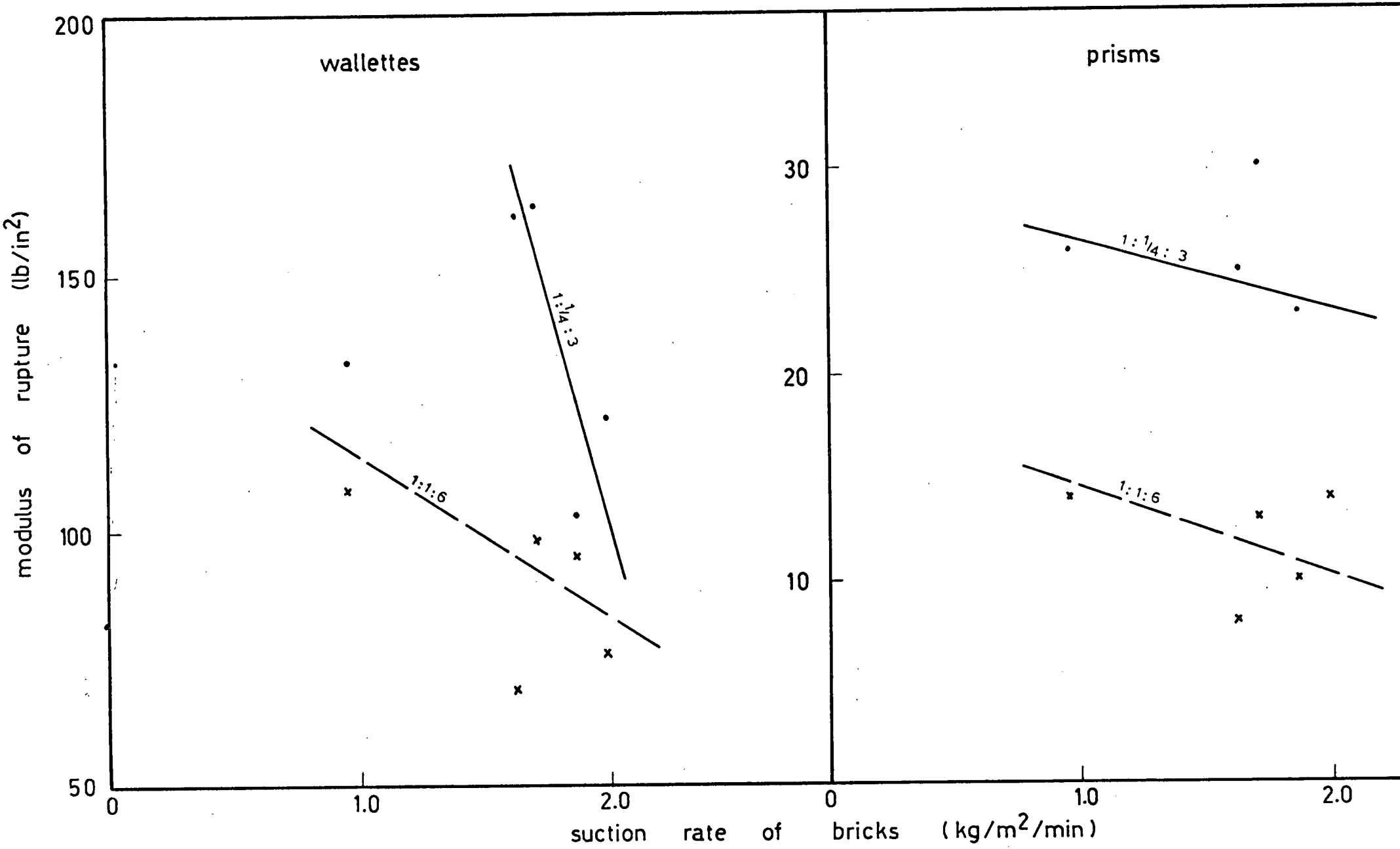
wallettes
prisms
modulus of rupture (lb/in²)
200
150
100
50
30
20
10
1:¼:3
1:1:6
1:¼:3
1:1:6
0
1.0
2.0
0
1.0
2.0
suction rate of bricks (kg/m²/min)

FIG. 7.25

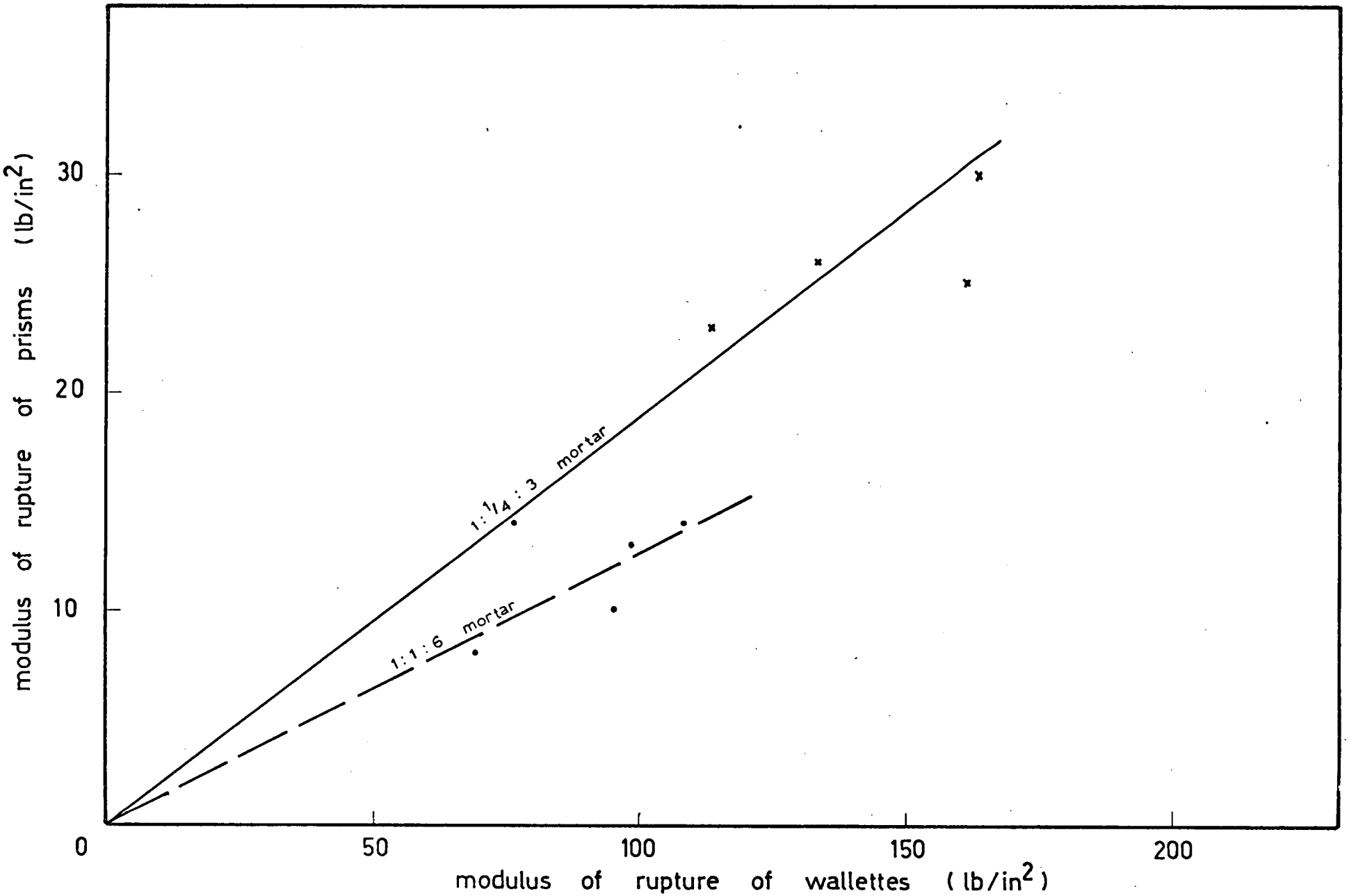
modulus of rupture of prisms (lb/in²)
30
20
10
0
50
100
150
200
modulus of rupture of wallettes (lb/in²)
1:¼:3 mortar
1:1:6 mortar

FIG. 7.26

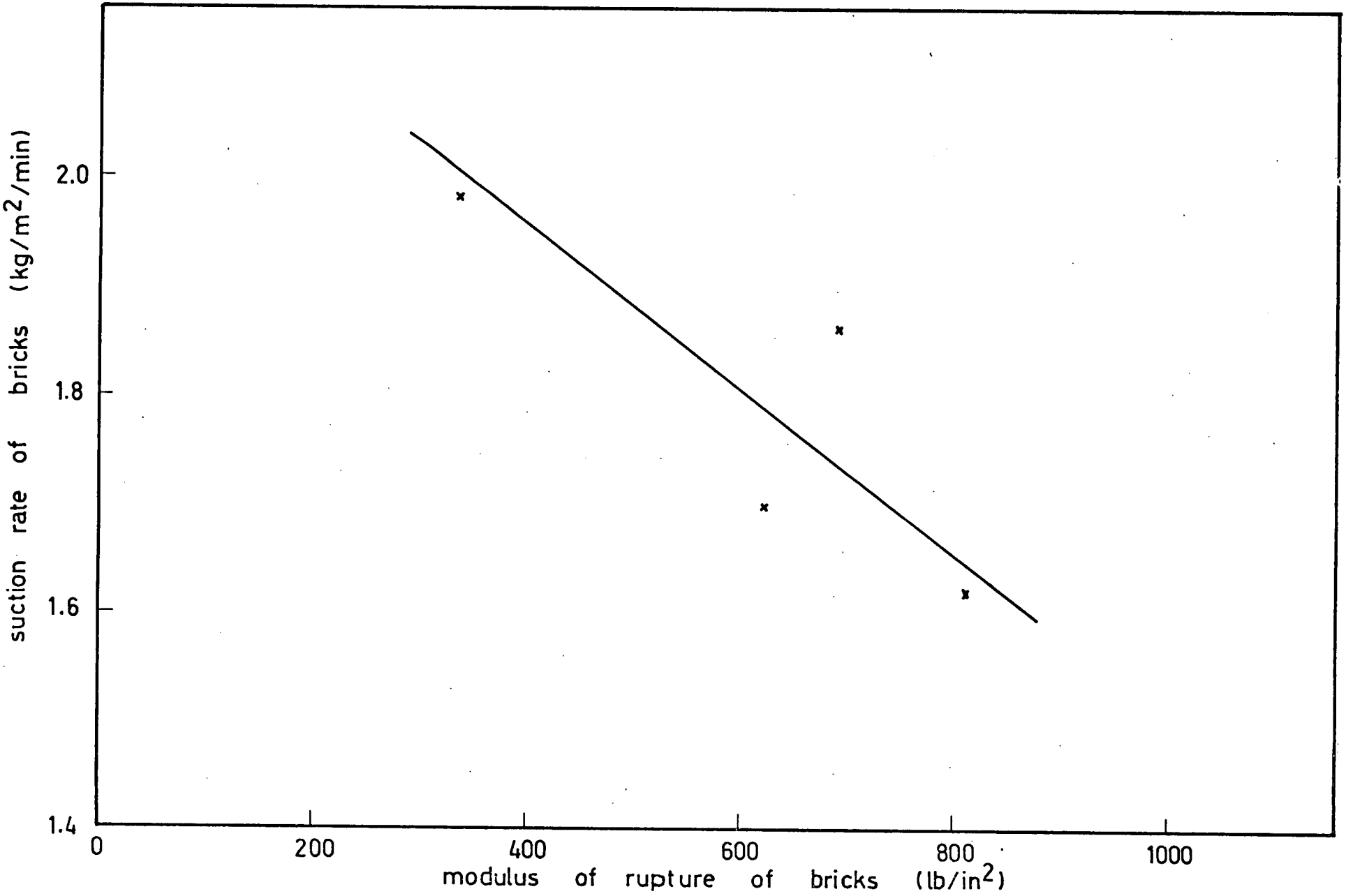
suction rate of bricks (kg/m2/min)
2.0
1.8
1.6
1.4
0
200
400
600
800
1000
modulus of rupture of bricks (lb/in2)

FIG. 7.27

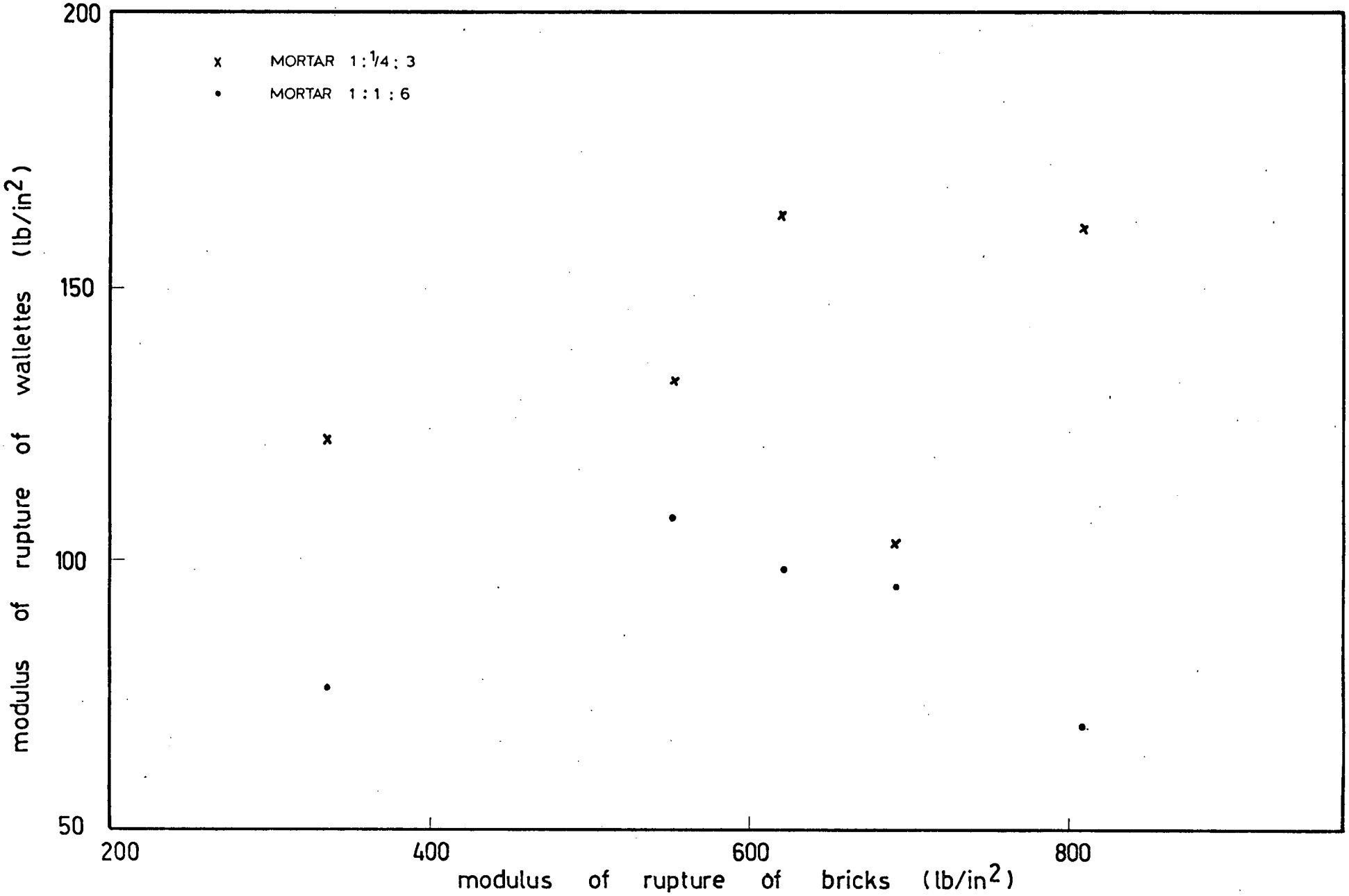
200
150
100
50
x MORTAR 1 : 1/4 : 3
• MORTAR 1 : 1 : 6
modulus of rupture of wallettes (lb/in2)
200
400
600
800
modulus of rupture of bricks (lb/in2)

FIG. 7.28

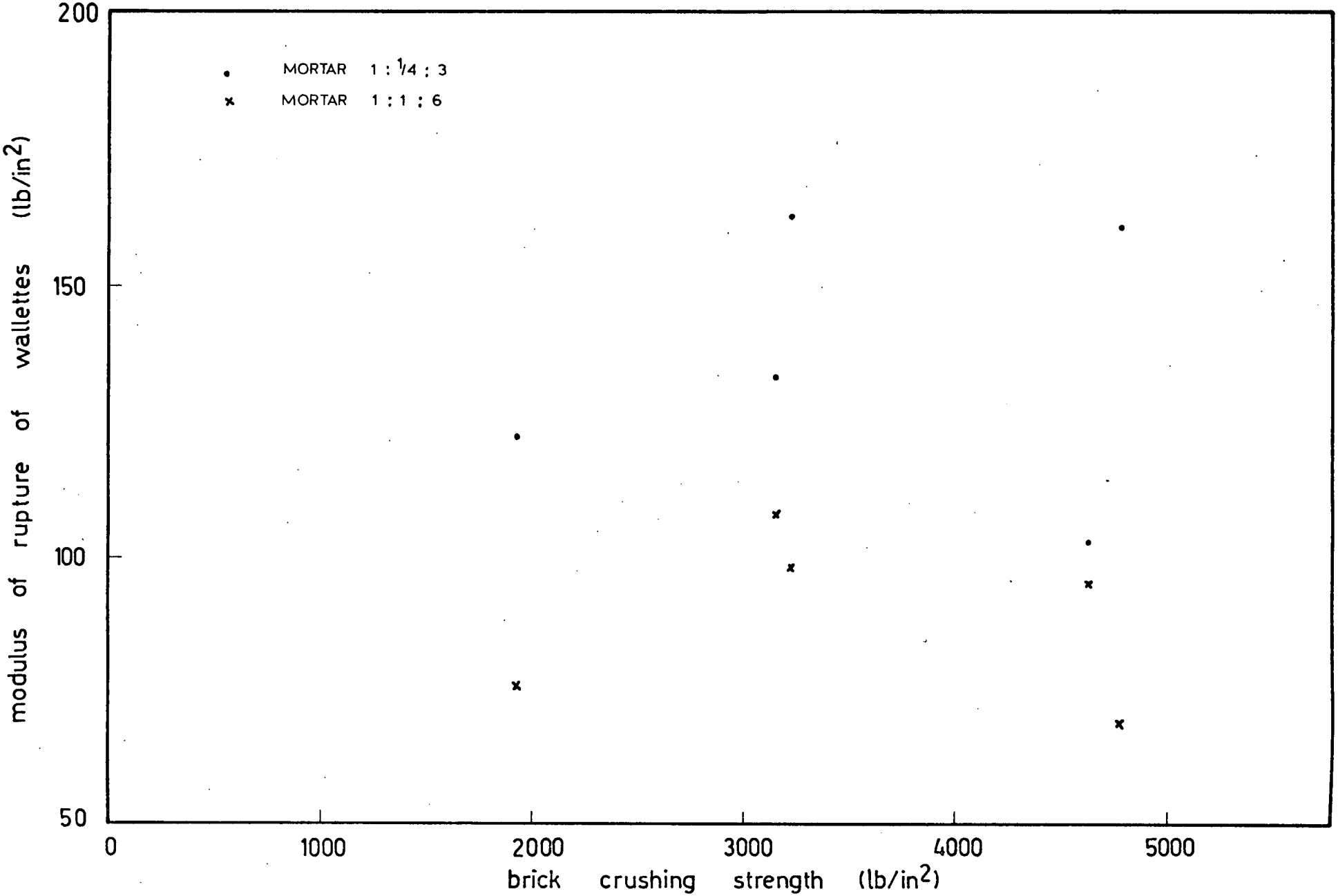
MORTAR 1 : 1/4 : 3
MORTAR 1 : 1 : 6
modulus of rupture of wallettes (lb/in2)
200
150
100
50
0
1000
2000
3000
4000
5000
brick crushing strength (lb/in2)

FIG. 7.29

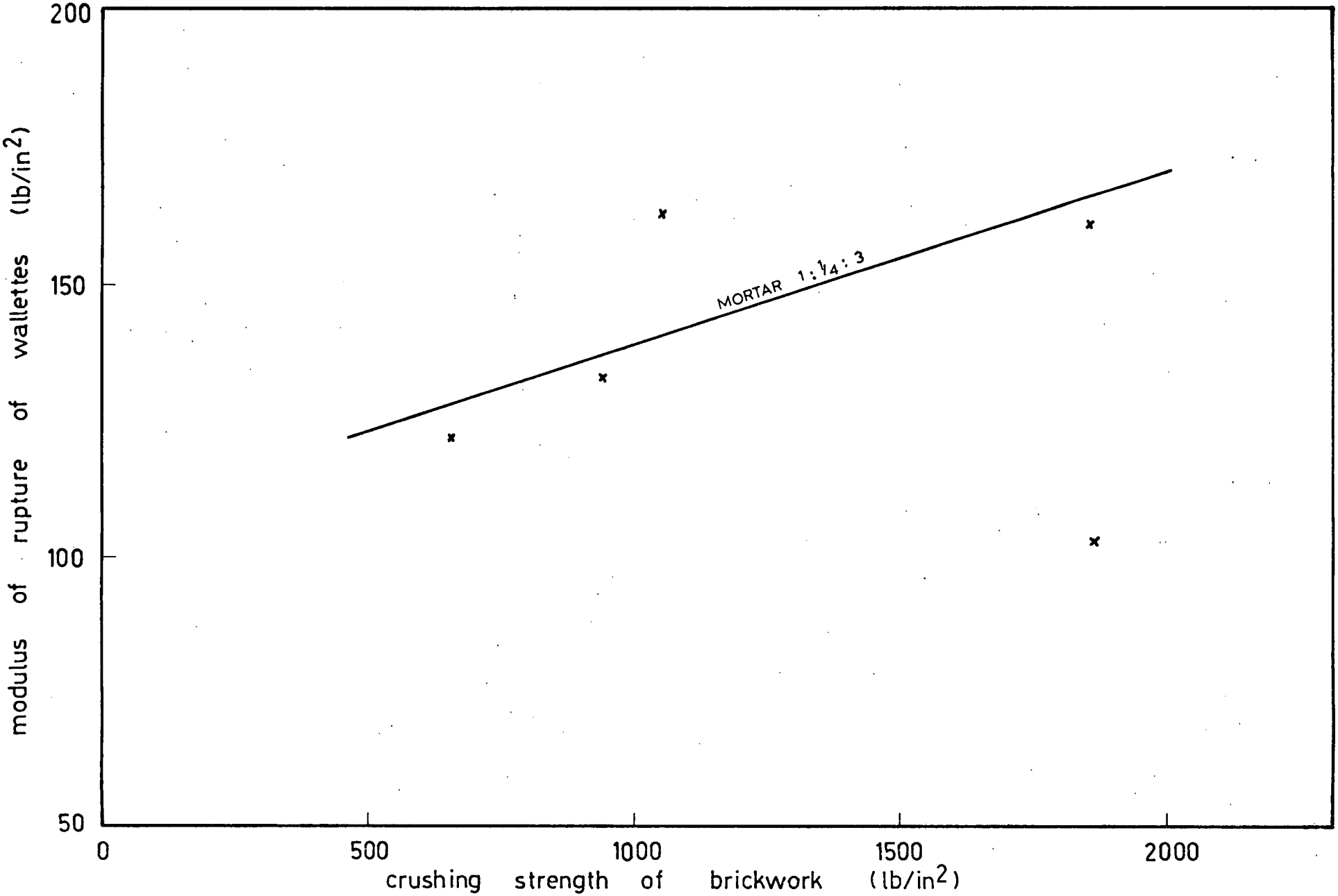
200
150
100
50
0
500
1000
1500
2000
modulus of rupture of wallettes (lb/in²)
crushing strength of brickwork (lb/in²)
MORTAR 1:¼:3

FIG. 7.30

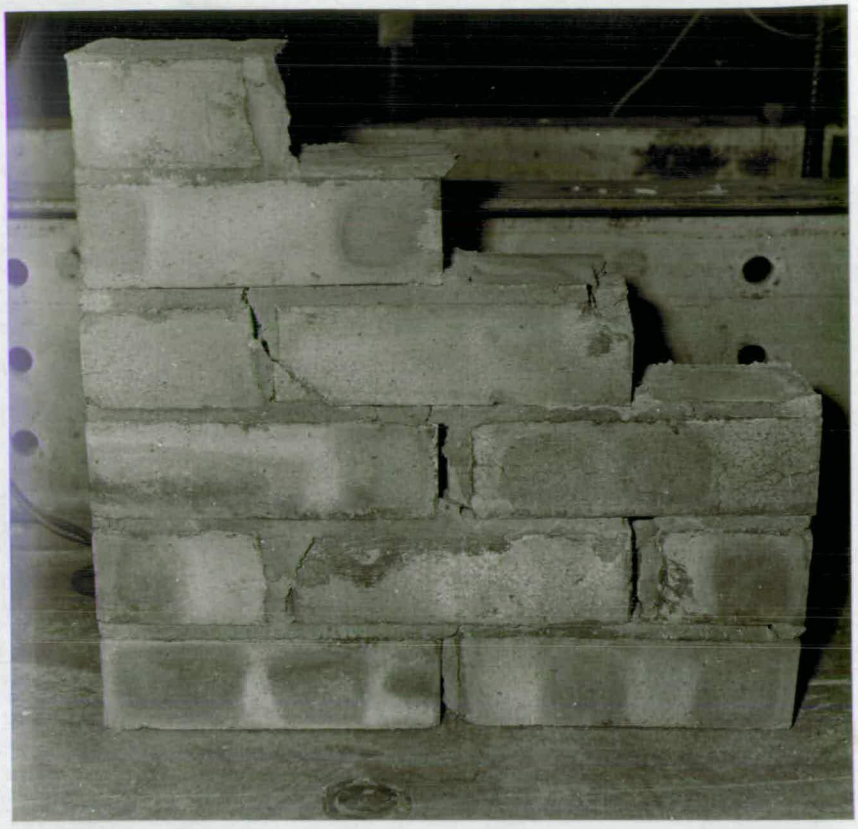

FIG. 7.31 FAILURE OF A WALLETTE OF THE SECOND SERIES

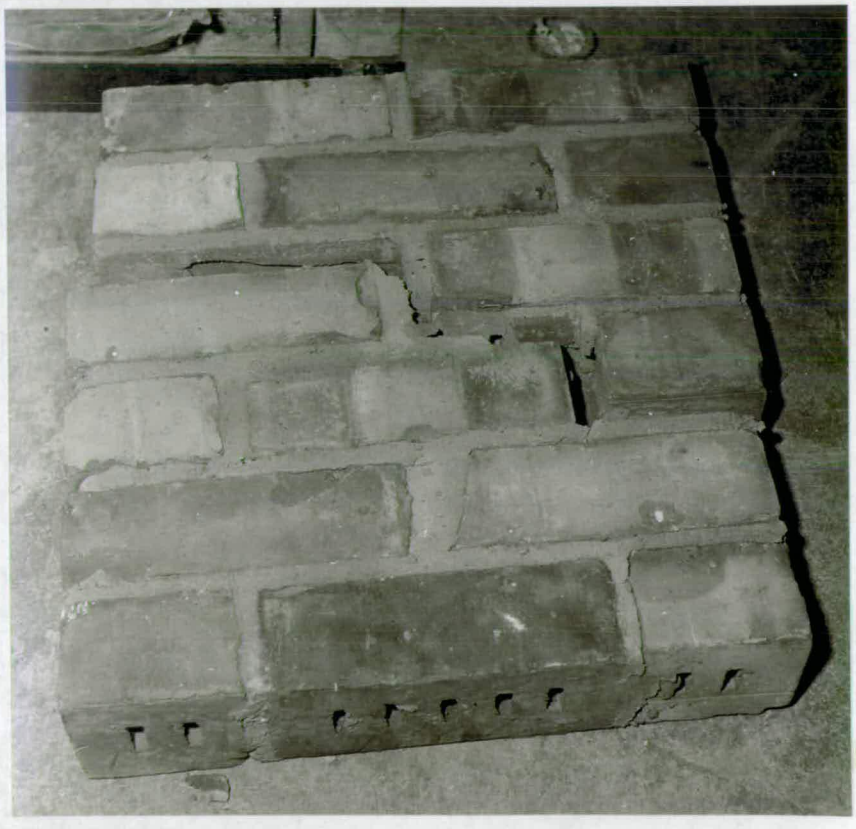

FIG. 7.32 FAILURE OF A WALLETTE OF THE SECOND SERIES

FIG. 7.33 FAILURE OF A WALLETTE OF THE SECOND SERIES

FIG. 7.34 FAILURE OF A WALLETTE OF THE SECOND SERIES

FIG. 7.35 FAILURE OF A WALLETTE OF THE SECOND SERIES

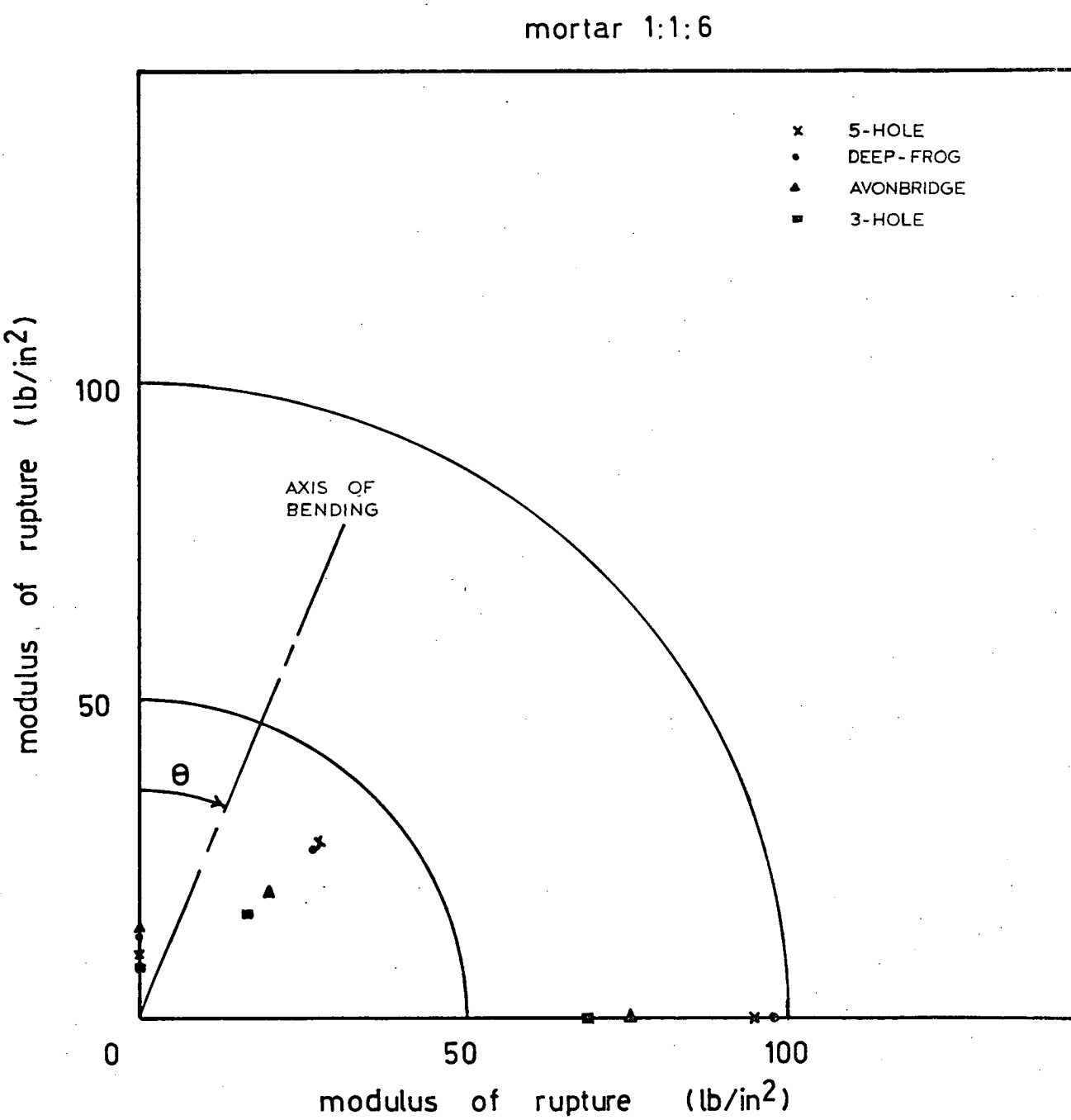
mortar 1:1:6
5-HOLE
DEEP-FROG
AVONBRIDGE
3-HOLE
AXIS OF BENDING
θ
modulus of rupture (lb/in²)
100
50
0
50
100
modulus of rupture (lb/in²)

FIG. 7.36

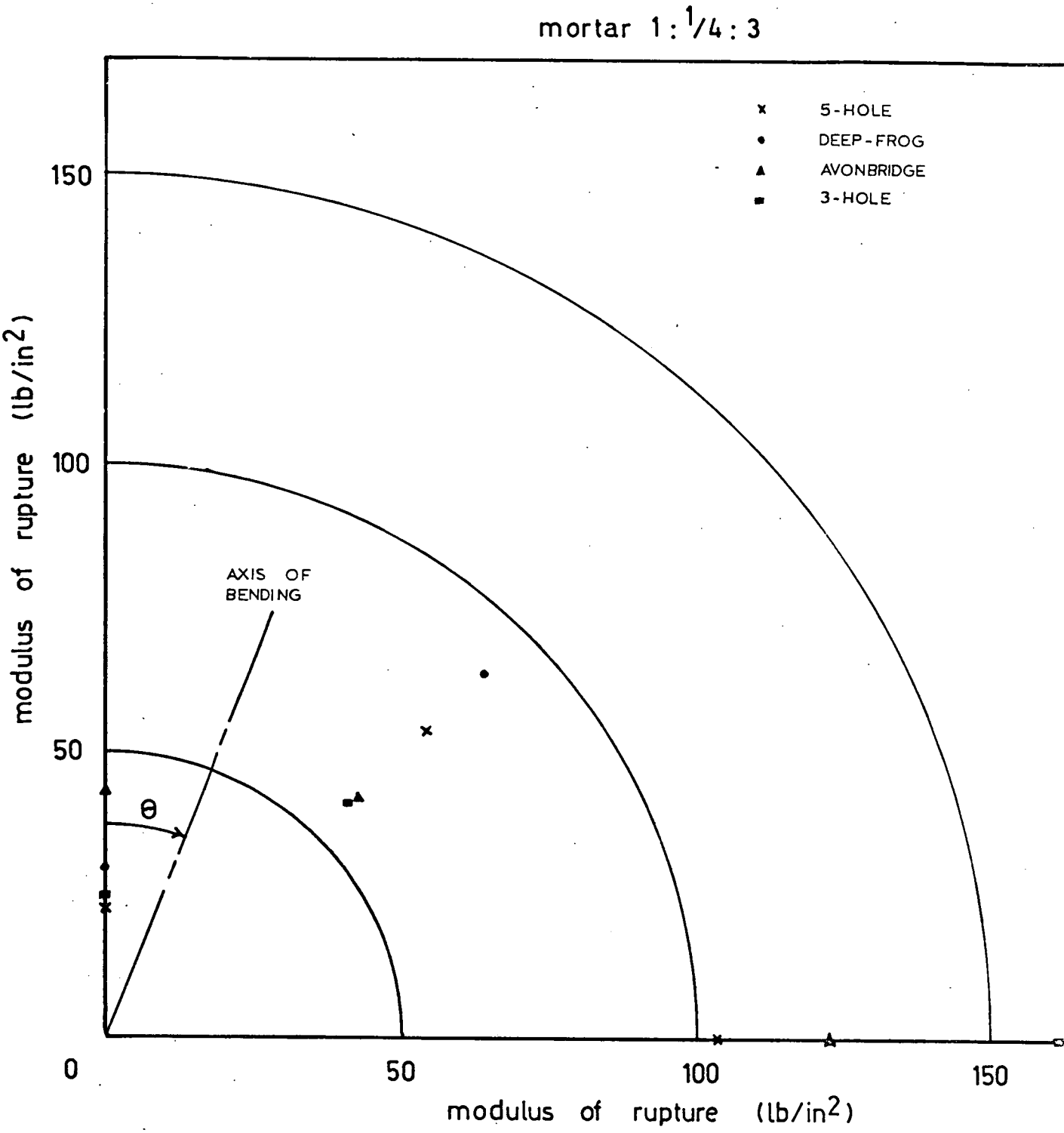
mortar 1 : 1/4 : 3
5-HOLE
DEEP-FROG
AVONBRIDGE
3-HOLE
150
100
50
0
modulus of rupture (lb/in2)
AXIS OF BENDING
θ
50
100
150
modulus of rupture (lb/in2)

FIG. 7.37

CHAPTER 8

GENERAL CONCLUSIONS

The conclusions reached from the investigations presented in this thesis are summarised as follows:

(a) With normal mortars, failure under lateral loading in brick walls supported on three or four sides is due to the breakdown of bond at the brick/mortar interface, leading to diagonal cracks stepping through the vertical and horizontal mortar joints. In some cases it may occur through the brick as well.

(b) Under lateral load with sufficient precompression, failure of brick walls supported on three or four sides would occur by a yield line pattern of cracks passing through both the brick and mortar; in this case the ultimate strength of walls is governed by both the modulus of rupture of the brickwork and the applied precompression.

(c) Walls in the uppermost storeys of high buildings fail at lower lateral loads compared to those at lower heights as precompression, which is due to self weight, decreases with height.

(d) In the tests, walls under precompression failed at higher lateral loads than those which caused failure of identical walls under less or no precompression.

(e) Under/

(e) Under combined axial and lateral loads the lateral rigidity of brick walls increases with increase of axial precompression. For the same value of precompression, lateral rigidity increases with decrease of length of walls of the same height and thickness.

(f) The lateral strength of brick walls can be estimated analytically using The Yield Line Theory provided that the moment of resistance is based on the modulus of rupture of the brickwork obtained from data provided by transverse tests of specimens prepared from the same materials used in construction. In the case of walls with axial precompression the moment of resistance is adjusted to allow for these precompressions. The use of The Yield Line Theory here is only empirical as it could not be proved that all yield lines have had the same maximum bending moment simultaneously.

(g) Stresses and deflections in a laterally loaded brick wall can be calculated reasonably accurately, and the yield line pattern of cracks predicted using The Finite Element Method.

(h) Transverse strength of brickwork is related indirectly to the crushing strength and modulus of rupture of the bricks, and the crushing strength of the brickwork.

(i) The most significant factors determining the modulus of rupture of brickwork are the mortar water retentivity and brick suction rate. There is a conflict between these two properties: the mortar trying to retain its water for proper hydration of cement/

cement and the brick trying to absorb water out of mortar. The resulting moisture balance is a deciding factor of the modulus of rupture.

(j) The modulus of rupture of brickwork at an axis of bending through a mortar bed joint has been related directly to the modulus at an axis of bending normal to the bed joints, depending on the type of mortar used. It was found that for 1:$\frac{1}{4}$:3 mortar the modulus of rupture at a bed joint is about one-fifth of that at an axis of bending normal to the bed joint. For 1:1:6 mortar the ratio is one-eighth.

(k) The modulus of rupture of brickwork gradually increases with increasing angle between the bed joints and the axis of bending up to 90 degrees.

(l) It is suggested that the permissible tensile stresses of brickwork be increased when the suction rate of the units is controlled and mortars of high water retentivity are used.

Recommendations for future research:

1. As the use of the yield-line theory was empirical an investigation could be carried out to verify the existence at all yield-lines of maximum bending moments.
2. Some further study of the relationship between the moment of resistance in the horizontal and vertical directions in brickwork walls could be made.
3. Application of the yield-line theory to panels of more complicated boundary conditions and openings could also be made.

LIST OF REFERENCES

1. British Standard Code of Practice, C.P. 111: Part 2: 1970
Structural Recommendations for Loadbearing Walls.

2. THOMAS, F.G.
The Strength of Brickwork,
The Structural Engineer, February 1953, pp 35 - 46

3. DAVEY, N.
Modern Research on Loadbearing Brickwork,
The Brick Bulletin, The National Federation of Clay Industries.

4. TASKER, H.E.
Report on simulated Wind Pressure Tests carried out on Four Full-size Test Walls,
Technical Study 13, April 1947, Commonwealth Experimental Building Station, Australia.

5. BRADSHAW, R.E. and ENTWISLE, F.D.
Wind Forces on Non-Loadbearing Brickwork Panels,
CPTB - Technical Note, Vol. 1, No. 6, May 1965.

6. British Standard Code of Practice, C.P. 114 (1957),
The Structural Use of Reinforced Concrete in Buildings.

7. MONK, C.B.
SCR Brick Wall Tests, SCPRF, Research Report No. 1

8. SCPRF
Research Report No. 8, Compressive and Transverse Tests of Five-Inch Brick Walls, May 1965.

9. SCPRF/

9. SCPRF

Research Report No. 9, Compressive, Transverse and Racking Strength Tests of Four-Inch Brick Walls, August 1965.

10. SCPRF

Research Report No. 10, Compressive and Transverse Strength Tests of Eight-Inch Brick Walls, October 1966.

11. THOMPSON, J.N., JOHNSON, F.B., and WHEELESS, L.A.

Transverse strength of Masonry Bonded Hollow Walls, The University of Texas, August 1965.

12. MONK, C.B.

Transverse strength of Masonry Walls.

ASTM, Special Technical Publication No. 166, 1954.

13. O'CONNOR, J.P.

NCMA Tests on Flexural Strength of Concrete Masonry Walls, National Concrete Masonry Association, Virginia.

14. HALLQUIST, A.

Lateral Loads on Masonry Walls, Norwegian Building Research Institute, Reprint 172, 1970.

15. HASELTINE, B.A., THOMAS, K., WEST, H.W.H. and HODKINSON, H.R.

Loadbearing Brickwork - Design for The Fifth Amendment: Lateral Loading Tests, BDA Tech. Note, September 1970.

16. GRENLEY, D.G., CATTANEO, LE and PFRANG, E.O.

Effect of Edge Load on Flexural Strength of Clay Masonry Systems Utilizing Improved Mortars, The National Bureau of Standards.

17. HENDRY, A.W. SINHA, B.P. and MAURENBRECHER, AHP/

17. HENDRY, A.W. SINHA, B.P. & MAURENBRECHER, A.H.P.
Full Scale Tests on The Lateral Strength of Brick Cavity Walls with Precompression, Department of Civil Engineering and Building Science, University of Edinburgh.

18. JOHANSEN, K.W.
Yield-Line Theory, Cement and Concrete Association, 1962.

19. JONES, L.L.
Ultimate Load Analysis of Reinforced and Prestressed Concrete Structures, Chatto and Windus, London, 1968.

20. WOOD, R.H. and JONES, L.L.
Yield-Line Analysis of Slabs, Thames and Hudson, Chatto and Windus, London 1967.

21. WESTERGAARD, H.M. and SLATER, W.A.
Moments and Stresses in Slabs, Proc. A.C.I., 1921.

22. TIMOSHENKO, S.P. and WOINOWSKY-KRIEGER, S.
Theory of Plates and Shells, McGraw-Hill 1959

23. McNEICE, G.M.
Elastic-Plastic Bending Analysis of Plates and Slabs by The Finite Element Method.

24. TURNER, M.J. CLOUGH, R.W, MARTIN, H.C. and TOPP, L.J.
Stiffness and Deflection Analysis of Complex Structures, Jr. Aero, Sc., Vol. 23, No. 9, September 1956.

25. CLOUGH, RW
The Finite Element Method in Structural Mechanics, Chapter 7 of Stress, Analysis, John Wiley & Sons, 1965.

26. ZIENKIEWICZ, O.C.
Finite Element Procedures in The Solution of Plate and Shell Problems,/

Problems, Chapter 8 of Stress Analysis, John Wiley & Sons, 1965.

27. ZIENKIEWICZ, O.C.
The Finite Element Method in Structural and Continuum Mechanics, McGraw Hill, 1967.

28. Proceedings of The Conference on Matrix Methods in Structural Mechanics, Air Force Institute of Technology, Ohio, U.S.A. 1965.

29. ARGYRIS, J.H.
On The Analysis of Complex Elastic Structures, App. Mech. Rev., Vol. II, July 1958.

30. GALLAGHER, R.H.
A Correlation Study of Methods of Matrix Structural Analysis, Pergamon Press, 1964.

31. PEARSON, J.C.
Measurement of Bond Between Bricks and Mortar, ASTM "Proceedings" 1943, Vol. 43

32. McBURNEY, J.W.
Discussion of 31.

33. PLUMMER,H. and REARDON, L.
Principles of Brick Engineering: Handbook of Design, Structural Clay Products Institute, Washington, D.C. 1939.

34. HALLQUIST, A.
Wind Loads on Cavity Walls, Tegl, No. 2 and No. 4 1966, Norwegian Building Research Institute.

35. HEDSTROM, R.O.
Load/

35. HEDSTROM, R.O.
Load Tests of Patterned Concrete Masonry Walls, ACI Journal, Proceedings, Vol. 57, April 1961 P. 1265; PCA Development Department Bulletin D41.

36. FISHBURN, C.
Effect of Mortar Properties on Strength of Masonry, National Bureau of Standards, Monograph 36, Department of Commercen, Novementer 1961, Washington D.C.

37. YOUL, V.A. and COATS, E.R.
Some Studies in Brick-mortar Bond, Australian Building Research Congress 1961, Paper 2, CB1.

38. RYDER, J.F.
The Use of Small Brickwork Panels for Testing Mortars, Transactions of the British Ceramic Society, Vol. 62, No. 8, pp 615-629 August, 1963.

39. The British Ceramic Research Association,
Model Specification for Loadbearing Clay Brickwork, Spec. Publ. 56, Revised Edition 1971.

40. British Standard 3921: Part 2: 1969
Specification for Bricks and Blocks of Fired Brickearth, Clay or Shale.

APPENDIX A.1

FORMULAE FOR PANELS BY THE YIELD-LINE THEORY

(1) Rectangular Panels Simply Supported from Three Sides:

a) First Mode of Failure (Fig. A.1.1)

The principle of virtual work is used.

Assume a deflection δ at points e and f

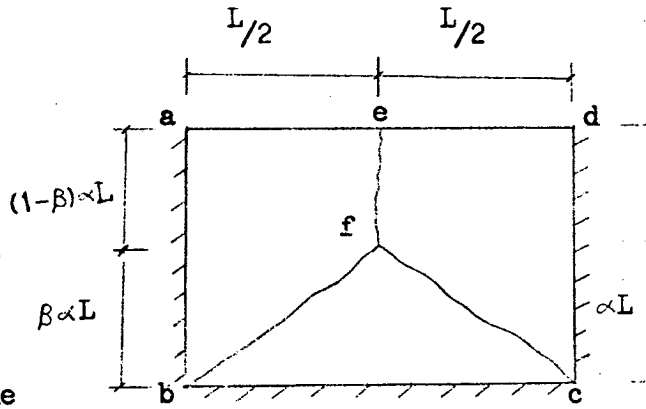

Fig. A.1.1.

The internal work done by rotation of the yield lines:

$$= m \times \alpha L \times \frac{2\delta}{L} \times 2 + m \times L \times \frac{\delta}{\beta \alpha L}$$

$$= m \alpha \delta \left(4 + \frac{1}{\beta \alpha^2}\right) \qquad \text{.....(1)}$$

External work done by load:

$$= p \left[\frac{1}{2} \times (1 - \beta) \alpha L \times \frac{\delta}{2} \times 2 + \frac{L}{2} \times \frac{\beta \alpha L}{2} \times \frac{\delta}{3} \times 2 + \beta \alpha L \times \frac{L}{2} \times \frac{\delta}{3} \right]$$

$$= \frac{pL^2}{6} \times \alpha \delta (3 - \beta) \qquad \text{.....(2)}$$

Internal work = External work

hence $m = \frac{pL^2}{6} \left[\frac{3\beta - \beta^2}{4\beta + \gamma} \right]$; $\gamma = \frac{1}{\alpha^2}$

$\frac{dm}{d\beta}$ /

$$\frac{dm}{d\beta} = 0 \quad \therefore \quad \beta = \frac{\gamma}{2}\left[\sqrt{1/4 + \frac{3}{\gamma}} - \frac{1}{2}\right]$$

and $$m = \frac{pL^2}{24}\left[\sqrt{3 + \frac{1}{4\alpha^2}} - \frac{1}{2\alpha}\right]^2$$

b) Second Mode of Failure (Fig. A.1.2)

For elements A and C, internal work =

$$m \times \frac{1}{\beta L} \times \alpha L \times 2 = 2m \times \frac{\alpha}{\beta}$$

For element B =

$$m \times \frac{1}{\alpha L} \times 2\beta L$$

Total internal work =

$$2\left(m\,\frac{\beta}{\alpha} + m\,\frac{\alpha}{\beta}\right) \qquad \ldots\ldots(1)$$

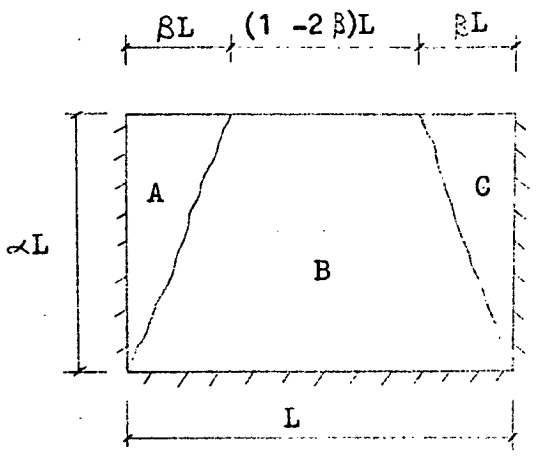

Fig A.1.2.

External work =

$$p\left[L(1-2\beta) \times \alpha L \times \frac{1}{2} + 4 \times \beta L \times \frac{\alpha L}{2} \times \frac{1}{3}\right]$$

$$= \frac{pL^2}{6} \times \alpha\,(3 - 2\beta) \qquad \ldots\ldots(2)$$

Equating (1) and (2) we get

$$m = \frac{pL^2}{12}\left(\frac{3\beta - 2\beta^2}{1 + \gamma\beta^2}\right); \quad \gamma = \frac{1}{\alpha^2}$$

$\frac{dm}{d\beta}$ /

$$\frac{dm}{d\beta} = 0 \quad \therefore \quad \beta = \frac{1}{\gamma}\left[\sqrt{\frac{4}{9} + \gamma} - {}^{2}/_{3}\right]$$

$$\text{and } m = \frac{p(\alpha L)^2}{24}\left[\sqrt{4 + \frac{9}{\alpha^2}} - 2\right]$$

(2) Rectangular Panels Simply Supported from Four Sides: (Fig.A.1.3)

Assume deflection δ along ef.

Internal work:

$$2 \times m \times \frac{\delta \times 2}{\alpha L} \times L + 2 \times m \times \frac{\delta}{\beta L} \times \alpha L$$

$$= m \times \delta\left(\frac{4}{\alpha} + \frac{2\alpha}{\beta}\right) \qquad \ldots\ldots(1)$$

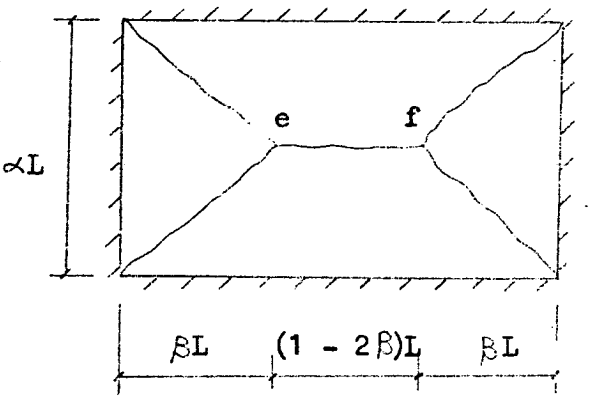

Fig A.1.3.

External work:

$$p\left(\left[\frac{1}{2} \times L \times (1 - 2\beta) \times \frac{\alpha L}{2} \times \frac{2\delta}{3} + \frac{1}{2} \times L \times \frac{\alpha L}{2} \times \frac{\delta}{3}\right] \times 2 + \right.$$

$$\left.\left[\frac{1}{2} \times \beta L \times \alpha L \times \frac{\delta}{3}\right] \times 2\right)$$

$$= \frac{p \quad L^2}{3}\left(\frac{3}{2} - \quad\right) \qquad \ldots\ldots(2)$$

Equating (1 and (2) gives

$$m = \frac{pL^2\alpha^2}{12} \times \frac{(3\beta - 2\beta^2)}{(2\beta + \alpha^2)}$$

$$\frac{dm}{d\beta} = 0 \quad \therefore \quad \beta = \frac{1}{2}\left[\sqrt{(3\alpha^2 + \alpha^4)} - \alpha^2\right]$$

$$\text{and} \quad m = \frac{p(\alpha L)^2}{24}\left[\sqrt{3 + \alpha^2} - \alpha\right]^2$$

APPENDIX A.2

Flow Chart 1.

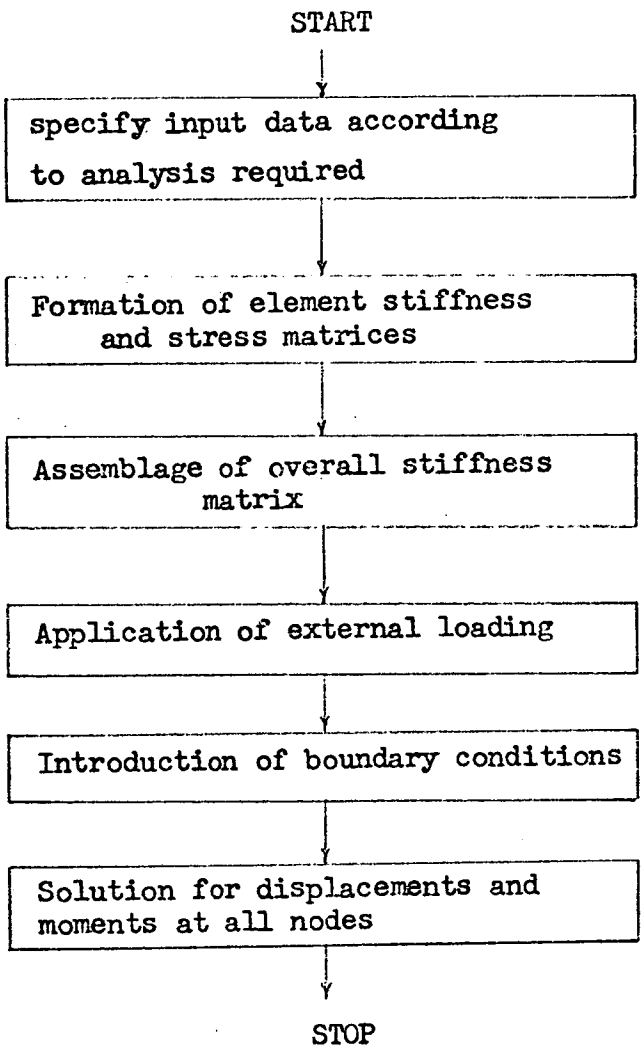

Flow Chart 2.